

Molecular Imaging

CME Learning Checkpoint Exhibit ED028 (PET-CT beyond 18FDG: A New Telling of an Old Tale)

All Day Room: Case of Day, Learning Center

MI

AMA PRA Category 1 Credit ™: .50

Participants

Cesar N. Cristancho Rojas, MD, Mexico City, Mexico (*Abstract Co-Author*) Nothing to Disclose Luis Azpeitia Espinosa, MD, Mexico City, Mexico (*Presenter*) Nothing to Disclose Mary C. Herrera-Zarza, MD, Mexico City, Mexico (*Abstract Co-Author*) Nothing to Disclose Jose L. Criales, MD, Mexico City, Mexico (*Abstract Co-Author*) Nothing to Disclose

Use of a Clinical Multislice CT for Preclinical Imaging

All Day Room: S503AB

Participants

Karen Briley, PhD, Columbus, OH (*Presenter*) Nothing to Disclose Ajay Siva, Columbus, OH (*Abstract Co-Author*) Nothing to Disclose Richard Jacko, BS, Columbus, OH (*Abstract Co-Author*) Nothing to Disclose Claudia Zindl, Cambridge, United Kingdom (*Abstract Co-Author*) Nothing to Disclose Matthew Allen, Cambridge, United Kingdom (*Abstract Co-Author*) Nothing to Disclose Michael V. Knopp, MD, PhD, Columbus, OH (*Abstract Co-Author*) Nothing to Disclose Michelle Williams, Columbus, OH (*Abstract Co-Author*) Nothing to Disclose

TEACHING POINTS

The aims of the educational exhibit are: 1) to illustrate the advantages of performing pre-clinical CT using a current generation, multislice clinical CT, 2) describe the optimization of clinical CT for imaging of rodents, 3) describe software adaptations to allow for morphometric cortical bone analysis, and 4) describe the optimization of clinical CT for bone analysis.

TABLE OF CONTENTS/OUTLINE

• Pre-clinical imaging using clinical CT. Advantages and limitations of clinical CT for pre-clinical imaging of animals (Fig.1).• Mouse Imaging on a clinical CT system. Optimization of the image acquisition and reconstruction parameters for rodent imaging (Fig.2).• Multiple mouse Imaging on a clinical CT system. Illustration of the possibility of scanning multiple mice and related acquisition optimization (Fig.3).• Quantitative pre-clinical CT using a clinical CT system. Introduction to morphometric cortical bone analysis on a clinical CT system in large animals e.g. canine. Adaptation of commercial validated microCT software for bone analysis of such CT data (Fig.4).• Example of Quantitative pre-clinical CT of the canine forelimb. Review of pre-clinical imaging obtained including optimization of current, pixel size/FoV, and reconstruction methods. Moprhometric data in the canine forelimb will be presented (Fig.5).

The Clinical Application of PSMA PET/MR for Treatment Planning and Staging of Prostate Cancer

All Day Room: S503AB

Participants

Daphne J. Prybyszczuk, BSC, Brisbane, Australia (Presenter) Nothing to Disclose

TEACHING POINTS

The education objective of this presentation is to describe the process involved in the formation of workflow, scan protocols and data analysis in PSMA Prostate PET/MR. This will enable the reader to appreciate the challenges and problems associated with these clinical protocols and to show their practical uses in the clinical setting.

TABLE OF CONTENTS/OUTLINE

A. Technical aspects of the PET/MR scanner.B .Indications for the procedureC.Contraindications and Precautions.D. PSMA pharmaceutical properties, dose and administration.E. Preparation of the patient.F. Description of the scan protocols and the adaptations used.G. Use of Gadolinium.H.Display and postprocessing.Many scans will have up to 10,000 images, therefore an efficient and effective means of data display is necessary. I. Identification of MR and PET artefacts.Methods to minimize these artefacts are discussed.K. Case StudiesIt will include comparison of the fused PET/MR to the colour maps from the Multiparametric MR. L.ConclusionIn PET/MR, it combines morphological detail,multiparametric functional MR data and molecular PET data for use in the detection of prostate cancer. The challenge is to use these different modalities in a way that complement, substantiate and add more information that each modality would do on its own.

MI101-ED-X

Ferumoxytol Enhanced MR Lymphography in Prostate Cancer: How We Do It

All Day Room: S503AB

FDA Discussions may include off-label uses.

Participants

Francesca Mertan, BS, Bethesda, MD (Presenter) Nothing to Disclose William Dahut, Bethesda, MD (Abstract Co-Author) Nothing to Disclose James Gulley, MD, PhD, Bethesda, MD (Abstract Co-Author) Nothing to Disclose Ravi A. Madan, MD, Bethesda, MD (Abstract Co-Author) Nothing to Disclose Soroush Rais-Bahrami, MD, Birmingham, AL (Abstract Co-Author) Nothing to Disclose Jeffrey Nix, MD, Bethesda, MD (Abstract Co-Author) Nothing to Disclose Ann Foo, Bethesda, MD (Abstract Co-Author) Nothing to Disclose Deborah Citrin, MD, Bethesda, MD (Abstract Co-Author) Nothing to Disclose Bradford J. Wood, MD, Bethesda, MD (Abstract Co-Author) Researcher, Koninklijke Philips NV; Researcher, Celsion Corporation; Researcher, BTG International Ltd; Researcher, W. L. Gore & Associates, Inc ; Researcher, Cook Group Incorporated; Patent agreement, VitalDyne, Inc; Intellectual property, Koninklijke Philips NV; Intellectual property, BTG International Ltd; ; ; ; Maria Merino, MD, Bethesda, MD (Abstract Co-Author) Nothing to Disclose Peter Pinto, Bethesda, MD (Abstract Co-Author) Nothing to Disclose Peter L. Choyke, MD, Rockville, MD (Abstract Co-Author) Researcher, Koninklijke Philips NV; Researcher, General Electric Company; Researcher, Siemens AG; Researcher, iCAD, Inc; Researcher, Aspyrian Therapeutics, Inc; Researcher, ImaginAb, Inc; Researcher, Aura Biosciences, Inc Baris Turkbey, MD, Bethesda, MD (Abstract Co-Author) Nothing to Disclose

TEACHING POINTS

Prostate cancer (PCa) has a variable natural history and can develop into an aggressive disease. Because of this, accurate nodal staging and detection of early metastasis is critical. Current imaging modalities such as CT, PET/CT, and sentinel lymphoscintigraphy have variable sensitivities, while the latter has a high false positive rate. Lymphotrophic nanoparticle enhanced MRI is a promising imaging modality in the detection of malignant nodal involvement in PCa patients showing improved sensitivities in several studies. Ferumoxytol, a semi-synthetic carbohydrate coated, magnetic iron oxide particle, allows for easy identification of possible metastatic lymph nodes in PCa patients. As metastatic tumor involvement in lymph nodes disrupts normal cellular texture, partial or total lack of accumulation of ferumoxytol over 24-48hrs results in MRI detectable lymph nodes suggestive of metastasis. The purpose of this exhibit is to provide tips to aid in image acquisition and interpretation of ferumoxytol enhanced MR lymphography (FEMRL) in the detection of nodal metastasis in PCa patients.

TABLE OF CONTENTS/OUTLINE

Definition of chemical and physical composition of ferumoxytol in comparison with ferumoxtran-10 FEMRL MRI protocol Qualitative and quantitative methods for FEMRL interpretation Case samples Current challenges in application of FEMRL

The 'ABC' of Manganese Enhanced Magnetic Resonance Imaging (MEMRI) from Well-Established Axononal Transport Imaging to Future Use in Bone Growth Visualisation and Cancer Research

All Day Room: S503AB

Participants

Francesca Rosa, MD, Genova, Italy (*Presenter*) Nothing to Disclose Luca Basso, MD, Genova, Italy (*Abstract Co-Author*) Nothing to Disclose Ilaria Verardo, Genova, Italy (*Abstract Co-Author*) Nothing to Disclose Lucia Secondini, Genova, Italy (*Abstract Co-Author*) Nothing to Disclose Stella Barbagallo, Genova, Italy (*Abstract Co-Author*) Nothing to Disclose Carlo Emanuele Neumaier, Genoa, Italy (*Abstract Co-Author*) Nothing to Disclose

TEACHING POINTS

Manganese-enhanced Magnetic Resonance Imaging (MEMRI) relies upon the several main properties of Mn2+, the teaching points of this work are: Review MEMRI established use in preclinical imaging; Review biological mechanisms which make Manganese an intracellular contrast agent (from voltage-gated calcium channel of myocardium to Calcium sensing Receptor pathway of breast cancer); Analyse rising applications of this technique especially in Cancer Research and Bone Growth disease.

TABLE OF CONTENTS/OUTLINE

This work highlight the utility of MEMRI as a "functional tool" able to study physiological and pathological conditions of :1. Axonal transport (Brain),2. Cardiovascular system,3. Digestive glands (liver).Meanwhile above applications are well established in literature and especially in preclinical research, a review of rising application of MEMRI focus on field of interest shown below:1. Advanced cancer disease (cachecxia),2. Bone growth disease,3. Cancer phenotype and behaviour,4. Digestive accessory gland (salivary glands)5. Endocrine glands (surrenal glands and thyroid).

Key Points for FDG-PET Reading and Reporting When Evaluating for Different Gynecological Malignancies, Essential for Surgical versus Non-surgical Treatment Planning

All Day Room: S503AB

Participants

Roberto C. Valentin, MD, Birmingham, AL (*Presenter*) Nothing to Disclose Rebecca C. Arend, MD, Birmingham, AL (*Abstract Co-Author*) Nothing to Disclose Janis P. O'Malley, MD, Birmingham, AL (*Abstract Co-Author*) Nothing to Disclose Jonathan E. McConathy, MD, PhD, Birmingham, AL (*Abstract Co-Author*) Research Consultant, Eli Lilly and Company; Research Consultant, Blue Earth Diagnostics Ltd; Research Consultant, Siemens AG; Research Consultant, General Electric Company; Michelle M. McNamara, MD, Birmingham, AL (*Abstract Co-Author*) Nothing to Disclose Samuel E. Almodovar-Reteguis, MD, Homewood, AL (*Abstract Co-Author*) Nothing to Disclose Taylor B. Turner, MD, Birmingham, AL (*Abstract Co-Author*) Nothing to Disclose

TEACHING POINTS

- To discuss what a PET reader should evaluate for and include in every report when analyzing initial and post-treatment/restaging PET studies, that will impact surgical versus non-surgical treatment planning in patients with gynecological malignancies.- To review the most common patterns of hematologic and lymphatic spread of cervical, endometrial, uterine body, and ovarian cancers.

TABLE OF CONTENTS/OUTLINE

FDG-PET is a non-invasive technique that allows for detection of abnormal metastatic metabolic activity prior to detection of any anatomical change. Hybrid imaging with CT or MR allows for anatomic characterization of lesions as well as accurate anatomic localization, essential for optimal treatment/surgical planning. We will review the anatomical boundaries of the intra and extraperitoneal regions within the pelvis, since location and extent of local tumor and metastatic lesions are of great importance when determining surgical versus non-surgical treatment planning. We will review the most common patterns of hematologic and lymphatic spread of cervical, endometrial, uterine body (leiomyosarcoma), and ovarian malignancies in order to provide a map for the PET reader when evaluating each study. We will also discuss the potential challenges a PET reader may encounter when evaluating for ovarian mucinous neoplasms.

PET Imaging of Hypoxia in Oncology: Implications on Patient Care and Available Tracers

All Day Room: S503AB

Participants

Sara Pourhassan Shamchi, MD, Philadelphia, PA (*Presenter*) Nothing to Disclose Sahra Emamzadehfard, MD, MPH, Philadelphia, PA (*Abstract Co-Author*) Nothing to Disclose Koosha Paydary, MD, MPH, Philadelphia, PA (*Abstract Co-Author*) Nothing to Disclose Thomas J. Werner, Philadelphia, PA (*Abstract Co-Author*) Nothing to Disclose Abass Alavi, MD, Philadelphia, PA (*Abstract Co-Author*) Nothing to Disclose

TEACHING POINTS

Tumor hypoxia in cancer has received a lot of attention in recent years due to its vital role in tumor aggressiveness and angiogenesis as well as its impact on disease prognosis and response to treatment. The goal of this educational exhibit is to discuss the importance of hypoxia imaging in oncology and introduction of currently available PET tracers for this purpose. We will further discuss how imaging of hypoxia can become incorporated into patient management.

TABLE OF CONTENTS/OUTLINE

1. How hypoxia develops in tumors. 2. Applications and impact of hypoxia imaging on patient care. 3. FMISO and other nitroimidazole compounds for PET imaging of hypoxia. 4. Non-nitroimidazole compounds for PET imaging of hypoxia 5. Newer agents for hypoxia imaging: HIF1a, CAIX

Preclinical Multimodality Imaging for Drug Development to Bridge Preclinical Trial and Clinical Trial

All Day Room: S503AB

Participants

Jinil Kim, MS, Seoul, Korea, Republic Of (*Presenter*) Jinil Kim is working for Center for Bioimaging in New Drug development in Korea, which has several collaboration projects with Korean pharmaceutical company. Kyung Won Kim, MD, Seoul, Korea, Republic Of (*Abstract Co-Author*) Nothing to Disclose Jeong Kon Kim, MD, Seoul, Korea, Republic Of (*Abstract Co-Author*) Nothing to Disclose YoonSeok Choi, Seoul, Korea, Republic Of (*Abstract Co-Author*) Nothing to Disclose Dong-Cheol Woo, PhD, Seoul, Korea, Republic Of (*Abstract Co-Author*) Nothing to Disclose

TEACHING POINTS

1. In preclinical phase of drug development, bioimaging can be used for evaluation of drug efficacy, drug toxicity, and biodistribution of a candidate drug.2. Preclinical imaging is an important tool to bridge preclinical trial and clinical trial

TABLE OF CONTENTS/OUTLINE

Table of Contents/Outline:1. Overview of role of preclinical imaging in the drug development2. Imaging modalities for small animal: MRI, CT, PET, and optical imaging.3. Evaluation of drug efficacy using multimodality imaging4. Evaluation of drug toxicity using imaging5. Evaluation of biodistribution of drug using imaging6. Utilization of preclinical trial data in designing clinical trial7. Comprehensive imaging platform for drug development

Molecular Imaging Sunday Case of the Day

Sunday, Nov. 27 7:00AM - 11:59PM Room: Case of Day, Learning Center

MI

AMA PRA Category 1 Credit ™: .50

Participants

Jonathan E. McConathy, MD, PhD, Birmingham, AL (Presenter) Research Consultant, Eli Lilly and Company; Research Consultant, Blue Earth Diagnostics Ltd; Research Consultant, Siemens AG; Research Consultant, General Electric Company; Suzanne E. Lapi, PhD, Birmingham, AL (Presenter) Research Grant, AbbVie Inc; Spouse, Consultant, General Electric Company; Consultant, Siemens AG; Consultant, Blue Earth Diagnostics Ltd; Consultant, Eli Lilly and Company Matthias J. Eiber, MD, Muenchen, Germany (Abstract Co-Author) Nothing to Disclose Thomas A. Hope, MD, San Francisco, CA (Abstract Co-Author) Research Grant, Consultant, GE Healtcare Robert R. Flavell, MD, PhD, San Francisco, CA (Abstract Co-Author) Nothing to Disclose Samuel J. Galgano, MD, Birmingham, AL (Abstract Co-Author) Nothing to Disclose Asim K. Bag, MD, Birmingham, AL (Abstract Co-Author) Nothing to Disclose David M. Schuster, MD, Atlanta, GA (Abstract Co-Author) Institutional Research Grant, Nihon Medi-Physics Co, Ltd; Institutional Research Grant, Blue Earth Diagnostics Ltd; Consultant, WellPoint, Inc; ; Ephraim E. Parent, MD, PhD, Saint Louis, MO (Abstract Co-Author) Nothing to Disclose Bital Savir-Baruch, MD, Maywood, IL (Abstract Co-Author) Nothing to Disclose Pamela K. Woodard, MD, Saint Louis, MO (Abstract Co-Author) Research Grant, Astellas Group; Research Grant, Bayer AG; Research agreement, Siemens AG; ; ; ; Sebastian R. McWilliams, MBBCh, Saint Louis, MO (Abstract Co-Author) Nothing to Disclose Amir K. Durrani, MD, St Louis, MO (Abstract Co-Author) Nothing to Disclose Robert J. Gropler, MD, Saint Louis, MO (Abstract Co-Author) Nothing to Disclose

Michael Hofman, PhD, San Francisco, CA (Abstract Co-Author) Nothing to Disclose

TEACHING POINTS

1) Interpret amyloid-PET scans as positive or negative. 2) Apply appropriate use criteria for selecting patients for amyloid-PET study. 3) Understand the goals of the IDEAS study as it relates to coverage with evidence development for clinical amyloid-PET scans.

Science Session with Keynote: Gastrointestinal (Rectal Cancer)

Sunday, Nov. 27 10:45AM - 12:15PM Room: E353A

CT GI MR MI

AMA PRA Category 1 Credits ™: 1.50 ARRT Category A+ Credits: 1.50

Participants

Kedar Jambhekar, MD, Little Rock, AR (*Moderator*) Nothing to Disclose Mukesh G. Harisinghani, MD, Boston, MA (*Moderator*) Nothing to Disclose

Sub-Events

SSA07-01 Gastrointestinal Keynote Speaker: Evolving Expectations from Imaging in the Management of Rectal Cancer

Sunday, Nov. 27 10:45AM - 10:55AM Room: E353A

Participants

Mukesh G. Harisinghani, MD, Boston, MA (Presenter) Nothing to Disclose

SSA07-02 Clinical Impact of Preoperative Gadoxetic Acid-enhanced Liver MRI in the Evaluation of Synchronous Liver Metastasis of Colon Cancer

Sunday, Nov. 27 10:55AM - 11:05AM Room: E353A

Awards

Student Travel Stipend Award

Participants

Cherry Kim, MD, Seoul, Korea, Republic Of (*Presenter*) Nothing to Disclose So Yeon Kim, MD, Seoul, Korea, Republic Of (*Abstract Co-Author*) Nothing to Disclose Min-Ju Kim, Seoul, Korea, Republic Of (*Abstract Co-Author*) Nothing to Disclose Seong Soo Lee, MD, Seoul, Korea, Republic Of (*Abstract Co-Author*) Nothing to Disclose Seong Ho Park, MD, Seoul, Korea, Republic Of (*Abstract Co-Author*) Research Grant, DONGKOOK Pharmaceutical Co, Ltd Kyu-Pyo Kim, Pittsburgh, PA (*Abstract Co-Author*) Nothing to Disclose Yong Sik Yoon, Seoul, Korea, Republic Of (*Abstract Co-Author*) Nothing to Disclose Chan Wook Kim, Seoul, Korea, Republic Of (*Abstract Co-Author*) Nothing to Disclose Jae Hoon Lee, Seoul, Korea, Republic Of (*Abstract Co-Author*) Nothing to Disclose Moon-Gyu Lee, MD, Seoul, Korea, Republic Of (*Abstract Co-Author*) Nothing to Disclose

PURPOSE

To investigate whether additional MRI with gadoxetic acid increases the survival rate of patients with synchronous liver metastasis of colon cancer (sCLM) planning to undergo curative-intended treatment, compared with patients assessed only with CT.

METHOD AND MATERIALS

We retrospectively identified 117 patients with sCLM who underwent curative-intended treatment for colon cancer with resectable sCLM from 2006 to 2010 and who were initially evaluated using CT. Among these patients, 65 underwent additional gadoxetic acidenhanced MRI (CT+MRI group) before surgery. The remaining 52 patients who were assessed using only CT constituted the CT group. We compared the baseline characteristics, including pathologic staging and the surgical margin status in the two groups. In the CT+MRI group, we analyzed patients with discrepancy between CT and MRI. We correlated the detected sCLM with the pathologic findings. The 5-year survival rate was compared between the two groups, and multivariable analyses were performed using a Cox proportional hazard model. The inverse probability treatment weighting analysis (IPTW) adjusted by propensity scores was done to reduce the effect of selection bias.

RESULTS

The CT and CT+MRI groups were comparable regarding the baseline characteristics. In the CT+MRI group, 43 patients (66.2%, 43/65) showed a discrepancy in the numbers of sCLM between CT and MRI and MRI detected 25 additional sCLM (38.5%, 25/65) which were initially missed on CT. The numbers of detected sCLM were correlated with the pathologic findings better in the CT+MRI group (86.2%) than in the CT group (65.4%) (P=0.014). The 5-year survival rate was significantly higher in the CT+MRI group than in the CT group (70.8% vs. 48.1%, P=0.003). On multivariate analyses, the CT+MRI group showed a lower mortality rate (HR, 0.413; 95% CI, 0.256 - 0.830) than the CT group. After the IPTW, the CT+MRI group was associated with a significantly lower risk of overall mortality (HR, 0.434; 95% CI, 0.226 - 0.831) than the CT group.

CONCLUSION

In patients with colon cancer and sCLM who underwent CT, additional preoperative evaluation by gadoxetic acid-enhanced MRI allowed us to detect sCLM more precisely and consequently increased the overall survival.

CLINICAL RELEVANCE/APPLICATION

Optimal preoperative staging using gadoxetic acid-enhanced liver MRI for synchronous liver metastasis in patients with colon cancer can improve the overall survival.

SSA07-03 Tumor Enhancement on Gadoxetate-enhanced MRI is Associated with Long-term Survival in Patients with Colorectal Liver Metastases

Awards Student Travel Stipend Award

Participants Helen Cheung, MD, Toronto, ON (*Presenter*) Nothing to Disclose Paul Karanicolas, Toronto, ON (*Abstract Co-Author*) Nothing to Disclose Natalie Coburn, Toronto, ON (*Abstract Co-Author*) Nothing to Disclose Calvin Law, MD, FRCPC, Toronto, ON (*Abstract Co-Author*) Nothing to Disclose Laurent Milot, MD, MSc, Toronto, ON (*Abstract Co-Author*) Nothing to Disclose

PURPOSE

Surgical resection is the standard of care for treatment of colorectal liver metastases (CRLM) and gadoxetate-enhanced MRI is routinely used for preoperative diagnosis and staging. Tumor fibrosis on post-hepatectomy specimens is associated with long-term survival and delayed enhancement on gadolinium-enhanced MRI is associated with fibrosis in other disease processes. Therefore, the goal of this study is to determine whether tumor enhancement on preoperative delayed-phase gadoxetate-enhanced MRI can predict disease-specific survival in patients with CRLM post-hepatectomy.

METHOD AND MATERIALS

Patients who received a preoperative gadoxetate-enhanced MRI prior to liver resection for CRLM from January 1, 2010 to December 31, 2012 were included in this retrospective study. The signal-to-noise ratio (SNR) was measured on the noncontrast and 10minute delayed phases. Tumor enhancement was calculated as the percentage increase in SNR from noncontrast to 10-minute delayed phase. If there were multiple lesions, we calculated the mean tumor enhancement, weighted by size of tumor (largest axial diameter). Per patient tumor enhancement was stratified into weak and strong enhancement based on the a cutoff determined by the Youden J statistic for 3-year survival. Kaplan-Meier and Cox-Regression analyses were used to determine whether tumor enhancement could predict disease-specific survival, independent of potential confounders.

RESULTS

Eighty-four patients met inclusion/exclusion criteria. Based on the Youden Index, the threshold for weak and strong tumor enhancement was a 12% increase in SNR between noncontrast and delayed phase. Tumor enhancement predicted disease-specific death with 61.1% surviving at 3 years in those with weak enhancement vs. 85.5% surviving in those with strong enhancement (p=0.01). The adjusted hazard ratio of death in patients who had weak tumor enhancement after adjusting for potential confounders was 3.48 (p=0.009).

CONCLUSION

Tumor enhancement seen on gadoxetate-enhanced MRI is associated with survival in patients with CRLM post-hepatectomy.

CLINICAL RELEVANCE/APPLICATION

Tumor enhancement of colorectal liver metastases on preoperative delayed-phase gadoxetate-enhanced MRI is a biomarker of long-term survival and may be helpful in preoperative patient risk-stratification.

SSA07-04 Discriminating Stages of Rectal Cancer by Texture Analysis on Apparent Diffusion Coefficient Maps

Sunday, Nov. 27 11:15AM - 11:25AM Room: E353A

Participants

Liheng Liu, MD, Jinan, China (*Presenter*) Nothing to Disclose Wenwu Li, MD, Shandong, China (*Abstract Co-Author*) Nothing to Disclose

PURPOSE

To explore the potential of texture analysis based on apparent diffusion coefficient (ADC) maps, as a predictor of local invasion depth (stage T1-2 vs. T3-4) and nodal status (N0 vs. N1-2) of rectal cancer.

METHOD AND MATERIALS

In this retrospective study, 68 patients with rectal cancer who underwent preoperative MRI with diffusion-weighted sequence prior to the surgery were enrolled. Texture features of ADC maps of the mass lesions (skewness, kurtosis, entropy, contrast, correlation) and routine ADC variables (ADCmean, ADCmin, ADCmax) were compared between T1-2 and T3-4 stages, between N0 and N1-2 stages, as well as between overall stages.

RESULTS

Significant inter-group differences were observed with respect to skewness (P=0.015), entropy (P=0.004) and contrast (P=0.017) between T1-2 and T3-4 tumors. The three parameters were significantly lower in patients with T1-2 as compared to those with T3-4 tumors (skewness, 0.166 vs. 0.476; entropy, 3.212 vs. 3.441; contrast, 10.773 vs. 13.596). Further, skewness and entropy were identified as independent predictors for extramural invasion of tumors (stage T3-4). Using a logistic regression model that factored skewness and entropy to differentiate T3-4 from T1-2 tumors, we achieved an area under the receiver-operating characteristic curve (AUC) of 0.743. Significant differences were observed between N0 and N1-2 tumors with respect to ADCmean (P=0.023), ADCmax (P=0.005) and entropy (P=0.015). ADCmax. and entropy were independent predictors of positive nodal status. An AUC of 0.750 was achieved by using this logistic model. In addition, ADCmean, skewness, entropy and contrast were significantly different among the overall stages (stage I, II, III and IV).

CONCLUSION

Texture analysis on ADC maps could provide valuable information in indentifying locally advanced rectal cancer.

CLINICAL RELEVANCE/APPLICATION

The findings might be help for the preoperative evaluatation of rectal cancer.

SSA07-05 Survival Prediction in Patients Treated by Folfiri and Bevacizumab using Contrast-enhanced CT

Texture Analysis: Ancillary Study of a Multicenter Prospective Study (PRODIGE 9)

Sunday, Nov. 27 11:25AM - 11:35AM Room: E353A

Participants Anthony Dohan, MD, Montreal, QC (Presenter) Nothing to Disclose Benoit P. Gallix, MD, PhD, Montpellier, France (Abstract Co-Author) Nothing to Disclose Caroline Reinhold, MD, MSc, Montreal, QC (Abstract Co-Author) Consultant, GlaxoSmithKline plc Philippe A. Soyer, MD, PhD, Paris, France (Abstract Co-Author) Consultant, Guerbet SA; Boris Guiu, MD, Dijon, France (Abstract Co-Author) Nothing to Disclose Karine Le Malicot, Dijon, France (Abstract Co-Author) Nothing to Disclose Jaafar Bennouna, MD, Saint-Herblain, France (Abstract Co-Author) Nothing to Disclose Francois Ghiringhelli, Dijon, France (Abstract Co-Author) Nothing to Disclose Valerie Boige, MD, PhD, Villejuif, France (Abstract Co-Author) Research Grant, Merck KGaA; Research Consultant, Bayer AG; Research Consultant, Merck KGaA Julien Taieb, MD, PhD, Paris, France (Abstract Co-Author) Nothing to Disclose Olivier Bouche, Reims, France (Abstract Co-Author) Nothing to Disclose Eric Francois, MD, Nice, France (Abstract Co-Author) Nothing to Disclose Jean-Marc Phelip, MD, Saint-Priest-En-Jarez, France (Abstract Co-Author) Nothing to Disclose Christian Borel, MD, Strasbourg, France (Abstract Co-Author) Nothing to Disclose Roger Faroux, MD, La Roche Sur Yon, France (Abstract Co-Author) Nothing to Disclose Jean-Francois Seitz, MD, Marseille, France (Abstract Co-Author) Nothing to Disclose Stephane Jacquot, MD, Montpellier, France (Abstract Co-Author) Nothing to Disclose Dominique Genet, MD, Limoges, France (Abstract Co-Author) Nothing to Disclose Jean-Louis Jouve, MD, Dijon, France (Abstract Co-Author) Nothing to Disclose Francoise Desseigne, MD, Lyon, France (Abstract Co-Author) Nothing to Disclose Come Lepage I, MD, PhD, Dijon, France (Abstract Co-Author) Nothing to Disclose Thomas Aparicio, MD, PhD, Bobigny, France (Abstract Co-Author) Nothing to Disclose Christine C. Hoeffel, MD, Reims, France (Abstract Co-Author) Nothing to Disclose

PURPOSE

To determine whether surface area (SA) measurement and texture analysis (TA) on pre-treatment and two months postchemotherapy computed tomography (CT) images can predict 2-year survival in patients with liver metastases from colo-rectal cancer (CRC) treated by Folfiri and bevacizumab.

METHOD AND MATERIALS

This is an ancillary study from PRODIGE-9 multicenter prospective study for which 494 patients with CRC metastatic to the liver and treated by Folfiri and bevacizumab had been enrolled. In 223 patients, TA was performed by two radiologists in consensus using TexRAD® software on the dominant liver lesion during the venous phase of a contrast-enhanced CT examination, at baseline and two months post-chemotherapy. Metastasis SA, TA parameters and their changes were correlated with the 2-year survival status. Receiver operating characteristic (ROC) curves were performed and the 4 strongest parameters were incorporated into a multivariate logistic regression model to identify predictive factors for 2-year survival and their odd-ratios(OR). A score combining these 4 factors was built and optimal cutoff values for predicting 2-year survival status was determined with ROC curve analysis. Survival was estimated with the Kaplan-Meier method and compared between groups with the log-rank test.

RESULTS

The strongest independent predictive factors for 2-year survival status were decrease in SA(AUC=.67;(.59-.74)), decrease in kurtosis value (ssf=0)(AUC=.54;(.56-.62)), the baseline mean value (ssf=0)(AUC=.64;(.56-.72)) and the baseline Mean Positive Pixels (MPP) value (ssf=0)(AUC=.63;(.56-.71)). Using multivariate analysis, predictive factors of 2-year survival status were the decrease in SA>44%(OR=2.6,P=.002), the decrease in kurtosis value (ssf=0)(OR=2.49,P=.030), baseline mean value (ssf=0)>62.27UH (OR=2.15,P=.39) and baseline MPP value (ssf=0)>67.05 UH,(OR=2.15,P=.11). A score ranging from 0 to 16 was built. AUC of the score for predicting 2-year survival was .72(.66-.79) with a sensitivity of 67% and specificity of 61% for a cutoff value of 7. Patients with a score>7 had a higher survival rate (P<.001).

CONCLUSION

SA and TA parameters on baseline and first evaluation CT may be able to predict which patient will have an increased survival in CRC with liver metastases treated by Folfiri and bevacizumab.

CLINICAL RELEVANCE/APPLICATION

TA performed on liver metastases from CRC treated by Folfiri and bevacizumab allows prediction of patients 2-year survival.

Honored Educators

Presenters or authors on this event have been recognized as RSNA Honored Educators for participating in multiple qualifying educational activities. Honored Educators are invested in furthering the profession of radiology by delivering high-quality educational content in their field of study. Learn how you can become an honored educator by visiting the website at: https://www.rsna.org/Honored-Educator-Award/

Caroline Reinhold, MD, MSc - 2013 Honored Educator Caroline Reinhold, MD, MSc - 2014 Honored Educator

SSA07-06 Using Quantitative Imaging Features of Colorectal Liver Metastases on Pre-Treatment CT to Predict Volumetric Response to Chemotherapy

Sunday, Nov. 27 11:35AM - 11:45AM Room: E353A

Participants

Hairong Chen, New York, NY (*Abstract Co-Author*) Nothing to Disclose John M. Creasy, MD, New York, NY (*Abstract Co-Author*) Nothing to Disclose Richard Kinh Gian Do, MD, PhD, New York, NY (*Presenter*) Nothing to Disclose Lauryn B. Adams, New York, NY (*Abstract Co-Author*) Nothing to Disclose Camilla Gomes, New York, NY (*Abstract Co-Author*) Nothing to Disclose Mithat Gonen, PhD, New York, NY (*Abstract Co-Author*) Nothing to Disclose Patrick Seastedt, MD, New York, NY (*Abstract Co-Author*) Nothing to Disclose Michael D'Angelica, MD, New York, NY (*Abstract Co-Author*) Nothing to Disclose Amber Simpson, New York, NY (*Abstract Co-Author*) Nothing to Disclose

PURPOSE

To investigates whether quantitative imaging features that measure tumor heterogeneity can be used to predict volumetric response in patients with colorectal liver metastases (CRLM).

METHOD AND MATERIALS

An IRB approved retrospective study included 103 patients from two prospective clinical trials on hepatic arterial infusion chemotherapy. Index tumors were extracted from contrast enhanced CT using Scout Liver (Pathfinder Technologies Inc., TN) at baseline and at 8 weeks follow-up. Volumetric response (as a percentage change) was assessed as a continuous variable. Imaging features (summary statistics including Hounsfield Unit -HU, texture, and shape properties) were extracted from index tumor volumes in the baseline CT scan using Matlab (Natick, MA). Imaging features statistically significant for volumetric response on univariate analysis were included in the regression model. The data were randomly split into training (n=93) and test sets (n=10). Random forest regression models were employed with cross validation on the training set. Test data were input into the trained regression models. Predicted accuracy of volumetric response was averaged over the models. Imaging features of CRLM in patients with partial response (PR) and stable disease (SD) defined by RECIST were also compared.

RESULTS

Predicted accuracy of volumetric response for CRLM after chemotherapy was 86.68% (CI: 85.35% - 88%). HU and the short run emphasis (SRE: a feature measuring consecutive pixels with the same intensity values) were the top two predictors of volumetric response. Mean HU values in PR were 91.2 (n=56) and 82.2 for SD (n=47), while SRE for PR was lower than the SD group (0.0864 vs. 0.098), suggesting that higher density and coarser grained image texture (more heterogeneity) may be related to better response. Increased heterogeneity reflects greater intravenous contrast uptake, which may translate to greater intake of chemotherapy within CRLM and subsequent volumetric response.

CONCLUSION

Quantitative imaging features extracted from pre-treatment CT are promising predictors of volumetric response to chemotherapy in patients with CRLM. External validation is required prior to using these novel imaging marker in a clinical setting.

CLINICAL RELEVANCE/APPLICATION

Pre-treatment prediction of response to chemotherapy using quantitative data from CT imaging has the potential to better select patients for chemotherapy.

SSA07-07 Correlation between Intravoxel Incoherent Motion (IVIM) and Dynamic Contrast-enhanced Magnetic Resonance Imaging (DCE-MRI) Parameters in Rectal Cancer

Sunday, Nov. 27 11:45AM - 11:55AM Room: E353A

Participants

Yanyan Xu, Beijing, China (*Presenter*) Nothing to Disclose Hongliang Sun, MD, Beijing, China (*Abstract Co-Author*) Nothing to Disclose Wu Wang, MD, PhD, Beijing, China (*Abstract Co-Author*) Nothing to Disclose Kaining Shi, PhD, Beijing, China (*Abstract Co-Author*) Nothing to Disclose

PURPOSE

To determine the correlation between intravoxel incoherent motion (IVIM) and multiphase dynamic contrast-enhanced magnetic resonance imaging (DCE-MRI) quantitative parameters in rectal cancer.

METHOD AND MATERIALS

Ninety-seven patients with histological diagnosis of rectal cancer were included in this study. All pelvis magnetic resonance imaging were performed in a 3.0T MR unit including diffusion-weighted imaging with 16 b-values (0, 10, 20, 30, 40, 60, 80, 100, 150, 200, 400, 800, 1000, 1200, 1500 and 2000s/mm2) and DCE-MRI(40 dynamic phases) as reference. IVIM perfusion-related parameters (f, perfusion fraction; D*, pseudo-diffusion coefficient; f·D*, the multiplication of the two parameters) were calculated by bi-exponential analysis. Quantitative parameters included Ktrans [transfer constant between blood plasma and extravascular extracellular space (EES)], Kep (rate between EES and blood plasma), Ve (extravascular Volume fraction), Vp (plasma volume fraction). DCE-MRI parameters were automatically calculated after region of interest (ROI) being selected along the outline of tumor maximal dimension (axial view), meanwhile relevant signal intensity (SI) time curves were obtained. Correlations between f and quantitative DCE-MRI parameters were respectively analyzed using Pearson's or Spearman's correlation coefficients, D* and f·D* were also similarly analyzed. Interobserver agreements were evaluated using the intraclass correlation coefficient (ICC) and Bland-Altman analysis.

RESULTS

There were 75 males and 22 females with a median age of 58.8 years (range, 26-85 years). Interobserver reproducibility for IVIM parameters, DCE-MRI semi-quantitative and quantitative parameters were good to excellent (ICC=0.9417-0.9618, ICC=0.7695-0.9905, ICC=0.7826-0.9488, respectively; narrow with of 95% limits of agreement). D* demonstrated significant correlations with Vp (r= -0.370; p<0.001), meanwhile, f·D* demonstrated significant correlations with TTP(r= -0.387; p=0.001). However, no correlation was observed between f and DCE-MRI quantitative parameters.

CONCLUSION

 $IVIM \ perfusion-related \ parameters, \ especially \ f\cdot D^*, \ demonstrated \ moderate \ correlations \ with \ DCE-MRI \ quantitative \ parameters \ in \ rectal \ cancer.$

CLINICAL RELEVANCE/APPLICATION

IVIM imaging parameters can be used as alternatives to DCE-MRI in reflecting the changes of rectal cancer perfusion in longitudinal monitoring treatment response.

SSA07-08 The Development and Validation of a CT-based Radiomics Signature for the Preoperative Discrimination of Stage I-II and State III-IV Colorectal Cancer

Sunday, Nov. 27 11:55AM - 12:05PM Room: E353A

Participants Yanqi Huang, Guangzhou, China (*Presenter*) Nothing to Disclose Zaiyi Liu, Guangzhou, China (*Abstract Co-Author*) Nothing to Disclose

PURPOSE

To investigative the predictive ability of radiomics signature based on CT image for the preoperative staging (I-II vs. III-IV) of primary colorectal cancer (CRC).

METHOD AND MATERIALS

The ethical-approved retrospective study consisted of 494 consecutive patients (training dataset: n=286; and validation cohort, n=208) with stage I–IV CRC. A radiomics signature was constructed based on the radiomics features extracted from CT images using LASSO logistic regression model. The potential association between the radiomics signature and CRC staging was explored. The classification performance of the radiomics signature was explored with respect to the receiver operating characteristics (ROC) curve, with accuracy, sensitivity and specificity obtained.

RESULTS

The developed 16-feature based radiomics signature was an independent predictor for the staging of CRC patients, which successfully discriminate stage I-II and stage III-IV CRC patients (p < 0.0001) in both the training and validation dataset. The median value of the radiomics signature of stage III-IV patients was significantly higher than that of the stage I-II patients. As for the classification performance of the radiomics signature in CRC staging, the yielded AUC was 0.792 (95%CI: 0.741-0.853), with a sensitivity of 0.667 and a specificity of 0.874. The validity of the signature in the validation dataset obtained an AUC of 0.708 (95%CI: 0.639-0.778), a sensitivity of 0.685, and a specificity of 0.690.

CONCLUSION

A radiomics signature was developed and validated to be a significant predictor for the discrimination of stage I-II from stage III-IV CRC, which may serve as a complementary tool for the preoperative tumor staging in CRC patients.

CLINICAL RELEVANCE/APPLICATION

The developed and validated radiomics signature could be used to discriminate stage I-II from stage III-IV CRC patients, which may serve as a noninvasive tool for the preoperative tumor staging in CRC patients.

SSA07-09 Can MRI Predict Recurrence in Patients with Locally Advanced Rectal Cancer?

Sunday, Nov. 27 12:05PM - 12:15PM Room: E353A

Awards

Student Travel Stipend Award

Participants Cinthia Cruz, MD, Boston, MA (*Presenter*) Nothing to Disclose Betsa Parsai Salehi, MD, Boston, MA (*Abstract Co-Author*) Nothing to Disclose James H. Thrall, MD, Boston, MA (*Abstract Co-Author*) Stockholder, Peregrine Pharmaceuticals, Inc; Stockholder, iBio, Inc; Stockholder, Antares Pharma, Inc; Speaker, Bracco Group; ; Mukesh G. Harisinghani, MD, Boston, MA (*Abstract Co-Author*) Nothing to Disclose

PURPOSE

Determine MRI findings in locally advanced rectal cancer that can be used as predictors of disease recurrence.

METHOD AND MATERIALS

Single center retrospective study. 152 potential consecutive subjects. Inclusion criteria: diagnosis of locally advanced rectal cancer(T3) between 2010-2015, neo-adjuvant therapy, radical surgery and availability of a baseline MR imaging scan and 1 year follow up pelvic MRI within our PACS (Picture Archiving and Communications System). Recurrence: abnormal follow-up MRI in the evaluated period. Scans were performed in a $1.5T(GE^{TM})$ or $3T(Siemens^{TM})$ clinical scanners, using the standard departmental rectal protocol. Scans were read by two radiologists blinded to outcomes. Recorded data: location (upper, mid or lower rectum or combination); transverse diameter of the tumor, length, shortest distance from the tumor to the mesorectal fascia (DMRF), lymphnode involvement (≥ 5) (LI), sphincter and extramural vessel involvement (EMV). Interobserver variability was evaluated. Fisher's exact and Z tests were applied.

RESULTS

Sixty-nine patients, 22 women, 47 men. Mean age 57.8 years(y). No gender difference in recurrence incidence. Recurrent(19/69 28%) versus non-recurrent(50/69 72%) tumors showed no significant differences in length, diameter, LI or EMV. Length 48.8:51.5mm (p>0.05), diameter 19.1:17.7mm(p>0.05), MRF 3.1:5.1mm (p=0.03), LI 9/19(47%):30/50(60%)(p=0.3), mid-lower rectum 14/19(74%): 21/50(42%) (p=0.01), sphincter involvement 9/19(47%):10/50(20%) (p=0.02) and EMV 2/19(10%):2/50(4%) (p>0.05). Tumors with DMRF <3.9mm(14/19, 74%) as well as those located in the mid-lower rectum(14/19, 74%), were highly associated with recurrence (p=0.01 and p=0.03, respectively). Mid-lower rectum involvement, MRF<4mm and sphincter involvement in combination (9/19(47%) vs 0/50(0) p=0.03), were highly associated with recurrence (OR=91, 95% CI:5 to 1695, p=0.002) demonstrating a sensitivity and specificity of 100% and 83%, respectively. Acceptable variation among readers ranged from 1.2-5.5%.

CONCLUSION

Mid-lower rectum involvement and MRF<4mm are highly associated with rectal cancer recurrence when found on 1 year follow-up MRI. In combination with sphincter involvement, such tumors demonstrated a 91-fold greater chance of recurring.

CLINICAL RELEVANCE/APPLICATION

MRI features and tumor location may be used to predict recurrence and markers of worst prognosis in locally advanced rectal cancer at 1-year-follow up scans.

Molecular Imaging (Cardiovascular/Nanoparticles)

Sunday, Nov. 27 10:45AM - 12:15PM Room: S504CD

MI

AMA PRA Category 1 Credits ™: 1.50 ARRT Category A+ Credits: 1.50

Participants

Markus Schwaiger, MD, Munich, Germany (*Moderator*) Research Grant, Siemens AG; Speaker, Siemens AG Jan Grimm, MD, PhD, New York, NY (*Moderator*) Nothing to Disclose

Sub-Events

SSA13-01 Accelerated Blood Clearance Phenomenon Reduces Passive Targeting of Nanoparticles in Peripheral Arterial Disease

Sunday, Nov. 27 10:45AM - 10:55AM Room: S504CD

Participants

Hyung-Jun Im, MD, Madison, WI (*Presenter*) Nothing to Disclose Christopher England, PhD, Madison, WI (*Abstract Co-Author*) Nothing to Disclose Reinier Hernandez, MSc, Madison, WI (*Abstract Co-Author*) Nothing to Disclose Steve Cho, MD, Madison, WI (*Abstract Co-Author*) Nothing to Disclose Robert J. Nickles, PhD, Madison, WI (*Abstract Co-Author*) Nothing to Disclose Dong Soo Lee, MD, Seoul, Korea, Republic Of (*Abstract Co-Author*) Nothing to Disclose Weibo Cai, PhD, Palo Alto, CA (*Abstract Co-Author*) Nothing to Disclose

PURPOSE

Accelerated blood clearance (ABC) phenomenon refers to loosing long circulating characteristics of polyethylene glycol (PEG) conjugated nanomaterials, when the nanomaterials are injected twice in the same animal. The phenomenon is of concern for in vivo imaging and drug delivery using nanomaterials, but has only been evaluated using lipid based or polymeric nanomaterials. We tested if ABC phenomenon occurs by long circulating hybrid nanoparticles, and if the phenomenon affects the passive targeting in the murine model of peripheral arterial disease (PAD).

METHOD AND MATERIALS

Hindlimb ischemia was induced by ligation and cut of the femoral artery. 64Cu labeled PEGylated reduced graphene oxide – iron oxide nanoparticles (64Cu-RGO-IONP-PEG) were prepared for imaging of PAD. At post-surgery day 3, 10, and 17, positron emission tomography (PET) was performed until 72 h after injection of the nanoparticles. At post-surgery day 10 and 17, non-injected mice were used for Naïve group, and the mice which were injected at post-surgery day 3 were used for Re-injection group. To confirm the existence of the integral nanoparticles in the liver tissues, photoacoustic (PA) imaging and Prussian blue staining of liver were performed.

RESULTS

At post-surgery day 3, the nanoparticles showed a long circulation time (> 30 h) and high accumulation in the ischemic hindlimb. At post-surgery day 10 and 17, Re-injection group showed significantly shorter circulation time and lower accumulation of the nanoparticles in the ischemic hindlimb than naïve group (Day 10: P < 0.001, Day 17: P < 0.001). Also, liver uptake was significantly higher in the Re-injection group (Day 10: P < 0.001, Day 17: P < 0.001). Also, liver uptake was significantly higher in the Re-injection group (Day 10: P < 0.001, Day 17: P < 0.05), indicating that the nanoparticles were cleared by the liver. Furthermore, increased PA signal in the liver and positive Prussian blue staining in the liver tissue confirmed the accumulation of the integral nanoparticles.

CONCLUSION

ABC phenomenon appeared when hybrid nanoparticles (64Cu-RGO-IONP-PEG) were re-injected. The phenomenon reduced efficiency of the passive targeting of the nanoparticles in the murine model of PAD.

CLINICAL RELEVANCE/APPLICATION

Our findings may be valuable information for future translational in vivo imaging and drug delivery applications using the long circulating nanoparticles in PAD.

SSA13-02 Re-assessing the Enhanced Permeability and Retention Effect in Peripheral Arterial Disease with 64Cu-labeled Long Circulating Nanoparticles

Sunday, Nov. 27 10:55AM - 11:05AM Room: S504CD

Participants

Christopher England, PhD, Madison, WI (*Presenter*) Nothing to Disclose Hyung-Jun Im, MD, Madison, WI (*Abstract Co-Author*) Nothing to Disclose Reinier Hernandez, MSc, Madison, WI (*Abstract Co-Author*) Nothing to Disclose Steve Cho, MD, Madison, WI (*Abstract Co-Author*) Nothing to Disclose Robert J. Nickles, PhD, Madison, WI (*Abstract Co-Author*) Nothing to Disclose Dong Soo Lee, MD, Seoul, Korea, Republic Of (*Abstract Co-Author*) Nothing to Disclose Weibo Cai, PhD, Palo Alto, CA (*Abstract Co-Author*) Nothing to Disclose

PURPOSE

It has been claimed that nanoparticles can passively accumulate in ischemic tissues through the enhanced permeability and retention (EPR) effect. As peripheral arterial disease (PAD) results in muscle ischemia and neovascularization, nanoparticle

accumulation may allow for molecular imaging of PAD. At this time, a quantitative evaluation of the passive targeting capabilities of nanoparticles has not been reported in PAD.

METHOD AND MATERIALS

Using a murine model of hindlimb ischemia, we quantitatively assessed the passive targeting capabilities of 64Cu-labeled PEGylated reduced graphene oxide – iron oxide nanoparticles (64Cu-RGO-IONP-PEG) through the EPR effect using positron emission tomography (PET) imaging. A surgical procedure recreated the conditions found in PAD patients, and as the ischemic hindlimb healed (15-20 days), blood flow was restored to normal in the diseased hindlimb. Serial laser Doppler imaging was performed to monitor changes in blood perfusion upon surgical induction of ischemia. In addition, photoacoustic imaging confirmed the accumulation of nanoparticles in ischemic tissues.

RESULTS

Nanoparticle accumulation was assessed at 3, 10, and 17 days post-surgery and found to be highest at 3 days post-surgery, with the ischemic hindlimb displaying an accumulation of 14.7 ± 0.5 percent injected dose per gram (%ID/g). Accumulation of 64Cu-RGO-IONP-PEG was lowest at 17 days post-surgery, with the ischemic hindlimb displaying only 5.1 ± 0.5 %ID/g. Furthermore, nanoparticle accumulation was confirmed by photoacoustic imaging (PA), showing increased PA signal in the ischemic hindlimb. The combination of PET and serial Doppler imaging showed that nanoparticle accumulation in the ischemic hindlimb negatively correlated with blood perfusion.

CONCLUSION

Thus, we quantitatively confirmed that 64Cu-RGO-IONP-PEG passively accumulated in ischemic tissue via the EPR effect, which is reduced as the perfusion normalizes. As 64Cu-RGO-IONP-PEG displayed substantial accumulation in the ischemic tissue, this nanoparticle platform may function as a future theranostic agent, providing both imaging and therapeutic applications.

CLINICAL RELEVANCE/APPLICATION

Nanoparticles passively accumulate in ischemic tissues via the EPR effect; thus, long circulating nanoparticles may be employed for drug delivery and therapeutic monitoring in ischemia-related diseases.

SSA13-03 High-Performance Upconversion Nanoprobes for Rats' MR Angiography Imaging

Sunday, Nov. 27 11:05AM - 11:15AM Room: S504CD

Participants

Jing Wang, Shanghai, China (*Presenter*) Nothing to Disclose Yue Wu, Shanghai, China (*Abstract Co-Author*) Nothing to Disclose Tianyong Xu, Shanghai, China (*Abstract Co-Author*) Nothing to Disclose Zhenwei Yao, Shanghai, China (*Abstract Co-Author*) Nothing to Disclose

PURPOSE

To address the low T1 relaxivity, short circulation time and high leakage rate of clinical used MR contrast agents which hindered the contrast enhanced MR angiography (MRA).

METHOD AND MATERIALS

Firstly, we synthesize UCNPs of core/shell structure (NaYF4:Yb/Er@NaGdF4) through a two-step pyrolysis process. Then, PEG was used to modify UCNPs. Cell Counting Kit-8 assay was used to test cytotoxicity using Murine macrophage cells (RAW264.7), Brain capillary endothelial cells (BCECs) and Buffalo rat liver cells (BRL). To investigate the amount of PEG-UCNPs and Magnevist leaking through the vessel walls, *in vitro* transwell assay was used with the transwell filters seeded with a compact BCECs monolayer. Relaxivities of PEG-UCNPs were measured using a 3.0 T MR scanner (Discovery MR 750, GE Medical Systems, Milwaukee, WI, USA). Healthy male SD rats (mean weight, 250 g) were used for *in vivo* MRA imaging. Time-resolved magnetic resonance imaging of contrast kinetics (TRICKS-MRA) was acquired in coronal view after the injection of CAs at a rate of 1 mL/s.

RESULTS

PEG-UCNPs were successfully synthesized with high monodispersity and stability (Figure a-c), which possess superior advantages over Magnevist, such as higher relaxivity (r1 = 12.01 mM-1s-1), longer circulation time (t1/2= 79.8 min), and lower leakage rate (Figure g), which guarantee better imaging efficiency. Cellular viabilities of all three types of cells are around 90% after 24 h of incubation with a relatively high concentration (1 mg/mL) of PEG-UCNPs (Figure d-f). The upconversion luminescence of PEG-UCNPs under 980 nm NIR excitation is observed in the cytoplasm of RAW264.7 cells after 4 h of co-incubation (Figure h). Remarkably, an extremely small dosage (5 mg Gd/kg) of PEG-UCNPs (Figure i) provides high-resolution MRA imaging with the vascular system delineated much clearer than the Magnevist with clinical dosage as high as 108 mg Gd/kg (Figure j).

CONCLUSION

In summary, the PEG-UCNPs with high T1 relaxivity have been proved as efficient MR CAs. The PEG-UCNPs can be used for MRA at a small dosage of 5 mg Gd/kg with the vascular system delineated much clearer than that using clinical MR CAs at clinical dosage.

CLINICAL RELEVANCE/APPLICATION

PEG-UCNPs are expected to be a promising candidate for substituting clinical Magnevist in MRA, which will significantly lengthen the imaging time window and improve the overall diagnostic efficiency.

SSA13-04 In Vivo Quantitative Dynamic Angiography with Gold Nanoparticles and Spectral Photon-Counting Computed Tomography K-Edge Imaging

Sunday, Nov. 27 11:15AM - 11:25AM Room: S504CD

Participants

Salim Si-Mohamed, Bron, France (*Presenter*) Nothing to Disclose David P. Cormode, DPhil, MS, Philadelphia, PA (*Abstract Co-Author*) Research Grant, Koninklijke Philips NV; Monica Sigovan, PhD, Lyon, France (*Abstract Co-Author*) Nothing to Disclose Daniel Bar-Ness, Bron, France (*Abstract Co-Author*) Nothing to Disclose Philippe Coulon, PhD, Suresnes, France (*Abstract Co-Author*) Employee, Koninklijke Philips NV Pratap Naha, PhD, Philadelphia, PA (*Abstract Co-Author*) Nothing to Disclose Jean-Baptiste Langlois, Bron, France (*Abstract Co-Author*) Nothing to Disclose Franck Lavenne, Bron, France (*Abstract Co-Author*) Nothing to Disclose Matthias Bartels, PhD, DIPLPHYS, Hamburg, Germany (*Abstract Co-Author*) Employee, Koninklijke Philips NV Bernhard Brendel, Hamburg, Germany (*Abstract Co-Author*) Researcher, Koninklijke Philips NV Heiner Daerr, DIPLPHYS, Hamburg, Germany (*Abstract Co-Author*) Employee, Koninklijke Philips NV Axel Thran, Hamburg, Germany (*Abstract Co-Author*) Employee, Koninklijke Philips NV Ewald Roessl, PhD, Hamburg, Germany (*Abstract Co-Author*) Employee, Koninklijke Philips NV Michal Rokni, PhD, Haifa, Israel (*Abstract Co-Author*) Employee, Koninklijke Philips NV Ira Blevis, Haifa, Israel (*Abstract Co-Author*) Employee, Koninklijke Philips NV Ira Blevis, Haifa, Israel (*Abstract Co-Author*) Employee, Koninklijke Philips NV Loic Boussel, MD, Lyon, France (*Abstract Co-Author*) Nothing to Disclose Philippe C. Douek, MD, PhD, Lyon, France (*Abstract Co-Author*) Nothing to Disclose

PURPOSE

To investigate the potential of spectral photon-counting computed tomography (SPCCT) in performing quantitative dynamic angiography with gold nanoparticles in order to obtain absolute quantification for arterial input function assessment.

METHOD AND MATERIALS

We used SPCCT with multiple energy bins (Philips Healthcare, Haifa, Israel), anode tube current of 100 mA, tube voltage of 120 kVp and gantry rotation time of 1 second. In vitro, imaging was first performed on a phantom containing a range of dilutions of gold nanoparticles (0 to 65 mg/mL) to validate the quantification of gold using K-edge data. In vivo, SPCCT was used to acquire at the level of the heart every 2 seconds over a period of 30 seconds starting 2 seconds after iv administration of 12 ml of 18 nm blood pool gold nanoparticles at 1 ml/s (dose 250 mg Au/kg) in two NZW rabbits, following approval by an ethics committee. Regions of interest were manually drawn in the thoracic vessels, the cardiac cavities, the myocardium and the pulmonary parenchyma for measuring gold concentration.

RESULTS

In vitro, phantom imaging showed that concentrations measured on the K-edge specific images correlated well with known concentrations (R2 = 0.98, slope = 1.02). In vivo, K-edge specific imaging of gold allowed the visualization of the blood compartment (thoracic vessels, cardiac cavities, myocardial and pulmonary perfusion) with the benefit of the removal of all other anatomical structures. Peak gold concentration decreased from 25.6 ± 0.8 mg/ml (right ventricle) to 17.1 ± 1.0 mg/ml and 16.7 ± 0.3 mg/ml (pulmonary artery, left ventricle) to 13.0 ± 0.9 mg/ml (aorta), 6.0 ± 0.7 mg/ml (myocardium) and 4.9 ± 0.9 mg/ml (lung). After 30 seconds, mean concentration (6.7 ± 0.4 mg/mL) was similar between all systemic vessels, with an early steady state in the myocardium at 3.6 ± 0.5 mg/mL during the last 16 seconds.

CONCLUSION

SPCCT allows specific quantification of blood pool gold nanoparticles concentration during first-pass dynamic angiography.

CLINICAL RELEVANCE/APPLICATION

Absolute quantification of contrast media is achievable by K-edge gold dynamic angiography for assessment of arterial input function for potential quantification of abnormal tissue perfusion

SSA13-05 Dynamic Positron Emission Tomography Imaging of Renal Clearable Gold Nanoparticles

Sunday, Nov. 27 11:25AM - 11:35AM Room: S504CD

Participants

Shreya Goel, Madison, WI (*Presenter*) Nothing to Disclose Feng Chen, PhD, Madison, WI (*Abstract Co-Author*) Nothing to Disclose Reinier Hernandez, MSc, Madison, WI (*Abstract Co-Author*) Nothing to Disclose Stephen Graves, Madison, WI (*Abstract Co-Author*) Nothing to Disclose Robert J. Nickles, PhD, Madison, WI (*Abstract Co-Author*) Nothing to Disclose Weibo Cai, PhD, Palo Alto, CA (*Abstract Co-Author*) Nothing to Disclose

PURPOSE

To study the dynamic distribution patterns of ultra-small gold (Au) nanoparticles by labeling them with coper-64 (64Cu, t1/2=12.7 h) and using dynamic positron emission tomography imaging (PET) imaging.

METHOD AND MATERIALS

Glutathione (GSH)-capped ultra-small Au nanoparticles (Au-GSH) were synthesized by reacting gold(III) chloride trihydrate (HAuCl4·3H2O) with reduced glutathione in a 90 °C water bath for 35 min followed by conjugation of NOTA (a chelator for labeling 64Cu). 64CuCl2 diluted in of 0.1 M sodium acetate buffer (pH 6.5) was reacted with NOTA-Au-GSH at 37 °C for 30 min. For PET imaging, healthy BALB/c mice were injected with 5-10 MBq of 64Cu-NOTA-Au-GSH intravenously. For PET/CT imaging, a mixture of 64Cu-NOTA-Au-GSH (hot) and NOTA-Au-GSH (cold) was used. A 60-min dynamic scan was performed and framed into 46 frames. Image reconstruction, and region of interest (ROI) analysis of the PET data were then performed.

RESULTS

Au-GSH with a hydrodynamic (HD) size of 2.5 ± 0.1 nm was synthesized. The dynamic light scattering measurement showed slightly increased HD to 2.6 ± 0.1 nm after NOTA conjugation. The labeling yield of 64Cu to NOTA-Au-GSH was estimated to be over 90% within 30 min. Serum stability study showed a high radio-stability with <5% of 64Cu being detached after 24 h incubation. Systematic characterization demonstrated efficient renal clearance of nanoparticles with >75 %ID 64Cu-NOTA-Au-GSH being cleared at 24 h post-injection. The majority of 64Cu-NOTA-Au-GSH was found in mouse kidney and liver with their uptake measured to be 1.69 \pm 0.54 and 0.33 \pm 0.22 %ID/g at 24 h post-injection, respectively. Dynamic PET imaging provided more accurate information regarding the rapid clearance kinetics of nanoparticles in organs, such as heart, kidneys and liver. The elimination half-life of 64Cu-NOTA-Au-GSH was calculated to be less than 6 min.

CONCLUSION

In conclusion, the dynamic PET imaging of 64Cu-NOTA-Au-GSH addresses the current challenges in accurate and noninvasive iamging of the organ kinetics, and provides a highly useful tool for studying renal clearance mechanism of other ultra-small nanoparticles, as well as the diagnosis of kidney diseases in the future.

CLINICAL RELEVANCE/APPLICATION

The study provides a highly useful tool for studying renal clearance mechanism of other ultra-small nanoparticles, as well as the diagnosis of kidney diseases in the future.

SSA13-06 In Vivo Quantification of Gold Nanoparticles Biodistribution Kinetics with Spectral Photon-Counting Computed Tomography K-Edge Imaging

Sunday, Nov. 27 11:35AM - 11:45AM Room: S504CD

Participants

David P. Cormode, DPhil, MS, Philadelphia, PA (Abstract Co-Author) Research Grant, Koninklijke Philips NV; Salim Si-Mohamed, Bron, France (Presenter) Nothing to Disclose Daniel Bar-Ness, Bron, France (Abstract Co-Author) Nothing to Disclose Monica Sigovan, PhD, Lyon, France (Abstract Co-Author) Nothing to Disclose Caroline Bouillot, Bron, France (Abstract Co-Author) Nothing to Disclose Pratap Naha, PhD, Philadelphia, PA (Abstract Co-Author) Nothing to Disclose Franck Lavenne, Bron, France (Abstract Co-Author) Nothing to Disclose Philippe Coulon, PhD, Suresnes, France (Abstract Co-Author) Employee, Koninklijke Philips NV Matthias Bartels, PhD, DIPLPHYS, Hamburg, Germany (Abstract Co-Author) Employee, Koninklijke Philips NV Bernhard Brendel, Hamburg, Germany (Abstract Co-Author) Researcher, Koninklijke Philips NV Heiner Daerr, DIPLPHYS, Hambrg, Germany (Abstract Co-Author) Employee, Koninklijke Philips NV Axel Thran, Hamburg, Germany (Abstract Co-Author) Employee, Koninklijke Philips NV Ewald Roessl, PhD, Hamburg, Germany (Abstract Co-Author) Employee, Koninklijke Philips NV Michal Rokni, PhD, Haifa, Israel (Abstract Co-Author) Employee, Koninklijke Philips NV Ira Blevis, Haifa, Israel (Abstract Co-Author) Employee, Koninklijke Philips NV Loic Boussel, MD, Lyon, France (Abstract Co-Author) Nothing to Disclose Philippe C. Douek, MD, PhD, Lyon, France (Abstract Co-Author) Nothing to Disclose

PURPOSE

To study the capabilities of spectral photon-counting computed tomography (SPCCT) to quantify the organ biodistribution kinetics of gold nanoparticles in vivo.

METHOD AND MATERIALS

Imaging was performed with SPCCT with multiple energy bins (Philips Healthcare, Haifa, Israel), anode tube current of 100 mA, tube voltage of 120 kVp and gantry rotation time of 1 second, first on a phantom containing a range of dilutions of gold nanoparticles (0 to 65 mg/mL, 18 nm) to validate the quantification of gold using K-edge data. In vivo imaging was then performed on 3 NZW rabbits, following approval by an ethics committee. The rabbits were iv injected with gold nanoparticles (250 mg Au/kg). The aorta, liver, spleen, kidneys and bone marrow were imaged before and after injection at different time points from 30 seconds to 30 min, one week and one month. Regions of interest (ROIs) were manually drawn in the organs on K-edge specific images to measure gold concentrations.

RESULTS

Phantom imaging showed that concentrations measured on the K-edge specific images correlated well with known concentrations (R2 = 0.98, slope = 1.02). In vivo, gold K-edge specific images showed differential temporal uptake between organs: gold nanoparticles remained at high concentrations in blood up to the 30 min post injection $(4.9\pm0.5 \text{ mg/mL})$ and decreased at 1 week $(1.8\pm0.6 \text{ mg/mL})$ to same value at 1 month $(1.9\pm0.5 \text{ mg/mL})$. Two concentration peaks were observed for liver and spleen, one related to the vascular phase $(3.1\pm0.6 \text{ mg/mL})$ and $4.3\pm0.5 \text{ mg/mL}$ at 2 min) and one related to tissue uptake that increased from 30 min $(2.7\pm0.5 \text{ mg/mL})$ and $4.1\pm0.3 \text{ mg/mL})$ to similar values at 1 week $(5.61\pm0.61 \text{ mg/mL})$ and $5.6\pm0.5 \text{ mg/mL})$ and 1 month $(5.9\pm0.6 \text{ mg/mL})$ and $5.4\pm0.3 \text{ mg/mL})$. Compared to liver and spleen, bone marrow showed slower uptake in the early phase (<30 min, 2.2\pm0.9 \text{ mg/mL}) and similar values at 1 week and 1 month.

CONCLUSION

SPCCT is capable of assessing distribution of gold nanoparticles and quantitative in-vivo imaging of pharmacokinetics in organs over time.

CLINICAL RELEVANCE/APPLICATION

SPCCT may result in clinically applicable imaging protocols for specific detection, and assessment of biodistribution and quantification of contrast media.

SSA13-07 Lisinopril-functionalized near Infrared Fluorescent (NIRF) Nanoparticles for Molecular Imaging of Angiotension-converting Enzyme (ACE) Expression

Sunday, Nov. 27 11:45AM - 11:55AM Room: S504CD

Participants

Stefan Harmsen, PhD, New York, NY (*Abstract Co-Author*) Nothing to Disclose Jason Gardenier, New York, NY (*Abstract Co-Author*) Nothing to Disclose Ilker Medine, New York, NY (*Abstract Co-Author*) Nothing to Disclose Raghu P. Kataru, New York, NY (*Abstract Co-Author*) Nothing to Disclose Gabriela Garcia Nores, New York, NY (*Abstract Co-Author*) Nothing to Disclose Thorsten R. Fleiter, MD, Baltimore, MD (*Abstract Co-Author*) Nothing to Disclose Oguz Akin, MD, New York, NY (*Abstract Co-Author*) Nothing to Disclose Mehrara Babak, New York, NY (*Abstract Co-Author*) Nothing to Disclose Omer Aras, MD, New York, NY (Presenter) Nothing to Disclose

PURPOSE

Optical imaging is a highly sensitive modality that provides multiscale imaging capabilities. Here we demonstrate the an application of NIRF nanoparticles for molecular imaging of ACE expression.

METHOD AND MATERIALS

NIRF nanoparticles were synthesized by a modified Stöber reaction in the presence of silane-functionalized dye. The as-synthesized NIRF nanoparticles were functionalized with thiol-groups, which were used to conjugate a lisinopril-modified linker to the NIRF nanoparticles yielding to yield the ACE-targeted NIRF nanoparticles. NIRF nanoparticles dispersions were characterized by transmission electron microscopy (TEM), nanoparticle tracking analysis (NTA), and NIRF imaging. The ACE-targeted NIRF ($\lambda ex=800$ nm) and control NIRF nanoparticles ($\lambda ex=700$ nm) were evaluated in vivo in wild-type mice (N=5) and molecular images were obtained by differential imaging of ACE-targeted NIRF and control-NIRF nanoparticles on the Odyssey small animal fluorescent imaging system.

RESULTS

Both the ACE-targeted and control NIRF nanoparticles were narrowly dispersed with a mean hydrodynamic diameter of 100 nm. The limit of detection for both nanoparticles was 100 fM. Wild type animals injected with 100 uL 25 nM mixture of ACE-targeted and control NIRF nanoparticles (1:1). The next day, the organs were excised and imaged ex vivo at λ ex=700nm and 800 nm. While the control NIRF nanoparticles demonstrated typical nanoparticle pharmacokinetics with high accumulation in organs of the mononuclear phagocytic system such as liver and spleen, the ACE-targeted NIRF nanoparticles accumulated in the lungs as well, which express high levels of ACE relative to other organs. To enable ACE-specific molecular imaging, a differential image was generated by subtracting the control NIRF nanoparticle signal from the ACE-targeted NIRF nanoparticle signal.

CONCLUSION

Highly specific molecular imaging of ACE was achieved by differential NIRF imaging of control and ACE-targeted NIRF nanoparticles in wild type animals.

CLINICAL RELEVANCE/APPLICATION

The Lisinopril conjugated NIRF particles have the potential to simultaneously enhance optical imaging contrast and facilitate tissue ACE tracking in the number of different disease processes.

SSA13-08 Molecular Imaging of Atherosclerosis using A Combined Magnetic Resonance and MALDI Imaging Approach

Sunday, Nov. 27 11:55AM - 12:05PM Room: S504CD

Awards

Student Travel Stipend Award

Participants

Fabian Lohoefer, MD, Munich, Germany (*Presenter*) Nothing to Disclose Almut Glinzer, Munich, Germany (*Abstract Co-Author*) Nothing to Disclose Laura Hoffmann, Munich, Germany (*Abstract Co-Author*) Nothing to Disclose Franz Schilling, Munchen, Germany (*Abstract Co-Author*) Nothing to Disclose Ernst J. Rummeny, MD, Munich, Germany (*Abstract Co-Author*) Nothing to Disclose Moritz Wildgruber, MD, PhD, Muenchen, Germany (*Abstract Co-Author*) Nothing to Disclose

PURPOSE

Evaluation of Gadofluorine P enhanced molecular magnetic resonance imaging (MRI) in a mouse model of atherosclerosis by Matrix Assisted Laser Desorption Ionization (MALDI) Imaging

METHOD AND MATERIALS

In this longitudinal study low density lipoprotein receptor deficient mice (LDLr-/-) were fed a Western Type diet. After 4, 8 and 16 weeks mice were imaged by high-field 7 Tesla MRI after injection of Gadofluorine P at a dosage of 0.1mmol/kg body weight. Age matched C57BL/6 mice on a chow diet were used as control group. Imaging planes were planned in line with the aortic arch. Vessel wall contrast enhancement was assessed by Late Gadolinium Enhancement (LGE) and quantified by T1-mapping. T1/R1 values were calculated from T1 maps based on a Look-Locker sequence. T1 images were calculated from source images based on a 3-parameter Levenberg-Marquardt curve fitting procedure with a correction for read-out-induced attenuation of the relaxation curve. Mice from each time point were sacrificed after completion of imaging. The aortic arch was further processed for immunohistochemistry and MALDI-IMS. Tissue slices were cut in line with the aortic arch accordingly to in vivo MRI. MALDI-IMS was performed for quantification of Gadofluorine P ex vivo.

RESULTS

R1 values in atherosclerotic plaques located in the aortic root peaked 30min after Gadofluorine P injection. A kinetic study showed that R1 values of the vessel wall returned to baseline levels after \sim 5h.R1 values in the aortic root in LDLr-/- mice were significantly higher compared to the control group. Contrast enhancement of the vessel wall increased over the time period of the high fat diet. Gadofluorine P accumulation in the atherosclerotic plaque and increase over the time of the high fat diet was confirmed by MALDI-IMS ex vivo.

CONCLUSION

Gadofluorine P enhanced MR imaging allows capturing of plaques even at early stages of atherosclerosis in mice. T1 mapping at high field strength allows semi-quantitative assessment of contrast agent accumulation in plaques in vivo, which can be further evaluated by ex vivo MALDI imaging.

CLINICAL RELEVANCE/APPLICATION

SSA13-09 Assessment and Precise Quantification of Post-Infarction Scar Remodeling using a Combined Molecular Magnetic Resonance and MALDI Imaging Approach

Sunday, Nov. 27 12:05PM - 12:15PM Room: S504CD

Participants

Fabian Lohoefer, MD, Munich, Germany (*Presenter*) Nothing to Disclose Laura Hoffmann, Munich, Germany (*Abstract Co-Author*) Nothing to Disclose Almut Glinzer, Munich, Germany (*Abstract Co-Author*) Nothing to Disclose Katja Kosanke, Muenchen, Germany (*Abstract Co-Author*) Nothing to Disclose Franz Schilling, Munchen, Germany (*Abstract Co-Author*) Nothing to Disclose Ernst J. Rummeny, MD, Munich, Germany (*Abstract Co-Author*) Nothing to Disclose Moritz Wildgruber, MD, PhD, Muenchen, Germany (*Abstract Co-Author*) Nothing to Disclose

PURPOSE

The aim of this study is to evaluate molecular magnetic resonance imaging (MRI) combined with Matrix assisted laser desorption ionization (MALDI) imaging approach using a collagen-targeted contrast agent to analyze and quantify mechanisms of myocardial remodeling and scar formation in a murine myocardial infarction model.

METHOD AND MATERIALS

In-vivo accumulation of Gadofluorine P, targeting collagen, tenascin and proteglycans within the infarct scar, was investigated in a mouse model of myocardial infarction. C57BL/6J mice were scanned by in-vivo MRI at 7 Tesla 1 and 6 weeks after coronary artery ligation. Gadofluorine P was injected at a dose of 0.1mmol/kg body weight and compared to conventional Gd-DTPA. Contrast enhancement of infarcted myocardium was assessed using Late Gadolinium Enhancement (LGE) and T1 mapping. T1/R1 values were calculated from T1 maps based on a Look-Locker sequence. T1 images were calculated from source images based on a 3-parameter Levenberg-Marquardt curve fitting procedure with a correction for read-out-induced attenuation of the relaxation curve. Cardiac function parameters were assessed by volumetric analysis based on short axis views in CINE sequences. Mice from each time point were sacrificed after completion of imaging. The heart was removed and further processed for immunohistochemistry and matrix-assisted laser desorption ionization imaging (MALDI) to quantify Gadofluorine P accumulation ex-vivo.

RESULTS

R1 values in myocardial infarction peaked 15min after Gadofluorine P injection. A slow linear decrease was seen over a time period of 1h. R1 values in vivo in infarcted myocardium were significantly higher 6 weeks after myocardial infarction compared to 1 week. This was confirmed by MALDI-IMS ex vivo. Gadofluorine P accumulation showed a positive correlation with the ejection fraction of the heart.

CONCLUSION

MR imaging using collagen-targeted Gadofluorine P allows capturing of extracellular matrix components in remodeling and scar formation after myocardial infarction. T1 mapping at high field strength enables a more precise quantification of signal enhancement which can be further evaluated and fully quantified by MALDI Imaging.

CLINICAL RELEVANCE/APPLICATION

Preclinical animal study

Molecular Imaging Sunday Poster Discussions

Sunday, Nov. 27 12:30PM - 1:00PM Room: S503AB

MI

AMA PRA Category 1 Credit [™]: .50

FDA Discussions may include off-label uses.

Participants

Steven P. Rowe, MD, PhD , Parkville, MD (Moderator) Nothing to Disclose

Sub-Events

MI201-SD-SUA2 Comparison Analysis of the Tumor Response to Chemotherapy using Diffusion Weighted Imaging and Hyperpolarized 13C MRSI

Station #2

Participants

Young-Suk Choi, Seoul, Korea, Republic Of (*Abstract Co-Author*) Nothing to Disclose Eun-Kyung Wang, Seoul, Korea, Republic Of (*Abstract Co-Author*) Nothing to Disclose Han-Sol Lee, Seoul, Korea, Republic Of (*Abstract Co-Author*) Nothing to Disclose Dong-Hyun Kim, PhD, Seoul, Korea, Republic Of (*Abstract Co-Author*) Nothing to Disclose Ho-Taek Song, MD, Seoul, Korea, Republic Of (*Presenter*) Nothing to Disclose

PURPOSE

To validate the reduction of exchange flux of hyperpolarized [1-13C]pyruvate to lactate after chemotherapy correlated with diffusion weighted imaging technique and hitopatholgy.

METHOD AND MATERIALS

We performed hyperpolarized [1-13C]pyruvate magnetic resonance spectroscopy and imaging after doxorubicin treatment comparison with diffusion weighted MRI (DWI) in orthotropic hepatocellular carcinoma mouse model. 1x10^6 HuH7 cells in PBS were injected into the median liver lobe in Balb/C nude mouse. 6mg/kg of doxorubicin was administrated once by i.p injection. Therapeutic efficacy was evaluate by three imaging techniques: 1) conventional T2W MRI to measure tumor volume, 2) diffusion weighted MR imaging for apparent diffusion coefficient mapping, and 3) hyperpolarized [1-13C]pyruvate MRSI to measure the flux of metabolism. According to the lapse of time, it performed at pre-treatment, post day 3, and post day 6.

RESULTS

From the ratio analysis of area under the curve of hyperpolarized [1-13C] MRSI, HCC showed remarkably higher conversion ratio from pyruvate to lactate than normal liver tissue. In the early response phase, tumor volumes showed 3.24 fold increases, metabolic flux shows 0.95 fold decreases, and ADC values did not show difference. In the late response phase, tumor volume shows 5.6 fold increases, metabolic flux showed 0.66 fold decrease, and ADC value of tumor showed no significant change. In vehicle treated group, increased in the flux and decreased in the ADC values were significant. In doxorubicin treated group, decrease in the flux was not significant and increase in the ACD was significant.

CONCLUSION

In this hepatocellular carcinoma model, the decrease of hyperpolarized [1-13C]lactate flux did not correlated with increase in ADC values. hyperpolarized [1-13C]pyruvate MRSI probably quantitate the viable cells in the tumor resistant to chemotherapy.

CLINICAL RELEVANCE/APPLICATION

Although ADC values of diffusion weighted image represent cellularity of tumor or even status of apotosis, the actual tumor viability was not reflected properly. Hyperpolarized [1-13]pyruvate MRSI could be a robust diagnostic metabolic imaging tool to evaluate the tumor viability to evaluate the therapeutic efficacy in clinic.

MI202-SD- [I-123] Ioflupane Study in Parkinsonian Patients: Utility of Putamen to Caudate Ratio SUA3

Station #3

Participants

Manuela C. Matesan, MD, PhD, Seattle, WA (*Presenter*) Nothing to Disclose Santhosh Gaddikeri, MD, Seattle, WA (*Abstract Co-Author*) Nothing to Disclose Katelan H. Longfellow, MD, Seattle, WA (*Abstract Co-Author*) Nothing to Disclose Robert Miyaoka, PhD, Seattle, WA (*Abstract Co-Author*) Nothing to Disclose Saeed Elojeimy, MD, PhD, Seattle, WA (*Abstract Co-Author*) Nothing to Disclose Shana Elman, MD, Seattle, WA (*Abstract Co-Author*) Nothing to Disclose Shu-Ching Hu, Seattle, WA (*Abstract Co-Author*) Nothing to Disclose David H. Lewis, MD, Seattle, WA (*Abstract Co-Author*) Research funded, Eli Lilly and Company Satoshi Minoshima, MD, PhD, Salt Lake City, UT (*Abstract Co-Author*) Royalties, General Electric Company; Research Consultant, Hamamatsu Photonics KK; Research Grant, Hitachi, Ltd; Research Grant, Nihon Medi-Physics Co, Ltd;

PURPOSE

Value of semi-quantitative analysis of [I-123]ioflupane uptake has been suggested in Parkinsonian patients. We hypothesized that PCR may not be suitable for evaluation of disease progression when both caudate and putamen are involved.

We retrospectively reviewed medical records of 32 patients (26 male, average age = 68 yrs) with a clinical diagnosis of Parkinson disease (PD) (n=22) or Parkinson-plus syndrome (PPS) (n=10; including 5 multisystem atrophy, 3 progressive supranuclear palsy, 1 corticobasal degeneration, & 1 non-specified) based on clinical follow- up by a movement disorder specialist. All subjects included in this study had a positive Datscan image by visual interpretation. Brain imaging was performed 4 hours after intravenous injection of 3-5 mCi [I-123]ioflupane using SPECT-CT acquisition. Images were reconstructed using filtered back projection and no attenuation correction was used. Semi-quantitative evaluation using Datquant was performed. We assessed the utility of PCR less than 0.7 as a diagnostic marker of nigrostriatal degeneration in the PD and PPS groups which were further stratified based on their caudate-to-background ratio (CBR) values into mild (CBR>2) and severe disease (CBR <2).

RESULTS

PCR for both hemispheres ranged from 0.58-0.91, with 24 patients (75%) having PCR above 0.7. In the group with mild disease CBR>2 (n=8; mean 2.65 \pm 0.81) mean PCR value was 0.79 \pm 0.087 (87.5% patients > 0.7) and in the group with advanced disease CBR <2 (n=24; mean 1.1467 \pm 0.353) the mean PCR value was 0.75 \pm 0.09 (70.83% patients >0.7). In PD group (mean CBR: 1.5593 \pm 0.879), the mean PCR was 0.75 \pm 0.09 (72.72 % patients >0.7) and in PSS group (mean CBR: 1.445 \pm 0.73) the mean PCR was 0.77 \pm 0.10 (80 % patients >0.7).

CONCLUSION

These findings suggest that PCR ratio may not be a reliable numeric marker in interpretation of [I-123]ioflupane studies, mainly in advanced disease, likely due to decreased both putamen and caudate [I-123]ioflupane uptake.

CLINICAL RELEVANCE/APPLICATION

Although other parameters like caudate to background binding ratio have a role in supporting Datscan visual interpretation, the putamen- to- caudate ratio (PCR) must be interpreted with caution especially in advanced cases of nigrostriatal degeneration when both caudate and putamen have decreased uptake.

MI203-SD-SUA4 Using a Long Circulating Blood Pool Tracer to Perform Multi-patch MPI for Whole Body Imaging of a Mice

Station #4

Participants

Caroline Jung, Hamburg, Germany (*Presenter*) Nothing to Disclose Johannes M. Salamon, MD, Hamburg, Germany (*Abstract Co-Author*) Nothing to Disclose Patryk Szwargulski, Hamburg, Germany (*Abstract Co-Author*) Nothing to Disclose Michael G. Kaul, Hamburg, Germany (*Abstract Co-Author*) Nothing to Disclose Gerhard B. Adam, MD, Hamburg, Germany (*Abstract Co-Author*) Nothing to Disclose Tobias Knopp, DIPLENG, Hamburg, Germany (*Abstract Co-Author*) Nothing to Disclose Kannan M. Krishnan, Seattle, WA (*Abstract Co-Author*) Nothing to Disclose Matthew Ferguson, Seattle, WA (*Abstract Co-Author*) Nothing to Disclose Harald Ittrich, MD, Hamburg, Germany (*Abstract Co-Author*) Nothing to Disclose

PURPOSE

Magnetic particle imaging (MPI) is a new imaging technology that allows the direct quantitative mapping of the spatial distribution of superparamagnetic iron oxide nanoparticles (SPIO). The aim of the study was to perform multi-patch MPI using LS-008 as long circulating blood tracer to achieve mice whole body imaging in a high spatial resolution.

METHOD AND MATERIALS

MPI Scans of FVB mice (n=4) were carried out using a 3D imaging sequence (2.5 T/m gradient strength, 14mT drive-field strength, FoV 22.4x22.4x11.2 mm3). Ten minutes after the injection of 60µl of LS-008 via the tailvein six different drive-field patches (two cranial, two middle and two caudal) each taking 1.5 min were performed. As MPI delivers no anatomic information, MRI scans at 7T ClinScan (Bruker) were performed before MPI examination using a T2-weighted 2D turbo spin echo sequence. Fiducial markers were used to enable MRI/MPI image fusion. Image reconstruction was performed offline using a custom reconstruction framework developed in the programming language Julia using the join formulation.

RESULTS

The combined MRI/MPI measurements were carried out successfully. The reconstruction of the drive-field patches generated no artifacts at the margins resulting in a whole mice body MP imaging. Compared to previous experiments that we carried out using a gradient strength of 1.5 T/m the multi-patch method with an increased gradient strength of 2.5 T/m resulted in a higher spatial resolution. Therefore we were able not only to visualize the inferior vena cava, the heart and the liver but also the cerebral vessels, liver venes, the thoracic aorta and the kidneys.

CONCLUSION

In vivo whole body imaging of mice using multi-patch MPI is feasible. The long circulating blood tracer LS-008 enabled us to visualize the whole mice.

CLINICAL RELEVANCE/APPLICATION

The presented technique may offer a strong tool for fast and radiation free whole body angiography.

MI103-ED-SUA5 Peptide Receptor Radionuclide Therapy (PRRT) of Medullary and Non-Medullary Thyroid Cancer Using Radiolabeled Somatostatin Analogs: A New Paradigm

Station #5

Participants

Ali Salavati, MD, MPH, Philadelphia, PA (*Presenter*) Nothing to Disclose Ameya D. Puranik, MBBS, Mumbai, India (*Abstract Co-Author*) Nothing to Disclose Hendra Budiawan, MD, Bad Berka, Germany (*Abstract Co-Author*) Nothing to Disclose Harshad R. Kulkarni, MBBS, MSc, Bad Berka, Germany (*Abstract Co-Author*) Nothing to Disclose Richard P. Baum, MD, PhD, Bad Berka, Germany (*Abstract Co-Author*) Stockholder, OctreoPharm Sciences GmbH; Research Consultant, Novartis AG; Research Consultant, Ipsen SA; Research Grant, ITG-Medical, Inc

TEACHING POINTS

1) To discuss the role of peptide receptor radionuclide therapy (PRRT) using 177Lu-/90Y-labeled somatostatin analogs in the management of medullary and non-medullary thyroid cancers. 2) To review the application of 68Ga-labeled somatostatin analogs PET/CT imaging in the management of somatostatin receptors (SSTR) expressing thyroid tumors.

TABLE OF CONTENTS/OUTLINE

Therapeutic options in advanced medullary and non-iodine-avid differentiated (non-medullary) thyroid cancers are limited and associated with significant toxicity. Theranostic (therapy and diagnosis) using radiolabeled somatostatin analogs have proved to be a promising alternative in the management of somatostatin receptors (SSTR) expressing tumors. In this educational exhibit, we will review the molecular basis and clinical application of peptide receptor radionuclide therapy (PRRT) using 177Lu-/90Y-labeled somatostatin analogs in the management of medullary and non-medullary thyroid cancer patients. In addition, the role of 68Ga-labeled somatostatin analogs PET/CT on the management of somatostatin receptors (SSTR) expressing thyroid tumors will be discussed.

Molecular Imaging Sunday Poster Discussions

Sunday, Nov. 27 1:00PM - 1:30PM Room: S503AB

MI

AMA PRA Category 1 Credit ™: .50

FDA Discussions may include off-label uses.

Participants

Steven P. Rowe, MD, PhD , Parkville, MD (Moderator) Nothing to Disclose

Sub-Events

MI204-SD-SUB1 The Synthesis of avß3 and EGFR Targeted SPECT/MRI Probe and its Application in the Diagnosis of Lung Cancer

Station #1

Participants Jiali Cai, Shanghai, China (*Presenter*) Nothing to Disclose Zhetao Liu, Shanghai, China (*Abstract Co-Author*) Nothing to Disclose Shiyuan Liu, PhD, Shanghai, China (*Abstract Co-Author*) Nothing to Disclose

PURPOSE

In this study, we constructed three dual-modality SPECT/MRI iron oxide nanoparticles probe which simultaneously target to $\alpha\nu\beta3$ receptors in tumor angiogenesis and EGFR on non-small cell lung cancer.

METHOD AND MATERIALS

The PEG coated USPIO surface was directly conjugated with peptide c(RGDfK) and GE11.We demonstrated the specificity of the probe to $\alpha\nu\beta3$ integrin and EGFR with Prussian blue staining and quantitative analysis of Fe contents in vitro. In vitro cytotoxicity testing was performed with three probes for 12, 24 and 48 hour with three concentrations. Blood clearance and biodistribution of these probes show excellent biocompatibility. T2-weighted MR and small-animal SPECT/CT imaging were acquired in a H1299 cell xenografted lung cancer model.

RESULTS

USPIOs were synthesized via the polyol method. The resulting 4.8 nm nanoparticles have low r2/r1 of 3.88 (r1 =15.2 mM-1·s-1, r2 = 59.09 mM-1·s-1). On this basis, USPIOs were used as carrier and were applied to conjugate targeting peptide RGD, GE11 and label 99mTc nuclide. The radiochemical purity of 99mTc labeled nanoparticle > 92%, radioactive stability > 95%. The results of Prussian blue staining indicated that three probes can target to H1299 cells, while the dual-targeting probe RGD-GE11@USPIO had better targeting performance than those of the single-targeting probes. The same results were verified in the Fe contents in each cell.MRI showed three probes can specifically target to tumor and decreased the MR signal intensity. SPECT images showed particles mainly gathered in liver and kidney indicated that the particles were metabolized by urine and faeces. The qualitative and quantitative analysis of SPECT/MRI images kept in good concordance, and suggested that tumor accumulation of dual-targeting probe was more efficient and the most accumulation culminated at 6 hour post injection. Histological studies revealed that $\alpha\gamma\beta$ 3 integrin and EGFR were expressed on H1299 tumor cells.

CONCLUSION

In this study, 99mTc-RGD-GE11@USPIO has higher specificity and sensitivity for detectingav β 3 integrin and EGFR-expressing H1299 lung cancer cells and xenografted tumor models. The dual-modal probe can be diagnosis for the specific imaging of lung cancer.

CLINICAL RELEVANCE/APPLICATION

Animal procedures were carried out according to a protocol approved by the Institutional Animal Care and Use Committee at Second Military Medical University, Shanghai, China.

MI205-SD- Molecular BLI/CT-imaging Reveals Local IFN-ß induction in the Heart in a Murine Model of Acute Viral SUB2 Myocarditis

Station #2

Participants

Wolfgang Koestner, Hannover, Germany (*Presenter*) Nothing to Disclose Vanessa Herder, Hannover, Germany (*Abstract Co-Author*) Nothing to Disclose Claudia N. Detje, Hannover, Germany (*Abstract Co-Author*) Nothing to Disclose Martijn Langereis, UTRECHT, Netherlands (*Abstract Co-Author*) Nothing to Disclose Stefan Lienenklaus, Hanover, Germany (*Abstract Co-Author*) Nothing to Disclose Wolfgang Baumgartner, Hannover, Germany (*Abstract Co-Author*) Nothing to Disclose Frank K. Wacker, MD, Hannover, Germany (*Abstract Co-Author*) Nothing to Disclose Frank K. Wacker, MD, Hannover, Germany (*Abstract Co-Author*) Research Grant, Siemens AG; Research Grant, Pro Medicus Limited; Research Grant, Delcath Systems, Inc; Ulrich Kalinke, Hannover, Germany (*Abstract Co-Author*) Nothing to Disclose

PURPOSE

The differentiation of acute, chronic, viral and autoimmune etiology of myocarditis is essential for the choice of treatment. However, non-invasive diagnostics are lacking. We hypothesized that molecular imaging of IFN- β induction can be used as a biomarker to determine etiology of myocarditis. Furthermore, the impact of host- and virus-associated factors on pathogenesis was investigated.

METHOD AND MATERIALS

To preferentially direct Coxsackie-virus B3 (CVB-3) infection to the heart muscle, mice with a myocyte-specific IFNAR-ablation were generated (α -MHC*cre/wt*-IFNARf//fl). IFNAR-/-, IFN- β -/- and WT-C57BL/6 mice were used as controls. Spatio temporal distribution of IFN- β induction p.i. was assessed by BLI/CT in IFN- β luciferase reporter mice (IFN- $\beta \Delta \beta$ -luc). To investigate the impact of host-associated factors, reporter mice on two different backgrounds, C57BL/6 and BALB/C, as well as male versus female mice were analyzed. For virus-associated factors different infection doses and different viral variants were studied. Furthermore, IFNAR-/-IFN- $\beta \Delta \beta$ -luc mice and α -MHC*cre/wt*-IFNARf//fl-IFN- $\beta \Delta \beta$ -luc mice were evaluated.

RESULTS

Following CVB-3 infection IFNAR-/-IFN- $\beta \Delta \beta$ -luc mice succumbed within 2 to 3 days. Prior to death, a significant BLI signal was detected in the liver of these mice. Signal strength was reduced in IFNARwt/wt-IFN- $\beta \Delta \beta$ -luc-C57BL/6 mice. Other significant BLI-signals were observed in cervical and abdominal lymph nodes. In the heart, a weak BLI signal was observed at d7 p.i.. Signal strength was enhanced in a-MHCcre/wt-IFN- $\beta \Delta \beta$ -luc mice. In addition, these mice developed severe myocarditis and died upon CVB-3 infection within 7 days, whereas C57BL/6 mice showed mild myocarditis and survived. In contrast, IFN- β -/- mice died around day 40 post infection and displayed interstitial fibrosis within the myocardium. Thus, BLI-signal distribution and strength varied depending on host- and virus-associated factors.

CONCLUSION

BLI/CT imaging was used to visualize IFN- β induction in liver, lymph nodes and heart *in vivo* after CVB-3 infection. Signal strength and spatiotemporal distribution of BLI-signals were identified as relevant biomarkers. BLI/CT-imaging revealed local IFN- β induction in the heart during acute viral myocarditis.

CLINICAL RELEVANCE/APPLICATION

In patients with myocarditis molecular imaging might help to define more homogeneous patient cohorts for the initiation of clinical studies.

MI206-SD- Diffusion Kurtosis Imaging of Human Nasopharyngeal Carcinoma Xenografts: Initial Experience with SUB3 Pathological Correlation

Station #3

Participants

Jing Zhong, Fuzhou, China (*Presenter*) Nothing to Disclose Chen Yunbin, MD, Fuzhou, China (*Abstract Co-Author*) Nothing to Disclose Peng Shi, Fuzhou, China (*Abstract Co-Author*) Nothing to Disclose Dechun Zheng, MS, Fuzhou, China (*Abstract Co-Author*) Nothing to Disclose Xiang Zheng, MS, Fuzhou, China (*Abstract Co-Author*) Nothing to Disclose

PURPOSE

The aim of this study was to investigate the relationship between the diffusion kurtosis imaging (DKI) related parameters and pathological measures using human nasopharyngeal carcinoma (NPC) xenografts in nude mice model.

METHOD AND MATERIALS

24 BALB/c-nu nude mice were divided into two groups which were injected with two different nasopharyngeal squamous cell carcinoma cell lines (CNE1 and CNE2). Mice were sacrificed when the tumor max diameter exceed 1.5cm after MR scanning. The DK MR imaging was performed on a 3 Tesla MR scanner. DKI related parameters-mean diffusivity (MD) and mean kurtosis (MK) were measured. Tumors were then processed for Hematoaylin and Eosin staining. The pathological images were analyzed using computer-aided pixel-wise clustering method to evaluate tumor cellularity, extracellular space portion, cytoplasm portion and ratio of nuclei to cytoplasm (N/C ratio). The relationship between DKI related parameters and pathological features were analyzed statistically.

RESULTS

The mean MD of CNE1 xenograft (2.19±0.39) was higher than CNE2 group (1.76±0.48, p<0.05), but the mean MK between the two groups has no significant difference (CNE1 0.55±0.14 and CNE2 0.47±0.23, p>0.05). The spearmen test showed that the MD values were significantly correlated with cell cytoplasm portion and extracellular space portion (rs=0.370, p<0.05, rs=-0.435, p<0.05). The MK values were significantly correlated with cell cytoplasm portion and N/C ratio (rs=0,528, p<0.01, rs=0.627, p<0.001). Both MD and MK values were not significantly correlated with tumor cellularity.

CONCLUSION

In the xenografted NPC model, the MD values were significantly correlated with cell cytoplasm portion and extracellular space portion, when the MK value were correlated with cell cytoplasm portion and N/C ratio. The DKI imaging might be utilized as surrogate biomarker for noninvasive assessment of tumor micro-structure.

CLINICAL RELEVANCE/APPLICATION

The preliminary animal results suggest that DKI findings could provide valuable information for NPC micro-characterization.

MI207-SD-SUB4 Bio-Imaging of Unstable Plaques Using Thrombus Targeted Nano-polymers in Severe Hypercholesterolemia

Station #4

Participants Kye S. Kim, MD, Boston, MA (*Presenter*) Nothing to Disclose Peter Kang, MD, Boston, MA (*Abstract Co-Author*) Nothing to Disclose

PURPOSE

Atheromatous plaques are prone to rupture, resulting in plaque hemorrhage. This can result in recurrent ischemic events, such as myocardial infarction and stroke that have been recognized as the top culprits associated with the highest mortality and morbidity,

respectively in U.S. This improving strategies to deal with these conditions are important. In this study, we developed a novel polymer based delivery system to effectively image these unstable plaques by thrombus targeted approach.

METHOD AND MATERIALS

For animal model of unstable plaques, the mice having homozygous knock-in mutations of the HDL receptor (scavenger receptor, class B, type I(SRBI)) and the mice having homozygous null mutations in the apolipoprotein E(ApoE) gene were mated to create SRBI/ApoE double KI/KO mice that exhibited severe hypercholesterolemia and cardinal features of ischemic disease. The polymer-based micelles were generated through hydrophilic-hydrophobic interacting lipid polymers and pluronic F-127. A pentapeptide, CREKA(H-Cys-Arg-Glu-Lys-Ala-OH), shown a high affinity to fibrinogen-fibrin complex, was covalently bonded to the micelle. For thrombus targeted imaging, we loaded the micelles with indocyanine green(ICG), a near-infrared fluorophore with peak absorption at ~800 nm.

RESULTS

We found that the SRBI/ApoE double KI/KO mice exhibited significantly increased atherosclerosis and plaque hemorrhage compared to WT, single ApoEKO or single SRBI KI mice throughout the vascular system, including aorta, carotid and coronary arteries. Cardiac output was significantly decreased in double KI/KO mice(~29% SRBI/ApoEKI/KO compared to ApoE only, p<0.01). Double KI/KO mice also exhibited histologic evidences of early myocardial infarction at 6-7 weeks. These mice started to die within 7 weeks of age and by 12-13 weeks, there were over 90% mortality due to infarctions and heart failure.

CONCLUSION

The novel polymer micelle-based bio-imaging system using thrombus targeting may be used for non-invasive targeted imaging of unstable plaques.

CLINICAL RELEVANCE/APPLICATION

This research could be useful in developing thrombus targeted theranostic system to diagnose and treat unstable plaques in myocardial infarction and stroke.

MI104-ED-SUB5 Evolution in Functional Imaging of Prostate Cancer-Role of PSMA PET/CT: The Pathophysiology, Normal Distribution and Clinical Utility of 68Ga-PSMA PET/CT in Prostate Cancer

Station #5

Awards Certificate of Merit

Participants Venkatesh Rangarajan, MBBS, Mumbai, India (*Presenter*) Nothing to Disclose Archi Agrawal, MBBS, Mumbai, India (*Abstract Co-Author*) Nothing to Disclose Nilendu C. Purandare, DMRD, Mumbai, India (*Abstract Co-Author*) Nothing to Disclose Sneha A. Shah, Mumbai, India (*Abstract Co-Author*) Nothing to Disclose Nilesh Sable, Mumbai, India (*Abstract Co-Author*) Nothing to Disclose

TEACHING POINTS

PSMA PET/CT is a useful imaging tool for identification of the primary tumor, nodal and skeletal metastases in prostate cancer. It has higher sensitivity for nodal disease as it can detect metastases in tiny sub centimetre sized nodes. It helps in assessment of response in skeletal metastases unlike bone scintigraphy. It helps in detection of tiny recurrences at the primary site and nodal metastases in patients with biochemical relapse.

It is a one-stop-shop imaging for staging and restaging of prostate cancer.

TABLE OF CONTENTS/OUTLINE

Advantages of 68Ga-PSMA PET/CT in evaluation of prostate cancer over conventional imaging modalities. Pathophysiology and imaging findings in diagnosis, staging, restaging and in response assessment will be discussed. The spectrum of imaging findings for detection of primary, nodal, visceral and skeletal metastases will be described. The potential pitfalls of 68Ga-PSMA PET/CT imaging.

Imaging of Atherosclerosis

Sunday, Nov. 27 2:00PM - 3:30PM Room: E352

CA VA CT MI MR

AMA PRA Category 1 Credits ™: 1.50 ARRT Category A+ Credits: 1.50

FDA Discussions may include off-label uses.

Participants

John J. Carr, MD, MS, Nashville, TN (Moderator) Nothing to Disclose

Sub-Events

RC103A The Biology of Atherosclerosis

Participants

Pamela K. Woodard, MD, Saint Louis, MO, (woodardp@mir.wustl.edu) (*Presenter*) Research Grant, Astellas Group; Research Grant, Bayer AG; Research agreement, Siemens AG; ; ; ; ;

LEARNING OBJECTIVES

1) Discuss the initiation of the atherosclerotic disease process, including chemical, mechanical and immunological factors. 2) Discuss the molecular biology of atherosclerosis and cellular mechanisms involved in plaque remodeling, progression, instability and repair. 3) Discuss potential molecular targets in atherosclerosis imaging.

ABSTRACT

RC103B Molecular Imaging of Atherosclerosis

Participants

Zahi A. Fayad, PhD, New York, NY, (zahi.fayad@mssm.edu) (Presenter) Nothing to Disclose

LEARNING OBJECTIVES

1) Define Nanomedicine and its opportunity in cardiovascular disease detection and treatment. 2) Demonstrate the methods of plaque molecular imaging with MR Imaging, PET, CT. 3) Discuss the advantages and limitations of plaque molecular imaging using MR Imaging, PET, CT. 4) Discuss the preclinical and clinical relevance of plaque molecular imaging by MR Imaging, PET, CT. 5) Discuss novel methods for atherosclerotic plaque treatment using nanomedicine.

ABSTRACT

Atherosclerosis is a chronic progressive disease, affecting the medium and large arteries, in which lipid-triggered inflammation plays a pivotal role. The major clinical manifestations of atherosclerosis are coronary artery disease (CAD), leading to acute myocardial infarction (MI) and sudden cardiac death; cerebrovascular disease, leading to stroke; and peripheral arterial disease, leading to ischemic limbs and viscera. These complications of atherosclerosis are leading causes of death worldwide. Despite progress in medical and revascularization therapies for atherothrombotic disease, the incidence of MI and stroke remain high under the current standard of care, and the past decade has generated few new medical therapies to prevent atherosclerosis-induced events. Similarly, current diagnostic approaches to atherosclerosis do not accurately identify those individuals who will suffer an ischemic complication. The field of atherosclerosis is therefore ripe for reengineering in both the therapeutic and diagnostic arenas. Research into the process of atheroma lesion development and maturation has implicated many immune cells including lymphocytes, dendritic cells, and neutrophils. The most numerous cells in atherosclerotic plaque are macrophages, which are leukocytes that are central to the innate immunity. Because they play a major role in instigating plaque development and complication-both of which are inflammation-related disease processes-leukocytes are promising targets for more effective atherosclerosis treatments. However, the complexity of the immune system and its role as a defensive force against infection require novel tools to very precisely identify and treat the inflammatory cells that promote atherosclerosis. Biomedical engineering offers unique possibilities for diagnosing and treating atherosclerotic plaque inflammation. Thus, interfacing engineering with immunology will be essential to meaningful advances in disease management. This talk will discuss how recent discoveries in atherosclerosis immunology can provide opportunities for diagnostic imaging of atherosclerotic plaques and cardiovascular complications of atherosclerosis, including translatable molecular imaging techniques. Integrated diagnostic modalities have uncovered new pathways that can serve as potential diagnostic and therapeutic targets, and show hat these pathways can be specifically modulated by nanomedicine based interventions.

RC103C MR Imaging of Atherosclerosis

Participants Chun Yuan, PhD, Seattle, WA (*Presenter*) Research Grant, Koninklijke Philips NV; ;

LEARNING OBJECTIVES

1) Identify the clinical goals of MRI of atherosclerosis, describe the critical information needed for different vascular beds. 2) Explain the technical need and challenges in imaging atherosclerosis. 3) Assess current approaches and applications and future directions.

ABSTRACT

RC103D CT Imaging of Atherosclerosis

Participants Pal Maurovich-Horvat, MD, PhD, Pecs, Hungary (*Presenter*) Nothing to Disclose

Molecular Imaging Monday Case of the Day

Monday, Nov. 28 7:00AM - 11:59PM Room: Case of Day, Learning Center

MI

AMA PRA Category 1 Credit ™: .50

Participants

Jonathan E. McConathy, MD, PhD, Birmingham, AL (Presenter) Research Consultant, Eli Lilly and Company; Research Consultant, Blue Earth Diagnostics Ltd; Research Consultant, Siemens AG; Research Consultant, General Electric Company; Suzanne E. Lapi, PhD, Birmingham, AL (Presenter) Research Grant, AbbVie Inc; Spouse, Consultant, General Electric Company; Consultant, Siemens AG; Consultant, Blue Earth Diagnostics Ltd; Consultant, Eli Lilly and Company Matthias J. Eiber, MD, Muenchen, Germany (Abstract Co-Author) Nothing to Disclose Thomas A. Hope, MD, San Francisco, CA (Abstract Co-Author) Research Grant, Consultant, GE Healtcare Robert R. Flavell, MD, PhD, San Francisco, CA (Abstract Co-Author) Nothing to Disclose Samuel J. Galgano, MD, Birmingham, AL (Abstract Co-Author) Nothing to Disclose Asim K. Bag, MD, Birmingham, AL (Abstract Co-Author) Nothing to Disclose David M. Schuster, MD, Atlanta, GA (Abstract Co-Author) Institutional Research Grant, Nihon Medi-Physics Co, Ltd; Institutional Research Grant, Blue Earth Diagnostics Ltd; Consultant, WellPoint, Inc; ; Ephraim E. Parent, MD, PhD, Saint Louis, MO (Abstract Co-Author) Nothing to Disclose Bital Savir-Baruch, MD, Maywood, IL (Abstract Co-Author) Nothing to Disclose Pamela K. Woodard, MD, Saint Louis, MO (Abstract Co-Author) Research Grant, Astellas Group; Research Grant, Bayer AG; Research agreement, Siemens AG; ; ; ; Sebastian R. McWilliams, MBBCh, Saint Louis, MO (Abstract Co-Author) Nothing to Disclose Amir K. Durrani, MD, St Louis, MO (Abstract Co-Author) Nothing to Disclose Robert J. Gropler, MD, Saint Louis, MO (Abstract Co-Author) Nothing to Disclose

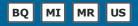
Michael Hofman, PhD, San Francisco, CA (Abstract Co-Author) Nothing to Disclose

TEACHING POINTS

1) Interpret amyloid-PET scans as positive or negative. 2) Apply appropriate use criteria for selecting patients for amyloid-PET study. 3) Understand the goals of the IDEAS study as it relates to coverage with evidence development for clinical amyloid-PET scans.

Molecular Imaging Symposium: Basics of Molecular Imaging

Monday, Nov. 28 8:30AM - 10:00AM Room: S405AB



AMA PRA Category 1 Credits ™: 1.50 ARRT Category A+ Credits: 1.50

FDA Discussions may include off-label uses.

Participants

Jan Grimm, MD, PhD, New York, NY (*Moderator*) Nothing to Disclose Zaver M. Bhujwalla, PhD, Baltimore, MD (*Moderator*) Nothing to Disclose

Sub-Events

MSMI21A MI Using Radioactive Tracers

Participants

Jan Grimm, MD, PhD, New York, NY (Presenter) Nothing to Disclose

LEARNING OBJECTIVES

1) In this course, we will discuss the various radio tracers and their applications in Molecular Imaging studies. Participants will understand in which situations to use which radio tracers, what to consider when developing the imaging construct and what controls to obtain for nuclear imaging studies. Examples will contain imaging with small molecules, with antibodies and nanoparticles as well as with cells in order to provide the participants with examples how o correctly perform their imaging studies. Most of the examples will be from the oncology field but their underlying principles are universally applicable to other areas as well.

ABSTRACT

Nuclear Imaging is currently the only true "molecular" imaging method utilized in clinic. It offers quantitative imaging of biological processes in vivo. Therefore, it is not surprising that it is also highly frequented in preclinical imaging applications since it is currently the only true quantitative imaging method. Multiple agents have been developed, predominantly for PET imaging but also for SPECT imaging.In this talk, we will discuss the application of radio tracers to molecular imaging and what to consider. Common pitfalls and mistakes as well as required measures to avoid these will be discussed. We will discuss various examples of imaging constructs, ranging from small molecules to antibodies, nanoparticles and even cells. In addition, the imaging modalities will also briefly discussed, including PET, SPECT and Cherenkov imaging.

MSMI21B Molecular MRI and MRS

Participants

Zaver M. Bhujwalla, PhD, Baltimore, MD (Presenter) Nothing to Disclose

LEARNING OBJECTIVES

1) To define the role of MRI and MRS in molecular and functional imaging and cover specific applications in disease processes. 2) The primary focus will be advances in novel theranostic approaches for precision medicine.

ABSTRACT

With an array of functional imaging capabilities, magnetic resonance imaging (MRI) and spectroscopy (MRS) techniques are valuable in obtaining functional information, but the sensitivity of detection is limited to the 0.1-1 mM range for contrast agents and metabolites, respectively. Nevertheless, MRI and MRS are finding important applications in providing wide-ranging capabilities to tackle key questions in cancer and other diseases with a 'molecular-functional' approach. An overview of these capabilities and examples of MR molecular and functional imaging applications will be presented with a focus on theranostic imaging for precision medicine.

MSMI21C Nanoparticles

Participants Heike E. Daldrup-Link, MD, Palo Alto, CA, (heiked@stanford.edu) (*Presenter*) Nothing to Disclose

LEARNING OBJECTIVES

1) Understand important safety aspects of USPIO. 2) Recognize the value of immediately clinically applicable iron oxide nanoparticles for tumor MR imaging applications. 3) Learn about intrinsic immune-modulating therapeutic effects of USPIO.

ABSTRACT

NanoparticlesNanoscale materials can be employed to develop novel platforms for understanding, diagnosing, and treating diseases. Integrating nanomedicine with novel multi-modality imaging technologies spurs the development of new personalized diagnostic tests and theranostic (combined diagnostic and therapeutic) procedures. This presentation will provide an overview over the safety, diagnostic applications and therapeutic implications of clinically applicable ultrasmall superparamagnetic iron oxide nanoparticles (USPIO). USPIO which are currently used for clinical applications include ferumoxytol (Feraheme), an FDA-approved iron supplement, and ferumoxtran-10 (Combidex/Sinerem), which is currently undergoing renewed clinical trials in Europe. Safety considerations for these agents will be discussed. Since USPIO are not associated with any risk of nephrogenic sclerosis, they can be used as alternative contrast agents to gadolinium chelates in patients with renal insufficiency or in patients in whom creatinine lab values are not available. Both ferumoxytol and ferumoxtran-10 provide long lasting blood pool enhancement, which can be used for MR angiographies and tissue perfusion studies. Subsequently, USPIO are slowly phagocytosed by macrophages in the reticuloendothelial system (RES), which can be used to improve MRI detection of tumors in liver, spleen, lymph nodes and bone marrow. A slow phagocytosis by tumor associated macrophages (TAM) in the tumor microenvironment can be used to grade tumor-associated inflammation and monitor the efficacy of new cancer immunotherapies. This opens opportunities for new discoveries in the area of cancer immunology and immunotherapy. TAM imaging concepts could represent a significant breakthrough for clinicians as a new means for risk stratification and as a new gold-standard imaging test for tracking treatment response in TAM-directed immunotherapy trials, which are currently entering clinical applications.

MSMI21D Contrast Ultrasound

Participants

Steven B. Feinstein, MD, Chicago, IL (*Presenter*) Research support, General Electric Company; Consultant, General Electric Company;

LEARNING OBJECTIVES

1) Inform: Clinical utility and safety of contrast enhanced ultrasound (CEUS) imaging. 2) Educate: Current diagnostic and therapeutic approaches. 3) Introduce: Newer concepts for combined diagnostic and therapeutic applications.

ABSTRACT

Contrast-Enhanced Ultrasound (CEUS) provides a novel, multi-faceted approach to diagnostic imaging and localized drug/gene delivery systems. The value-added proposition of CEUS centers on the pillars of safety, effectiveness, and economics. Specifically, in the field of diagnostic imaging, 3D CEUS ultrasound technology challenges the established formats CT, MR, and PET. CEUS provides distinct advantages including real-time volumetric imaging, unparalleled spatial and temporal resolution, economies of scale and all without exposure to unnecessary, ionizing radiation. Our efforts to develop 3D and contrast-enhanced ultrasound imaging continues to provide academic leadership while advancing the clinical field of cardiovascular medicine, urology (prostate imaging), and cancer (monitoring and therapy). In the evolving field of the ultrasound therapeutics, CEUS provides a novel, localized delivery system for ethical drugs and nucleic acids; all effectively delivered without viral-mediated agents. Further, the global installed base of ultrasound along with the safety record and ease of patient access highlights the utility of CEUS as a truly competitive, therapeutic delivery modality.In April 1, 2016, the USA FDA approved CEUS for liver imaging in adults and children. This is likely to have a major, paradigm chage in healthcare in the USA.

MSMI21E Quantitative Imaging Biomarkers

Participants

Richard L. Wahl, MD, Saint Louis, MO (Presenter) Consultant, Nihon Medi-Physics Co, Ltd;

LEARNING OBJECTIVES

1) Identify at least one method of quantitatively assessing anatomic tumor response . 2) Identify at least one method of quantitatively assessing metabolic tumor response using FDG PET . 3) Identify an MRI quantitative metric which is associated with cellularity of biological processes and which can be used in response assessments.

ABSTRACT

Radiology initially developed as an analog imaging method in which non quantitative data were interpreted in a "qualitative and subjective" manner. This approach has worked well, but modern imaging also is digital, quantitative and has the opportunity for more quantitative and objective interpretations. This lecture will focus on a few areas in which quantitative imaging is augmenting qualitative image assessments to lead to more precise interpretation of images. Examples of such an approach can include measuremental of tumor "metabolic" activity using formalisms such as PERCIST 1.0; methods of assessment of tumor size and volumes using the RECIST 1.1 and emerging formalisms and metrics of tumor heterogeneity, density, receptor density, diffusion, vascular permeability and elasticity using techniques incuding PET/SPECT, MRI, CT and ultrasound. With quantitative imaging, the opportunity to move from qualitative methods to precise in vivo quantitative pheontyping is a real one, with a quantitative "phenome" complementing other "omics" such as genomics. However, the quality of quantitation may vary and close attention to technical methodologies and process are required to have reliable and accurate quantitation. The RSNA QIBA effort will be briefly reviewed as one approach to achieve precise quantiative phenotyping. Examples of the use of quantitative phenotyping to inform patient management will be discussed.

Honored Educators

Presenters or authors on this event have been recognized as RSNA Honored Educators for participating in multiple qualifying educational activities. Honored Educators are invested in furthering the profession of radiology by delivering high-quality educational content in their field of study. Learn how you can become an honored educator by visiting the website at: https://www.rsna.org/Honored-Educator-Award/

Richard L. Wahl, MD - 2013 Honored Educator

BOOST: CNS-Oncologic Anatomy and Contouring Review: Emphasis on Molecular Markers and Role of MR/PET Imaging (An Interactive Session)

Monday, Nov. 28 8:30AM - 10:00AM Room: S103CD



AMA PRA Category 1 Credits ™: 1.50 ARRT Category A+ Credits: 1.50

Participants

Rajan Jain, MD, Hartsdale, NY (*Presenter*) Consultant, Cancer Panels; Royalties, Thieme Medical Publishers, Inc Michael D. Chan, MD, Winston-Salem, NC (*Presenter*) Advisory Board, NovoCure Ltd Christina I. Tsien, MD, Saint Louis, MO (*Presenter*) Speaker, Merck & Co, Inc

LEARNING OBJECTIVES

1) Describe how to differentiate gliomas from lymphoma, metastases as well as non-neoplastic etiologies such as demyelinating lesions: Role of functional imaging modalities. 2) Describe imaging characteristics of gliomas based on genomic differences: Imaging phenotype genotype correlation. 3) Advanced imaging techniques as a surveillance tool in post-therapy gliomas with emphasis on genomic markers.

ABSTRACT

Recent advances in glioma genomics have significantly changed our understanding of tumor biology and hence, affected how these patients are treated. Similarly, integrating imaging data with genomic markers has also helped create better prognostic and predictive biomarkers which offer promising future for personalized medicine. This session will highlight a multi-disciplinary approach with the focus on advanced imaging and genomics markers before and after therapy in gliomas.

OI

Molecular Imaging Symposium: Oncologic MI Applications

Monday, Nov. 28 10:30AM - 12:00PM Room: S405AB

MI AMA PRA Category 1 Credits ™: 1.50 ARRT Category A+ Credits: 1.50

FDA Discussions may include off-label uses.

Participants

Peter L. Choyke, MD, Rockville, MD, (pchoyke@nih.gov) (Moderator) Researcher, Koninklijke Philips NV; Researcher, General Electric Company; Researcher, Siemens AG; Researcher, iCAD, Inc; Researcher, Aspyrian Therapeutics, Inc; Researcher, ImaginAb, Inc; Researcher, Aura Biosciences, Inc

Umar Mahmood, MD, PhD, Charlestown, MA (Moderator) Research Grant, Sabik Medical Inc; Advisory Board, Blue Earth Diagnostics Ltd;

LEARNING OBJECTIVES

1) To understand the role of molecular imaging in cancer therapy. 2) To understand the impact that new molecular imaging agents could have on drug development. 3) To understand the barriers facing the development of new molecular imaging agents.

ABSTRACT

Molecular Imaging is expanding in many new directions. Most research is being performed for PET and SPECT agents. However, optical and MRI agents are also being developed. Molecular Imaging can play a role in accelerating the development and approval of new cancer therapeutics by quantifying the impact drugs have in early Phase studies and by selecting the most appropriate patients for trials. Molecular Imaging agents can be useful in determining the utility and mechanism of actions of drugs that are already approved and may provide insights to oncologists regarding the best treatment combinations for individual patients. Molecular Imaging methods have already expanded our knowledge of cancer behavior and this will ultimately lead to new forms of the therapy that will one day cure this dreaded disease.

Sub-Events

MSMI22A Hyperpolarized MRI of Prostate Cancer

Participants

Daniel B. Vigneron, PhD, San Francisco, CA (Presenter) Research Grant, General Electric Company; Research Grant, GlaxoSmithKline

LEARNING OBJECTIVES

View learning objectives under main course title.

MSMI22B Somatastatin Receptor Imaging

Participants Ronald C. Walker, MD, Nashville, TN (Presenter) Nothing to Disclose

LEARNING OBJECTIVES

1) Describe the advantages of 68Ga-somatostatin PET/CT over 111In-DTPA-octreotide]imaging. 2) Detect patients likely to benefit from peptide receptor radiotherapy (PRRT).

ABSTRACT

68Ga-labeled somatostatin analogs (DOTATATE, DOTATOC and DOTANOC) PET/CT imaging provides higher resolution scans than 111In-DTPA-octreotide with less radiation, comparable cost, and imaging completion within 2 hours vs. 2-3 days. 68Gasomatostatin analogs have a higher impact on care than 111In-DTPA-octreotide, including superior ability to identify patients likely to benefit from PRRT. This activity will provide results from the literature and the author's experience to illustrate the advantages of 68Ga-based PET/CT imaging of neuroendocrine tumors.

Active Handout:Ronald Clark Walker

http://abstract.rsna.org/uploads/2016/15003715/ACTIVE MSMI22B.pdf

MSMI22C Multimodal MI in Oncology

Participants

Umar Mahmood, MD, PhD, Charlestown, MA (Presenter) Research Grant, Sabik Medical Inc; Advisory Board, Blue Earth Diagnostics Ltd;

LEARNING OBJECTIVES

1) To understand strengths of various imaging modalities for specific target/disease assessment.

ABSTRACT

Each imaging modality has a set of characteristics that helps define optimal use. These constraints include sensitivity, depth of imaging, integration time for signal, and radiation dose, among other factors. Understanding when each modality can be used and when combining the relative strengths of differerent modalities can be synergistic allows greater molecular information to be

acquired.

MSMI22D Radiogenomics

Participants Michael D. Kuo, MD, Los Angeles, CA (*Presenter*) Nothing to Disclose

LEARNING OBJECTIVES

1) To discuss the principles behind radgiogenomics and to highlight areas of clinical application and future development.

ABSTRACT

MSMI22E Overview of MI in Oncology

Participants

Peter L. Choyke, MD, Rockville, MD, (pchoyke@nih.gov) (*Presenter*) Researcher, Koninklijke Philips NV; Researcher, General Electric Company; Researcher, Siemens AG; Researcher, iCAD, Inc; Researcher, Aspyrian Therapeutics, Inc; Researcher, ImaginAb, Inc; Researcher, Aura Biosciences, Inc

LEARNING OBJECTIVES

1) To understand the broad spectrum of activities in molecular imaging including PET, SPECT, optical and MRI. 2) To understand the potential impact of Molecular Imaging on cancer treatment.

ABSTRACT

Molecular Imaging is expanding at a rapid rate. This overview will provide a panoramic view of the field of Molecular Imaging and major trends that are emerging among the different modalities, PET, SPECT, optical, ultrasound and MRI that constitute molecular imaging.

Molecular Imaging Monday Poster Discussions

Monday, Nov. 28 12:15PM - 12:45PM Room: S503AB

MI

AMA PRA Category 1 Credit ™: .50

Participants

Rathan M. Subramaniam, MD, PhD, Dallas, TX (Moderator) Nothing to Disclose

Sub-Events

MI209-SD-Dual-Modal Positron-Emission Tomography (PET)/near Infrared Fluorescent Imaging-based in Vivo T Cell Tracking Platform

Station #2

Participants

Stefan Harmsen, PhD, New York, NY (*Presenter*) Nothing to Disclose Ilker Medine, New York, NY (*Abstract Co-Author*) Nothing to Disclose Fuat Nurili, New York, NY (*Abstract Co-Author*) Nothing to Disclose Jose Lobo, New York, NY (*Abstract Co-Author*) Nothing to Disclose Maxim A. Moroz, MD, New York, NY (*Abstract Co-Author*) Nothing to Disclose Richard Ting, PhD, New York, NY (*Abstract Co-Author*) Nothing to Disclose Nagavarakishore Pillarsetty, New York, NY (*Abstract Co-Author*) Nothing to Disclose Vladimir Ponomarev, MD, New York, NY (*Abstract Co-Author*) Nothing to Disclose Oguz Akin, MD, New York, NY (*Abstract Co-Author*) Nothing to Disclose Omer Aras, MD, New York, NY (*Abstract Co-Author*) Nothing to Disclose

PURPOSE

We explored the feasibility of labeling human T cells with a 89Zr-PET/NIRF imaging agent to enable in vivo T cell tracking over a range of scales.

METHOD AND MATERIALS

Human T cells were labeled with a dual-modal 89Zr-labeled NIRF nanoparticle using protamine sulfate (PS) and heparin (H). The effects of the labeling on cell viability were examined by Trypan blue staining. In vivo trafficking of 89Zr-PET/NIRF-labeled T cells were performed using a small animal PET and NIRF imager.

RESULTS

A high level of cell labeling was achieved after incubating T cells with the 89Zr/NIRF imaging agent for 30 min in the presence of the PS-H serum-free mixture. In vitro microPET imaging and gamma counting as well as optical imaging of the labeled T cells demonstrated that the PS-H labeling procedure resulted in improved labeling relative to other methods without affecting cell viability and functionality. Upon i.v. administration, we successfully tracked the dual-modal 89Zr/NIRF nanoparticle labeled T cells by small animal PET and end-point NIRF imaging. The labeled T cells were initially distributed to the lungs, and then migrated to the liver and spleen over longer periods of time.

CONCLUSION

We developed intrinsically 89Zr-labeled NIRF nanoparticles that can be used to introduce dual-modal PET/NIRF imaging capabilities to T cells using a protamine/heparin cell labeling procedure. Our results indicate that T cells can be safely and efficiently labeled with these dual-modal imaging probes without compromising their viability function to enable T cell tracking over long-periods of time and over a range of scales.

CLINICAL RELEVANCE/APPLICATION

Our method could be applied to various cell types and provides a new tool for sensitive in vivo cell tracking in a preclinical as well as clinical setting to monitor the fate of these cells.

MI210-SD-MOA3 Chemical Exchange Saturation Transfer (CEST) Imaging vs. Diffusion-Weighted MR Imaging vs. FDG-PET/CT: Capability of Molecular Information for Differentiation of Malignant from Benign Pulmonary Lesions

Station #3

Participants

Yoshiharu Ohno, MD, PhD, Kobe, Japan (*Presenter*) Research Grant, Toshiba Corporation; Research Grant, Koninklijke Philips NV; Research Grant, Bayer AG; Research Grant, DAIICHI SANKYO Group; Research Grant, Eisai Co, Ltd; Research Grant, Fuji Pharma Co, Ltd; Research Grant, FUJIFILM RI Pharma Co, Ltd; Research Grant, Guerbet SA; Masao Yui, Otawara, Japan (*Abstract Co-Author*) Employee, Toshiba Corporation Yuji Kishida, MD, Kobe, Japan (*Abstract Co-Author*) Nothing to Disclose Shinichiro Seki, Kobe, Japan (*Abstract Co-Author*) Nothing to Disclose Hisanobu Koyama, MD, PhD, Kobe, Japan (*Abstract Co-Author*) Nothing to Disclose Takeshi Yoshikawa, MD, Kobe, Japan (*Abstract Co-Author*) Research Grant, Toshiba Corporation Yoshiko Ueno, MD, PhD, Montreal, QC (*Abstract Co-Author*) Nothing to Disclose Katsusuke Kyotani, RT, Kobe, Japan (*Abstract Co-Author*) Nothing to Disclose Mitsue Miyazaki, PhD, Otawara, Japan (*Abstract Co-Author*) Nothing to Disclose Mitsue Miyazaki, PhD, Kobe, Japan (*Abstract Co-Author*) Nothing to Disclose Kazuro Sugimura, MD, PhD, Kobe, Japan (*Abstract Co-Author*) Nothing to Disclose Philips NV Research Grant, Bayer AG Research Grant, Eisai Co, Ltd Research Grant, DAIICHI SANKYO Group

PURPOSE

To directly and prospectively compare the capability for differentiation of malignant from benign pulmonary nodules and/ or masses among chemical exchange saturation transfer (CEST) imaging targeted to amide (-NH)groups, diffusion-weighted MR imaging (DWI) and FDG-PET/CT.

METHOD AND MATERIALS

Eighty-eight consecutive patients (54 men and 34 women; mean age 70 years) with pulmonary nodules and/ or masses underwent CEST imaging and DWI at a 3T MR system, FDG-PET/CT and pathological and/or follow-up examinations. According to final diagnoses, all lesions were divided into malignant (n=49) and benign (n=39) groups. To obtain CEST imaging data in each subject, respiratory-synchronized fast advanced spin-echo images were conducted following a series of magnetization transfer (MT) pulses. Then, magnetization transfer ratio asymmetry (MTRasym) was calculated from z-spectra at 3.5ppm in each pixel, and MTRasym map was computationally generated. To evaluate the capability for differentiation between two groups at each lesion, MTRasym, apparent diffusion coefficient (ADC) and SUVmax were assessed by ROI measurements. To compare each index between two groups, Student's t-test was performed. Then, ROC analysis was performed to determine each feasible threshold value for differentiation of two groups. Finally, sensitivity, specificity and accuracy were compared each other by McNemar's test.

RESULTS

Mean MTRasym (1.97±6.38%), ADC (1.17±0.25×10-3mm2/sec) and SUVmax (3.19±1.60) of malignant group had significant difference with those of benign group (MTRasym: -2.9±4.9%, p=0.0002; ADC: $1.33\pm0.18\times10-3mm2/sec$, p=0.0024, SUVmax: 2.27±0.48, p=0.0008). Results of ROC analysis showed that there were no significant differences of area under the curve (Az) among all indexes (MTRasym: Az=0.72, ADC: Az=0.67, SUVmax: Az=0.72) (p>0.05). When applied each feasible threshold value, there were no significant differences of diagnostic performance among all indexes (p>0.05).

CONCLUSION

CEST imaging is considered at least as valuable as DWI and FDG-PET/CT for differentiation of malignant from benign pulmonary lesions.

CLINICAL RELEVANCE/APPLICATION

CEST imaging is considered at least as valuable as DWI and FDG-PET/CT for differentiation of malignant from benign pulmonary nodules and/ or masses.

MI106-ED- Beyond VQ Scan-Nuclear Medicine and Molecular Imaging in the Chest

Station #4

Participants

Joanna E. Kusmirek, MD, Richmond, VA (Presenter) Nothing to Disclose

Jeffrey P. Kanne, MD, Madison, WI (*Abstract Co-Author*) Research Consultant, PAREXEL International Corporation; Advisory Board, F. Hoffmann-La Roche Ltd

Cristopher A. Meyer, MD, Madison, WI (Abstract Co-Author) Stockholder, Cellectar Biosciences, Inc Investor, NeuWave, Inc

TEACHING POINTS

The exhibit will:- review commonly used nuclear medicine applications in chest imaging- provide helpful tips in interpretationhighlight technical and interpretative pitfalls- describe rare and evolving techniques to include molecular imaging Familiarity with nuclear medicine thoracic imaging applications is crucial for radiologists serving as consultants to referring clinicians, especially in unusual and challenging cases, when routine imaging tests fail to establish the diagnosis.

TABLE OF CONTENTS/OUTLINE

Major topics:VQ scintigraphy in the era of CTA and MRA: imaging during pregnancy (dose reduction options), chronic thromboembolic disease and preoperative quantitative scans, tips for interpretation, examples of non-embolic abnormalities, right-to-left shunt quantification. Oncologic imaging: gallium and thallium scintigraphy, neuroendocrine imaging (MIBG, Octreotide, DOTA-TATE), and newer PET tracers in cancer imaging (F18-FMISO, F18-FLT, C11-thymidine). Inflammation/infection imaging: sarcoidosis (gallium, FDG PET/CT, and cardiac PET), labeled WBC imaging, FDG PET/CT for relapsing polychondritis and vasculitis, radiolabeled antibodies and peptides. in vascular graft infection. Pleura and miscellaneous: FDG PET/CT for pleural pathology, scintigraphic evaluation of abdominal-pleural fistulas, hepatic hydrothorax, splenosis.

Honored Educators

Presenters or authors on this event have been recognized as RSNA Honored Educators for participating in multiple qualifying educational activities. Honored Educators are invested in furthering the profession of radiology by delivering high-quality educational content in their field of study. Learn how you can become an honored educator by visiting the website at: https://www.rsna.org/Honored-Educator-Award/

Jeffrey P. Kanne, MD - 2012 Honored Educator Jeffrey P. Kanne, MD - 2013 Honored Educator

Molecular Imaging Monday Poster Discussions

Monday, Nov. 28 12:45PM - 1:15PM Room: S503AB

MI

AMA PRA Category 1 Credit ™: .50

FDA Discussions may include off-label uses.

Participants

Rathan M. Subramaniam, MD, PhD, Dallas, TX (Moderator) Nothing to Disclose

Sub-Events

MI211-SD-MOB1 CT Perfusion Differences between Primary and Secondary Pulmonary Malignancies and Certain Genetic Mutation (KRAS or EGFR)

Station #1

Awards

Student Travel Stipend Award

Participants Shaun M. Nordeck, MS, RRA, Dallas, TX (*Presenter*) Nothing to Disclose Gary Arbique, PhD, Dallas, TX (*Abstract Co-Author*) Research Grant, Toshiba Corporation Yin Xi, Dallas, TX (*Abstract Co-Author*) Nothing to Disclose Monica Patel, BS, Dallas, TX (*Abstract Co-Author*) Nothing to Disclose Lori M. Watumull, MD, Dallas, TX (*Abstract Co-Author*) Research Grant, Toshiba Corporation Cecelia Brewington, MD, Dallas, TX (*Abstract Co-Author*) Research Grant, Toshiba Corporation

PURPOSE

To evaluate CT Perfusion differences between primary and metastatic pulmonary malignancies based on histopathology. In addition, those with and without genetic mutations were compared with CT perfusion.

METHOD AND MATERIALS

Retrospective analysis of CT Perfusion (CTP) was performed on 29 participants for an indeterminate pulmonary nodule < 3cm and ≥ 0.6 cm with a pathologic diagnosis of malignancy. CTP data was analyzed using commercial perfusion software. Single and dual input CTP assessments were based on defined ROI analysis.

RESULTS

Of the 29 malignancies, 18 were primary and 11 metastatic. Single and Dual input CTP methods successfully differentiated primary versus metastatic lesions (p=0.01 and p=0.04 with AUC of 0.8 and 0.7 respectively). Sixteen (16) underwent further genetic testing in which 8 were positive for either KRAS or EGFR mutations. Those with mutations had different dual input pulmonary flow values than those without (p=0.03). A dual input pulmonary flow cutoff value of 103 provided a sensitivity of 100% and specificity of 62% for the presence of a gene mutation.

CONCLUSION

CTP values of pulmonary flow are significantly different between primary and metastatic pulmonary malignancies using single or dual input. Furthermore, dual input CTP pulmonary flow values were significantly different between malignancies with and without gene mutations.

CLINICAL RELEVANCE/APPLICATION

Non-invasive CTP demonstrates differences between primary and secondary lung cancers and offers promise in differentiating between the presence or absence of certain gene mutations.

MI212-SD- Contrast Ultrasound Imaging of Tumor Vasculature with Positively Charged Microbubbles

Station #2

Participants

Elizabeth Herbst, BS, Charlottesville, VA (*Abstract Co-Author*) Nothing to Disclose Galina Diakova, MS, Charlottesville, VA (*Abstract Co-Author*) Spouse, Co-founder, Targeson, Inc; Spouse, Shareholder, Targeson, Inc Zhongmin Du, PhD, Charlottesville, VA (*Abstract Co-Author*) Nothing to Disclose John A. Hossack, PhD, Charlottesville, VA (*Abstract Co-Author*) Nothing to Disclose

Alexander L. Klibanov, PhD, Charlottesville, VA (*Presenter*) Co-founder, Targeson, Inc; Minority Shareholder, Targeson, Inc; Institutional research collaboration, AstraZeneca PLC;

PURPOSE

Molecular ultrasound imaging is usually based on microbubble contrast agents targeted to endothelial markers of disease. A universal method of targeting tumor vasculature independent of specific ligands is desirable. We present enhanced accumulation of positively charged microbubbles in murine tumor vasculature, i.e., tumor-specific ultrasound imaging.

METHOD AND MATERIALS

Microbubbles were prepared from C4F10, with lipid shell made of DSPC and PEG stearate, with a fraction of positively charged lipids, distearoyl trimethylammoniumpropane (DSTAP) or a biodegradable distearoyl ethyl phospatidylcholine (DSEPC). Bubble size and

concentration was assessed by Coulter, zeta potential - by Zetasizer. Murine colon adenocarcinoma model was used (MC38 cells, J. Schlom, NIH, inoculated in the hind leg of C57BL/6 mice). Ultrasound conditions: Sequoia c512, 15L8 probe, CPS, 7 MHz, MI 0.2. We monitored contrast signal of tumor vs contralateral leg muscle up to 30 min following an iv bolus of 2.10^7 microbubbles.

RESULTS

Without positive lipid, microbubble zeta potential was close to zero; it increased with the fraction of positive lipid. Following iv bolus, neutral bubbles cleared bloodstream and tumor within ~10 min. For bubbles with high DSTAP load, adherent contrast signal in the tumor was high, but its level in normal muscle was also high: at DSTAP:DSPC molar ratio 1:4, at 10 min contrast signal of tumor vs muscle was not different (p>0.3). At 30 min, tumor/muscle signal ratio was 2.1. To reduce normal muscle retention, we reduced bubble charge surface density. For DSTAP:DSPC 1:13, tumor/muscle signal ratio was >3 at 30 min. DSTAP:DSPC ratio 1:22 was optimal for tumor targeting: at 10 min, tumor/muscle ratio was >7 (p=0.00015); at 20 min, >15 (p=0.0034); at 30 min, >16 (p=0.00011), with excellent tumor delineation. Bubbles with DSEPC:DSPC 1:20 ratio also provided excellent delineation of tumor mass (at 10 min, p<0.001), with >5 tumor/muscle signal ratio. We assume that selective targeting is via retention of positively charged microbubbles on the negatively charged endothelium in slow-flow tortuous tumor vasculature.

CONCLUSION

Positively charged microbubbles selectively accumulate in the tumor vasculature and provide high target-to-muscle contrast; optimized formulations are a universal ultrasound contrast agent for tumor imaging.

CLINICAL RELEVANCE/APPLICATION

This study proposes a translatable ultrasound contrast for tumor vasculature delineation.

MI213-SD-MOB3 The Comparison of Effects of Varenicline and Nicotine on NMDA Receptors in Animal Model by Using Proton Magnetic Resonance Spectroscopy at 9.4T

Station #3

Participants

Song-I Lim, BSC,BSC, Seoul, Korea, Republic Of (*Presenter*) Nothing to Disclose Kyu-Ho Song, Seoul, Korea, Republic Of (*Abstract Co-Author*) Nothing to Disclose Chi-Hyeon Yoo, Seoul, Korea, Republic Of (*Abstract Co-Author*) Nothing to Disclose Bo-Young Choe, PhD, Seoul, Korea, Republic Of (*Abstract Co-Author*) Nothing to Disclose

PURPOSE

Nicotine exerts its effects through the activation of nicotinic acetylcholine receptors (nAChRs) 1. Varenicline, a smoking cessation aid, is a partial agonist acting at the $\alpha 4\beta 2$ nAChRs. Although nicotine and varenicline contribute to the reward system at the same time, the influence of the substances on hippocampal neurochemical changes has not been investigated yet. We therefore studied the effects of repeated nicotine exposure and varenicline administration on hippocampus of rats by using in vivo proton magnetic resonance spectroscopy (1H MRS) at 9.4T.

METHOD AND MATERIALS

Eight-week-old male Wistar rats (n = 11; mean body weight, 304.9 ± 9.9 g; range, 290.1-323.21 g) were divided into 3 groups: control rats (control, saline injection, n = 3); nicotine-induced rats (nicotine, subcutaneous injection of nicotine, 0.4 mg/kg/day free base, n = 4); and nicotine- and varenicline-induced rats (varenicline, subcutaneous injection of nicotine, 0.4 mg/kg/day free base, intraperitoneal injection of varenicline 0.3 mg/kg/day free base, n = 4). On day 5, ¹H MRS was performed on 9.4T Agilent MR scanner approximately 1 h after the last injection. After the T2 weighted image acquisition, in vivo ¹H MRS were acquired in the voxel ($1.5 \times 2.5 \times 3$ mm³) using PRESS sequence and T2-weighted images for anatomical guidance with the following parameters: TR = 5000 ms, TE = 13.4 ms, 256 averages. The LC Model software was used to quantify the metabolites in the frequency domain.

RESULTS

In this study, the results show the tendency of increased Glu level in nicotine group than in the control and varenicline groups. Moreover, GSH and NAA levels tended to decrease in the nicotine group in comparison with those in the control and varenicline groups.

CONCLUSION

In conclusion, the hippocampus is integrally linked to the brain reward sensitization involved in addiction and glutamate release through mobilization of intracellular calcium stores. Further, oxidative stress and toxicity of nicotine on brain would cause the decline of GSH and NAA. Therefore, we suggest that varenicline effectively inhibits the reward cycle.

CLINICAL RELEVANCE/APPLICATION

MRS can evaluate regional cerebral neurochemical levels precisely and is recommended as part of a MR study prior to neurodegenerative disease.

NR

MI

Molecular Imaging Symposium: Neurologic MI Applications

Monday, Nov. 28 1:30PM - 3:00PM Room: S405AB

AMA PRA Category 1 Credits ™: 1.50 ARRT Category A+ Credits: 1.50

FDA Discussions may include off-label uses.

Participants

Satoshi Minoshima, MD, PhD, Salt Lake City, UT (*Moderator*) Royalties, General Electric Company; Research Consultant, Hamamatsu Photonics KK; Research Grant, Hitachi, Ltd; Research Grant, Nihon Medi-Physics Co, Ltd; Peter Herscovitch, MD, Bethesda, MD (*Moderator*) Nothing to Disclose

Sub-Events

MSMI23A Overview of MI in Neurology

Participants

Satoshi Minoshima, MD, PhD, Salt Lake City, UT (*Presenter*) Royalties, General Electric Company; Research Consultant, Hamamatsu Photonics KK; Research Grant, Hitachi, Ltd; Research Grant, Nihon Medi-Physics Co, Ltd;

LEARNING OBJECTIVES

1) Learn recent development of molecular imaging in the field of neurosciences. 2) Understand technologies used in molecular brain imaging. 3) Discuss opportunities and challenges in molecular brain imaging.

MSMI23B MI in Dementia

Participants

Alexander Drzezga, MD, Cologne, Germany (*Presenter*) Consultant, Siemens AG; Consultant, Bayer AG; Consultant, General Electric Company; Consultant, Eli Lilly and Company; Consultant, The Piramal Group; Speakers Bureau, Siemens AG; Speakers Bureau, Bayer AG; Speakers Bureau, General Electric Company; Speakers Bureau, Eli Lilly and Company; Speakers Bureau, The Piramal Group

LEARNING OBJECTIVES

1) Gain overview on types of molecular neuropathology involved in the development of different forms of dementia and understand currently discussed disease concepts. 2) Learn about the currently available methods for imaging molecular pathology such as amyloid-deposition and tau-aggregation in dementia and their current status of validation. 3) Gain insights on the clinical value of the individual available methods and their combination with regard to earlier detection, more reliable diagnosis and therapy monitoring of disease.

MSMI23C MI in Movement Disorders

Participants

Kirk A. Frey, MD, PhD, Ann Arbor, MI (*Presenter*) Consultant, MIM Software Inc; Consultant, Eli Lilly and Company; Stockholder, General Electric Company; Stockholder, Johnson & Johnson; Stockholder, Novo Nordisk AS; Stockholder, Bristol-Myers Squibb Company; Stockholder, Merck & Co, Inc;

MSMI23D Emerging Molecular Brain Imaging

Participants

Jonathan E. McConathy, MD, PhD, Birmingham, AL, (jmcconathy@uabmc.edu) (*Presenter*) Research Consultant, Eli Lilly and Company; Research Consultant, Blue Earth Diagnostics Ltd; Research Consultant, Siemens AG; Research Consultant, General Electric Company;

LEARNING OBJECTIVES

1) Participants will be familiar with newer molecular imaging approaches to dementia including tracers targeting tau, alphasynuclein, and neuroinflammation as well as simultaneous PET/MRI which is particularly well-suited to neuroimaging.

ABSTRACT

Imaging biomarkers for Alzheimer's disease (AD) and other neurodegenerative diseases are playing increasingly important roles in both research and patient care. Many neurodegenerative diseases involve the deposition of characteristic proteins including amyloid, tau, and alpha-synuclein which are target for molecular neuroimaging and potentially for therapy. Additionally, processes such as neuroinflammation appear to contribute to the pathophysiology of many neurodegenerative diseases including AD. In this talk, these newer approaches to molecular neuroimaging in dementia will be discussed including their potential clinical applications in patients with cognitive impairment and dementia.

MSMI23E Clinical Translation in Molecular Brain Imaging

Participants Peter Herscovitch, MD, Bethesda, MD (*Presenter*) Nothing to Disclose

LEARNING OBJECTIVES

1) Discuss the FDA approval process for diagnostic radiopharmaceuticals Describe the current status of CMS coverage for diagnostic radiopharmaceuticals. 2) Describe the current status of CMS coverage for amyloid PET radiopharmaceuticals and coverage with evidence development (CED). 3) Understand the design and implementation of the Imaging Dementia—Evidence for Amyloid Scanning (IDEAS) Study.

ABSTRACT

The final steps in clinical translation of molecular imaging radiopharmaceuticals for neurological studies are approval by the U.S. Food and Drug Administration (FDA) for marketing and by insurance carriers for reimbursement. Given the age of patients most likely to require brain imaging studies for neurodegenerative disorders, coverage approval by the U.S. Centers for Medicare and Medicaid ("Medicare") is crucial. This talk will discuss the steps required that lead to FDA approval of a radiopharmaceutical, including the IND process and Phase 1, 2, and 3 clinical trials. It should be noted that FDA approval does not necessarily lead to Medicare approval, especially for PET agents. The CMS approval process will be outlined, including the increasing need to demonstrate the ability of PET imaging to provide improved health outcomes. CMS coverage with evidence development (CED) of PET amyloid imaging agents will be described, with a focus on the design and implementation of the Imaging Dementia—Evidence for Amyloid Scanning (IDEAS) Study.

MSMI24

Molecular Imaging Symposium: Teaching Residents and Their Teachers about Molecular Imaging with Cases: Has the Time Come?

Monday, Nov. 28 3:30PM - 5:00PM Room: S405AB

MIED

AMA PRA Category 1 Credits ™: 1.50 ARRT Category A+ Credits: 1.50

FDA Discussions may include off-label uses.

Participants

Vikas Kundra, MD, PhD, Houston, TX, (vkundra@mdanderson.org) (*Moderator*) License agreement, Introgen Therapeutics, Inc Jeffrey T. Yap, PhD, Salt Lake City, UT (*Moderator*) Nothing to Disclose

LEARNING OBJECTIVES

1) Identify molecular imaging. 2) Comprehend the basis of aspects of molecular imaging. 3) Describe molecular imaging performed in a radiology setting.

ABSTRACT

This course will describe molecular imaging, identify the mechanisms of some aspects of molecular imaging, and give examples of molecular imaging in oncology. Cases will include those from current practice. Mechanisms and scientific basis of examples will be discussed. Sample applications will be discussed and illustrated. Translational examples, including those that have good potential for clinical application, will be used to illustrate interesting aspects of molecular imaging in oncology.

Sub-Events

MSMI24A Oncology

Participants

Vikas Kundra, MD, PhD, Houston, TX, (vkundra@mdanderson.org) (Presenter) License agreement, Introgen Therapeutics, Inc

LEARNING OBJECTIVES

View learning objectives under main course title.

ABSTRACT

MSMI24B Neurology

Participants Rathan M. Subramaniam, MD, PhD, Dallas, TX (*Presenter*) Nothing to Disclose

LEARNING OBJECTIVES

View learning objectives under main course title.

ABSTRACT

MSMI24C Cardiology

Participants Robert J. Gropler, MD, Saint Louis, MO (*Presenter*) Nothing to Disclose

LEARNING OBJECTIVES

1) Identify molecular imaging for CV disease. 2) Describe CV molecular imaging performed in a radiology setting

ABSTRACT

MSMI24D Vascular Inflammation

Participants Chun Yuan, PhD, Seattle, WA (*Presenter*) Research Grant, Koninklijke Philips NV; ;

LEARNING OBJECTIVES

1) Explain the basic pathophysiology of vascular inflammation and needs for imaging. 2) Learn the basic imaging approaches for vascular inflammation, quantitative measurements, and their clinical and research applications. 3) Discuss challenges and future directions.

ABSTRACT

MSMI24E Instrumentation

Jeffrey T. Yap, PhD, Salt Lake City, UT (Presenter) Nothing to Disclose

LEARNING OBJECTIVES

View learning objectives under main course title.

ABSTRACT

Molecular Imaging Tuesday Case of the Day

Tuesday, Nov. 29 7:00AM - 11:59PM Room: Case of Day, Learning Center

MI

AMA PRA Category 1 Credit ™: .50

Participants

Jonathan E. McConathy, MD, PhD, Birmingham, AL (Presenter) Research Consultant, Eli Lilly and Company; Research Consultant, Blue Earth Diagnostics Ltd; Research Consultant, Siemens AG; Research Consultant, General Electric Company; Suzanne E. Lapi, PhD, Birmingham, AL (Presenter) Research Grant, AbbVie Inc; Spouse, Consultant, General Electric Company; Consultant, Siemens AG; Consultant, Blue Earth Diagnostics Ltd; Consultant, Eli Lilly and Company Matthias J. Eiber, MD, Muenchen, Germany (Abstract Co-Author) Nothing to Disclose Thomas A. Hope, MD, San Francisco, CA (Abstract Co-Author) Research Grant, Consultant, GE Healtcare Robert R. Flavell, MD, PhD, San Francisco, CA (Abstract Co-Author) Nothing to Disclose Samuel J. Galgano, MD, Birmingham, AL (Abstract Co-Author) Nothing to Disclose Asim K. Bag, MD, Birmingham, AL (Abstract Co-Author) Nothing to Disclose David M. Schuster, MD, Atlanta, GA (Abstract Co-Author) Institutional Research Grant, Nihon Medi-Physics Co, Ltd; Institutional Research Grant, Blue Earth Diagnostics Ltd; Consultant, WellPoint, Inc; ; Ephraim E. Parent, MD, PhD, Saint Louis, MO (Abstract Co-Author) Nothing to Disclose Bital Savir-Baruch, MD, Maywood, IL (Abstract Co-Author) Nothing to Disclose Pamela K. Woodard, MD, Saint Louis, MO (Abstract Co-Author) Research Grant, Astellas Group; Research Grant, Bayer AG; Research agreement, Siemens AG; ; ; ; Sebastian R. McWilliams, MBBCh, Saint Louis, MO (Abstract Co-Author) Nothing to Disclose Amir K. Durrani, MD, St Louis, MO (Abstract Co-Author) Nothing to Disclose Robert J. Gropler, MD, Saint Louis, MO (Abstract Co-Author) Nothing to Disclose Michael Hofman, PhD, San Francisco, CA (Abstract Co-Author) Nothing to Disclose

Erik D. Roberson, MD, PhD, Birmingham, AL (Abstract Co-Author) Research Grant, Eli Lilly and Company

TEACHING POINTS

1) Interpret amyloid-PET scans as positive or negative. 2) Apply appropriate use criteria for selecting patients for amyloid-PET study. 3) Understand the goals of the IDEAS study as it relates to coverage with evidence development for clinical amyloid-PET scans.

Molecular Imaging Mini-Course: Basics of Molecular Imaging

Tuesday, Nov. 29 8:30AM - 10:00AM Room: S403B

CT MI NM PH

AMA PRA Category 1 Credits ™: 1.50 ARRT Category A+ Credits: 1.50

Participants

Sub-Events

RC323A Developing Molecular Imaging Agents

Participants

Julie L. Sutcliffe, PhD, Sacramento, CA (Presenter) Nothing to Disclose

LEARNING OBJECTIVES

1) Describe the ideal properties of a molecular imaging agent and molecular target. 2) Describe the in vitro and in vivo validation of the molecular imaging agent. 3) Describe specific examples of successful molecular imaging agents.

ABSTRACT

RC323B Instrumentation (PET and CT) and Image Reconstruction

Participants

John Sunderland, PhD, Iowa City, IA, (john-sunderland@uiowa.edu) (Presenter) Research Grant, Siemens AG

LEARNING OBJECTIVES

1) Identify the primary design components of a modern PET/CT system. 2) Design and implement a PET/CT quality control program to assure high quality and quantitatively accurate clinical imaging. 3) Describe commonly used PET reconstruction algorithms and the practical impact of reconstruction parameters upon image quality and quantitation.

ABSTRACT

RC323C Basic Clinical Applications

Participants

Hubert J. Vesselle, MD, PhD, Seattle, WA (Presenter) Consultant, MIM Software Inc

ABSTRACT

Science Session with Keynote: Molecular Imaging (Brain)

Tuesday, Nov. 29 10:30AM - 12:00PM Room: S504CD



AMA PRA Category 1 Credits ™: 1.50 ARRT Category A+ Credits: 1.50

FDA Discussions may include off-label uses.

Participants

Jonathan E. McConathy, MD, PhD, Birmingham, AL (*Moderator*) Research Consultant, Eli Lilly and Company; Research Consultant, Blue Earth Diagnostics Ltd; Research Consultant, Siemens AG; Research Consultant, General Electric Company; Satoshi Minoshima, MD, PhD, Salt Lake City, UT (*Moderator*) Royalties, General Electric Company; Research Consultant, Hamamatsu Photonics KK; Research Grant, Hitachi, Ltd; Research Grant, Nihon Medi-Physics Co, Ltd;

Sub-Events

SSG08-01 Molecular Imaging Keynote Speaker: A Short Overview on Relevant PET-Tracers for Brain Imaging

Tuesday, Nov. 29 10:30AM - 10:40AM Room: S504CD

Participants

Jonathan E. McConathy, MD, PhD, Birmingham, AL (*Presenter*) Research Consultant, Eli Lilly and Company; Research Consultant, Blue Earth Diagnostics Ltd; Research Consultant, Siemens AG; Research Consultant, General Electric Company;

SSG08-02 Radiogenomics Association and Comparison between Multiple Angiogenesis Imaging Surrogates derived from MR Perfusion Imaging and Molecular Genomic Biomarkers in Predicting Overall Survival in Patients with New Diagnosed Glioblastomas

Tuesday, Nov. 29 10:40AM - 10:50AM Room: S504CD

Participants

Xiang Liu, MD, Rochester, NY (*Presenter*) Nothing to Disclose Wei Tian, MD, PhD, Rochester, NY (*Abstract Co-Author*) Nothing to Disclose

PURPOSE

Angiogenesis plays an important role in tumor proliferation and invasion, which is associated with poor survival outcome in glioblastomas. The purpose of this study is to investigate the genomic mechanism of MR perfusion abnormalities, and compared their prognostic value in predicting overall survival (OS) in glioblastoma patients.

METHOD AND MATERIALS

41 new diagnosed glioblastoma cases (mean age is 62.32±12.09) were enrolled. The molecular and genomics biomarkers of TP53, Ki-67 labelling index, isocitrate dehydrogenase (IDH), mammalian target of rapamycin (mTOR), and epidermal growth factor receptor (EGFR) were evaluated. Multiple relative cerebral blood volume (rCBV) parameters were measured based on ROI-based approach and voxel-based histogram analysis, including mean and maximal rCBV ratio, as well as 15%, 25%, 50%, 75%, 85% quantiles and the interquartile range (IQR) of rCBV ratio in the enhancing tumor, and maximal rCBV ratio of peri-enhancing tumor area (rCBVperitumor). The radiogenomics association analysis, Cox regression and Kaplan-Meier survival analysis were performed to compare the predictive value between imaging parameters, and molecular genomic biomarkers.

RESULTS

The rCBVmax, and 50%, 75%, 85% quantiles and IQR had significant association with mTOR, (p = 0.047) without adjustment of age, gender and EGFR/mTOR. The rCBVperi-tumor showed significant correlation with mTOR and EGFR (p = 0.0183 and 0.0047 separately). The Cox regression analysis showed that rCBVperi-tumor and age were the two strongest predictors of OS (hazard ratio= 1.29 and 1.063 separately). ROC analysis showed that the rCBVperi-tumor had better prognostic value than molecular genomic biomarkers, and the rCBVperi-tumor threshold of 3.13 could be used to predict shorter OS with specificity of 78.9% and sensitivity of 77.3%.

CONCLUSION

The difference of radiogenomic association in enhancing and peri-enhancing areas may suggest different moderation of angiogenesis by the mTOR-EGFR pathway in glioblastomas. The rCBVperi-tumor had better prognostic value. These findings will be useful for development of new targeting therapies aiming to tumor proliferation and vasculature infiltration, and future design of personalized multimodality treatment.

CLINICAL RELEVANCE/APPLICATION

The mTOR-EGFR pathway had different moderation on rCBV change within glioblastomas, the rCBVperi-tumor had better prognostic value than molecular genomic biomarkers alone.

SSG08-03 In Vivo MR Tacking of Labeled Adoptive T Cells with Ultrasmall Muti-Modal Nanoprobes in Orthotopic Glioma

Tuesday, Nov. 29 10:50AM - 11:00AM Room: S504CD

Participants

Hua Zhang, ShangHai, China (*Presenter*) Nothing to Disclose Yue Wu, Shanghai, China (*Abstract Co-Author*) Nothing to Disclose Zhenwei Yao, Shanghai, China (*Abstract Co-Author*) Nothing to Disclose

PURPOSE

To establish a novel T1MR-based muti-modal nanoparticles to effectively label adoptive T cells and achieve in vivo noninvasive tracking in orthotopic glioma.

METHOD AND MATERIALS

In vivo MR tracking was performed on a 3-T unit scanner (Signa, GE Medical Systems) with an 8-channel mouse coil. Orthotopic GL261glioma were planted in C57/BL6 mice. HIV-1 transactivator (TAT) peptides were introduced into the surface of FITC-NaGdF4 to improve labeling effciency. The effects of muti-modal nanoprobes on adoptive T cells viability, proliferation and functions were measured by CCK-8, enzyme-linked immuno sorbent assay (ELISA) and flow cytometric analysis and compared with natural adoptive T cells. Axial T1 weighted images of mice brain were collected at different time points after intravenous infusion 107 labeled T cells (control group).

RESULTS

Ultrasmall T1MR-based muti-modal nanoparticles (TAT/FITC-NaGdF4) were successfully developed with high longitudinal relaxity (8.93 s-1mM-1) and favorable stability. It can label adoptive T cells with over 95% efficacy, remarkably superior to FITC-NaGdF4 nanoparticles. Quantitative ICP analysis showed that internalization of Gd contents reached a plateau at five hours after co-incubation with adoptive T cells. The results of CCK-8 indicated that the optimal nanoparticles concentration of labeling was 500 µg Gd/ml. There were no significant difference of the short and long-term viability, proliferative capacity, production of cytokines and expression levels of surface receptors between unlabeled and labeled T cells with TAT/FITC-NaGdF4 nanoprobes. Labeled T-cell clusters can be sensitively detected in C57/BL6 mouse orthotopic glioma at 24h by T1-weighted MR, which signal was distinctly higher than control group.

CONCLUSION

Adoptive T-lymphocytes can be efficiently labeled by novel muti-modal nanoparticles (TAT/FITC-NaGdF4) without measurable effects on their properties and be sensitively detected in vivo orthotopic glioma by T1MR.

CLINICAL RELEVANCE/APPLICATION

TAT/FITC-NaGdF4 nanoprobes act as the novel and high-performance T1MR-based muti-modal contrast agent, which can label T cells with high efficacy and without any measurable effects on T cells properties.

SSG08-04 Noninvasive Tracking the Kinetic Phases of Distribution and Glioblastoma Targeting of EGFRvIIIspecific Chimeric Antigen Receptor T Cells via MRI

Tuesday, Nov. 29 11:00AM - 11:10AM Room: S504CD

Participants

Xiao Chen, Chongqing, China (*Presenter*) Nothing to Disclose Weiguo Zhang, Chongqing, China (*Abstract Co-Author*) Nothing to Disclose Tian Xie, Chongqing, China (*Abstract Co-Author*) Nothing to Disclose

PURPOSE

Glioblastoma (GBM) is the most common primary malignant brain tumor in adults and is uniformly lethal. T-cell-based immunotherapy offers a promising platform for treatment given its potential to specifically target tumor tissue while sparing the normal brain. However, the challenge of monitoring the therapy in real time has been continually ignored. To address this issue, we developed MR imaging approaches to evaluate a recently reported novel CAR strategy for adoptive immunotherapy against glioma xenografts expressing EGFRvIII

METHOD AND MATERIALS

T cells, isolated from the peripheral blood of healthy donors, were transduced byEGFRvIII-specific human CAR (EGFRvIII-CAR). Flow cytometry was used to detect CAR expression on transduced T cells. Elevated concentration of USPIO was labeled CAR T cells. The biological properies of these cells were detected. Cytoxicity assay and cytokine production were anlynased in vitro. Then, USPIO-CAR T cells were transplanted into the nude mice bearing U87-EGFRvIII glioma. MRI and immunohistochemistry were performed.

RESULTS

We successfully labeled EGFRvIII-CAR T cells with USPIO without any influence on the biological properties and toxicity to tumor of these cells. After intravenous administration into glioma-bearing nude mice, the USPIO-EGFRvIII-CAR T cells specifically homed to gliomas and could be reliably tracked by 7.0 T MR as early as 1 day after transplantation, causing hypointensity on T2-weighted images. Prussian blue staining and CD3 immunohistochemistry stainingconfirmed the MRI findings. Infusion with EGFRvIII-CAR T cells led to cures in all mice with brain gliomas.

CONCLUSION

This therapeutic strategy offered efficient therapy effect to EGFRvIII+-glioma-bearing mice and implied that MR imaging is a highly useful tool in tracking the kinetic phases of CAR T cells distribution and monitor its therapuetic effect.

CLINICAL RELEVANCE/APPLICATION

We will establish a new technological paltform and evaluation system for in vivo tracking of CAR-T immunotherapy of GBM and other solid tumors to guide the design and improvement of new CAR with high penetration, proliferation and cytotoxicity in future, which will have great significance to the development of CAR-T immunotherapy and improvement of therapeutic effecacy in solid tumor.

SSG08-05 Imaging Aggregates, Fibrils, and Plaques using Small-Angle X-Ray Scattering: Initial Computational Modeling and Measurements Towards Designing an Anthropomorphic Phantom with Applications in Alzheimer's Disease

Tuesday, Nov. 29 11:10AM - 11:20AM Room: S504CD

Mina Choi, MS, Silver Spring, MD (*Abstract Co-Author*) Nothing to Disclose Eshan Dahal, Silver Spring, MD (*Abstract Co-Author*) Nothing to Disclose Nadia Alam, Silver Spring, MD (*Abstract Co-Author*) Nothing to Disclose Bahaa Ghammraoui, Silver Spring, MD (*Abstract Co-Author*) Nothing to Disclose Andreu Badal-Soler, Silver Spring, MD (*Abstract Co-Author*) Nothing to Disclose Aldo Badano, PhD, Silver Spring, MD (*Presenter*) Research Grant, Barco nv

PURPOSE

Protein aggregates play significant roles in many biological processes and diseases. For instance, beta-amyloid plaques and tau tangles have been shown to have an effect in the development of Alzheimer's (AD), a neurodegenerative disease characterized by impaired memory, reduce cognitive skills, and diminished ability to perform everyday tasks affecting over 5 million Americans for which there is currently no cure or effective treatment. This work discusses computational modeling and physical phantom studies that show the potential of small-angle x-ray scattering (SAXS) imaging for detecting and characterizing aggregates, fibrils, and plaques of relevance for Alzheimer's and other neurological diseases.

METHOD AND MATERIALS

Optical imaging techniques for the characterization of the molecular AD hallmarks lack the ability to image deep tissue. PET imaging is used to locate beta-amyloid plaques in the brain but suffers from low spatial resolution and low specificity. SAXS can characterize and selectively image structures based on electron density maps without any additional contrast agents. We report SAXS measurements of beta-amyloid-42 aggregation in a 50% dimethyl sulfoxide solution and Bovine Serum Albumin (BSA) under various temperatures which form amyloid-like fibrils. We compare measured signals with theoretical estimates and use the measured and theoretical cross sections to perform simulations using a publicly available, GPU-accelerated, Monte Carlo radiation transport tool. This tool is modified for cross-section sampling at relevant small scattering angles allowing user-generated cross sections accounting for interference effects using uniform and anatomically accurate phantoms.

RESULTS

We obtained reconstructed scatter profiles for different target materials using experimentally measured cross sections showing increased contrast at peak scattering angles consistent with the structure of the BSA aggregates. Various phantom design approaches will be discussed including a flowing sample design and an encasing approach.

CONCLUSION

The findings of the study indicate that BSA aggregation states can be reproduced by controlling pH levels in solvents. A physical phantom for imaging aggregates might be feasible.

CLINICAL RELEVANCE/APPLICATION

These studies will contribute to assessing the feasibility and providing the tools needed for the design and optimization of SAXS imaging systems to measure AD biomarkers in vivo.

SSG08-06 Quantitative Analysis of Amide Proton Transfer (APT) and Nuclear Overhauser Enhancement (NOE) Contrasts in Rat Glioma

Tuesday, Nov. 29 11:20AM - 11:30AM Room: S504CD

Participants

Yuwen I. Zhou, PhD, Charlestown, MA (*Presenter*) Nothing to Disclose Takahiro Takahiro, Charlestown, MA (*Abstract Co-Author*) Nothing to Disclose Phillip Zhe Sun, PhD, Charlestown, MA (*Abstract Co-Author*) Nothing to Disclose

PURPOSE

Amide proton transfer (APT), a specific form of Chemical Exchange Saturation Transfer (CEST) MRI, detects endogenous amide protons and has been increasingly used for tumor detection and grading. However, the origin of APT CEST contrast in tumors has not been fully explained, because the routine asymmetry analysis (MTRasym) is susceptible to confounding effects, such as spillover saturation and concomitant semisolid magnetization transfer (MT). In addition to APT, nuclear Overhauser enhancement (NOE) effects upfield from water also contributes to the observed CEST contrast. Here we combined analytic solution and numerical fitting to correct for spillover effect and decompose the contributions from APT, NOE and MT effects to CEST contrast in rat glioma.

METHOD AND MATERIALS

The non-infiltrating D74-rat glioma model was used. The animals (N=8) were imaged 11-13 days after tumor cell implantation using a 4.7T scanner. Multi-parametric MRI including T1, T2 mapping and CEST MRI was performed. CEST Z-spectrum were acquired with continuous-wave saturation pulses (0.75μ T for 5 s) with 49 frequency offsets evenly distributed from -6 to 6 ppm relative to the water resonance.

RESULTS

The spillover corrected Z-spectrum was obtained by subtracting the experimental Z-spectrum from the Z-spectrum analytically derived from relaxation measurements (Fig1a). After corrections for spillover effect, multi-Lorentzian fitting of the corrected Z decoupled the contribution of different pools (Fig1b). The fitted APT, NOE and MT effects were further corrected for the influence of the longitudinal relaxation of the water pool (Fig2). Fig3 shows that corrected APT in tumors significantly increased in tumor tissues (p<0.005, paired t-test), while corrected NOE and MT effects in tumors showed significant decreases compared with those in normal tissues (p<0.001, paired t-test).

CONCLUSION

By combining analytic solution and numerical fitting, we were able to decouple individual contributions from APT, NOE and MT effects, providing better understanding of the CEST contrast in tumors and assisting in the development of improved APT and NOE measurements for cancer imaging.

CLINICAL RELEVANCE/APPLICATION

Relaxation-based correction of spillover effects simplifies quantitative analysis of APT and NOE contrasts in rat glioma, providing better understanding of the CEST contrast in tumors and assisting in the development of improved APT and NOE measurements for cancer imaging.

SSG08-07 Therapeutic Efficacy of Treg in Diabetic Stroke: Measurement with an Ultrafast MMP Activatable Probe

Tuesday, Nov. 29 11:30AM - 11:40AM Room: S504CD

Participants

Yu Cai, Nanjing, China (*Presenter*) Nothing to Disclose Shenghong Ju, MD, PhD, Nanjing, China (*Abstract Co-Author*) Nothing to Disclose

PURPOSE

To measure the therapeutic efficacy of endogenous Treg cell in diabetic stroke by a novel and ultrafast MMP activatable probe.

METHOD AND MATERIALS

T2 diabetes mellitus was induced in C57BL/6(8-week-old) mice by administration of high-fat diet in combination with intraperitoneal injection of streptozotocin. CD28 superagonistic (200ug/mouse) was injected intraperitoneally 3-6 hours after photothrombotic stroke onset in wildtype mice and diabetic mellitus mice to boost the expression of endogenous regulatory T cells. Gelatin zymography assay, Immunofluorescent staining, T2-weighted MR scans and Near-infrared fluorescence (NIRF) imaging were performed on day 7 post stroke.

RESULTS

The group which was treated with CD28 SA, presented smaller infarct volume compared with control group, especially in diabetic mice $(9.73\%\pm2.25 \text{ vs.} 13.32\%\pm2.24$ in diabetic stroke group, p=0.16; $7.23\%\pm0.45 \text{ vs.} 9.29\%\pm1.64$ in wildtype stroke, p=0.014) (Figure 1). The results of Immunofluorescent staining and gelatin zymography assay demonstrated that the expression of MMP-9 were decreased in groups treated with CD28 SA (Figure 2). Here, we used a novel MMP activated optical imaging probe to visualize the MMP activity in vivo. Our preliminary results showed that TBR values were increased in diabetic stroke mice and significantly down regulated after treated with CD28 SA(2.05 vs.1.57 in diabetic stroke; 1.78 vs.1.40 in wildtype stroke)(Figure 3).

CONCLUSION

Amplification of regulatory T Cells using a CD28 SA improves outcome of diabetic stroke. Moreover, using MMP activatable probe, we successfully demonstrated the MMP activity and stroke outcome by non-invasive molecular imaging method.

CLINICAL RELEVANCE/APPLICATION

The results of our study is strongly suggest that the molecular imaging approach is valuable for measuring molecular-specific effects of treatment (CD28 SA induced Treg) in diabetic stroke and has great potential for clinical translation.

SSG08-09 Molecular Image-Guided Biopsy in Patients with Newly Diagnosed Gliomas Using Amide Proton Transfer-Weighted (APTw) MR Imaging

Tuesday, Nov. 29 11:50AM - 12:00PM Room: S504CD

Awards

Student Travel Stipend Award

Participants

Shanshan Jiang, MD, Baltimore, MD (Presenter) Nothing to Disclose Jinyuan Zhou, PhD, Baltimore, MD (Abstract Co-Author) License agreement, Koninklijke Philips NV Charles Eberhart, MD, PhD, Baltimore, MD (Abstract Co-Author) Nothing to Disclose Yi Zhang, Baltimore, MD (Abstract Co-Author) Nothing to Disclose Hye-Young Heo, Baltimore, MD (Abstract Co-Author) Nothing to Disclose Zhibo Wen, Guangzhou, China (Abstract Co-Author) Nothing to Disclose Lindsay Blair, Baltimore, MD (Abstract Co-Author) Nothing to Disclose Huamin Qin, Baltimore, MD (Abstract Co-Author) Nothing to Disclose Michael Lim, Baltimore, MD (Abstract Co-Author) Nothing to Disclose Alfredo Quinones-Hinojosa, Baltimore, MD (Abstract Co-Author) Nothing to Disclose Peter B. Barker, DPhil, Baltimore, MD (Abstract Co-Author) Nothing to Disclose Martin G. Pomper, MD, PhD, Baltimore, MD (Abstract Co-Author) Shareholder, CTS, Inc; Board Member, CTS, Inc; Research Grant, CTS, Inc; Advisor, CTS, Inc; Institutional license agreement, Progenics Pharmaceuticals, Inc; Institutional license agreement, Advanced Accelerator Applications SA; Institutional license agreement, LI-COR, Inc; Institutional license agreement, BIND Therapeutics, Inc John Laterra, Baltimore, MD (Abstract Co-Author) Nothing to Disclose

Peter C. Van Zijl, PhD, Baltimore, MD (Abstract Co-Author) Speakers Bureau, Koninklijke Philips NV; License agreement, Koninklijke Philips NV

Jaishri Blakeley, Baltimore, MD (Abstract Co-Author) Nothing to Disclose

PURPOSE

Pathological diagnosis remains the gold standard for determining the treatment for malignant gliomas. However, the accuracy of diagnostic neurosurgical procedures is often limited by the heterogeneous characteristics of these tumors. APT imaging is a molecular imaging technique that generates MRI contrast based on endogenous cellular proteins in tissue. We explored APTw image-guided neuro-navigation and radiopathologic correlation to assess the diagnostic accuracy of APT MRI in defining heterogeneous regions of malignant gliomas.

METHOD AND MATERIALS

Patients (n=24) with previously undiagnosed gliomas underwent a volumetric APTw imaging sequence. Pre-determined regions of interest on the APTw images were labeled on the co-registered clinical MR images in the BrainLab neuro-navigation system. The priority regions to sample included: (i) APTw hyperintense, Gd enhancing; (ii) APTw hyperintense, Gd non-enhancing; and (iii) APTw

isointense, Gd enhancing. 70 APTw image-directed stereotactic biopsies were obtained from these 24 patients. Pathologic indices (tumor grade, cellularity, necrosis degree, and proliferation) were analyzed and correlated with corresponding APTw signal intensities.

RESULTS

Based on the histopathological analysis, 33 specimens were diagnosed as WHO grade-II pathology, 14 specimens grade-III, 15 specimens grade-IV, and eight specimens peritumoral edema. Multiple grades were found within a single tumor lesion in six patients. APTw signal intensities of the biopsied sites were significantly higher for high-grade specimens ($2.65\pm0.96\%$) than for low-grade specimens ($1.82\pm0.54\%$; P<0.001), independent of Gd-enhancement patterns. APTw signal intensities of these biopsied sites showed strong positive correlations with cellularity and proliferation (R=0.751 and 0.538, respectively; both P<0.001). Multiple linear regression showed that tumor cellularity and proliferation index were the two best predictors of APTw signal intensities (R2=0.540; P<0.001).

CONCLUSION

Areas with APTw hyperintensity displayed higher cellularity and higher proliferation suggesting that APTw imaging highlights the most active and aggressive portions of heterogeneous gliomas.

CLINICAL RELEVANCE/APPLICATION

APTw molecular image-guided biopsy procedure can increase precision of tumor sampling in patients with gliomas, particularly in lesions that show no Gd enhancement.

Molecular Imaging Tuesday Poster Discussions

Tuesday, Nov. 29 12:15PM - 12:45PM Room: S503AB

MI

AMA PRA Category 1 Credit ™: .50

Participants

Donna J. Cross, PhD, Salt Lake City, UT (Moderator) Nothing to Disclose

Molecular Imaging Tuesday Poster Discussions

Tuesday, Nov. 29 12:45PM - 1:15PM Room: S503AB

MI

AMA PRA Category 1 Credit ™: .50

Participants

Donna J. Cross, PhD, Salt Lake City, UT (Moderator) Nothing to Disclose

Sub-Events

MI219-SD- USPIO-Labeling in Different Macrophage Population: A In Vitro and In Vivo MR Study

Station #2

Participants

Chiara Zini, MD, Rome, Italy (*Presenter*) Nothing to Disclose Maryanna Venneri, Rome, Italy (*Abstract Co-Author*) Nothing to Disclose Damiano Caruso, MD, Rome, Italy (*Abstract Co-Author*) Nothing to Disclose Selenia Miglietta, Roma, Italy (*Abstract Co-Author*) Nothing to Disclose Marco Rengo, MD, Rome, Italy (*Abstract Co-Author*) Nothing to Disclose Natale Porta, Latina, Italy (*Abstract Co-Author*) Nothing to Disclose Andrea Isidori, Rome, Italy (*Abstract Co-Author*) Nothing to Disclose Vincenzo Petrozza, Latina, Italy (*Abstract Co-Author*) Nothing to Disclose Andrea Laghi, MD, Rome, Italy (*Abstract Co-Author*) Nothing to Disclose Andrea Laghi, MD, Rome, Italy (*Abstract Co-Author*) Speaker, Bracco Group Speaker, Bayer AG Speaker, General Electric Company Speaker, Koninklijke Philips NV

PURPOSE

Tumor-associated macrophages (TAM) are recruited to the tumor site and programmed by tumor-derived factors in tumorsupportive M2-polarized macrophages, although M1-polarized TAM with anti-tumor activity have been described in several types of cancer.Aim of the present study was to evaluate if ultrasmall superparamagnetic iron oxide (USPIO) magnetic resonance (MR) could be used to depict distinct population of macrophages.

METHOD AND MATERIALS

Human monocytic cell line THP-1 were differentiated into macrophages using PMA and polarized according to the Tjiu method. A control population of macrophages, was developed from THP-1 cells with PMA (M0 macrophages). M1-polarized, M2-polarized and the M0 were incubated with USPIO research prototype (P904, CheMatech, Guerbet Research)(200 µg Fe/mL) for 36 hours. A M0 without P904 was the control non-treated population. M0, M0+P904, M1+P904 and M2+P904 were analyzed in gel phantoms containing at least 1x106 cells/milliliter with a 3.0T MR scan (Discovery MR750). Optical and electron microscopy was used as gold standard to evaluate the iron uptake.

RESULTS

M2+P904 showed a much greater T1 signal compared to the other population (p<0.0001), and the T2* signal was significantly lower compared to the other groups (p<0.0001); the R* was significantly higher for the M2+ P904 compared to the other populations (p<0.0001). Hystological analysis demonstrated higher iron content in the M2+P904 as compared to both the M1+904 (p=0.04) and the M0+P904 population (p=0.003). Ultrastructure analysis with a electron microscope demonstrated ubiquitous localization of P904 within the cellular compartments. Those results were confirmed with human macrophages.

CONCLUSION

Avid and selective USPIO-labeling for M2-like population was demonstrated with a 3.0T clinical scan.

CLINICAL RELEVANCE/APPLICATION

USPIO-RM is able to depict M2 macrophage population. Further studies on same topic would be highly desirable to investigate the possible role of non-invasive diagnosis in inflammation and cancer imaging

Molecular Imaging (Inflammation/Metabolism/Musculoskeletal)

Tuesday, Nov. 29 3:00PM - 4:00PM Room: S504CD



AMA PRA Category 1 Credit ™: 1.00 ARRT Category A+ Credit: 1.00

FDA Discussions may include off-label uses.

Participants

Tomio Inoue, MD, PhD, Yokohama, Japan (*Moderator*) Nothing to Disclose Michael S. Gee, MD, PhD, Jamaica Plain, MA (*Moderator*) Nothing to Disclose

Sub-Events

SSJ14-01 Whole-body Assessment of Fat Content and Insulin Sensitivity in Different Tissues of Healthy Volunteers and T2D Patients using a Fully Integrated PET/MR System

Tuesday, Nov. 29 3:00PM - 3:10PM Room: S504CD

Participants

Hakan Ahlstrom, Uppsala, Sweden (*Presenter*) Research funded, AstraZeneca PLC Emil Johansson, Uppsala, Sweden (*Abstract Co-Author*) Nothing to Disclose Mark Lubberink, Uppsala, Sweden (*Abstract Co-Author*) Nothing to Disclose Greta Boersma, Uppsala, Sweden (*Abstract Co-Author*) Nothing to Disclose Stanko Skrtic, Molndal, Sweden (*Abstract Co-Author*) Employee, AstraZeneca PLC Jan Eriksson, Uppsala, Sweden (*Abstract Co-Author*) Nothing to Disclose Joel Kullberg, DiplPhys, Uppsala, Sweden (*Abstract Co-Author*) Nothing to Disclose

PURPOSE

Parameters that are important for development of Type 2 Diabetes (T2D) are whole-body fat content and insulin sensitivity of all tissues in the body (expressed with the M-value). These parameters can be studied on a tissue level with a 18F- FDG PET/MR investigation. The main objective was to apply an integrated whole-body PET/ MR protocol for assessment of glucose uptake using 18F-FDG, during euglycemic clamp conditions, and fat content of various tissues, of healthy volunteers and TD2 patients, using a whole-body fully integrated PET/MR equipment.

METHOD AND MATERIALS

10 subjects (5 healthy, 5 T2D) were imaged using 18F-FDG and an integrated PET/MR system under steady state clamp conditions. PET: 1 dynamic acquisition (thorax,10 min) with simultaneous administration of 18F-FDG (average 330 MBq/subject), followed by 6 serial whole body scans (5 min/scan). MRI: 6 point Dixon for quantitative fat, water separated images were acquired after the PET scans. Standard Patlak model using image derived input function (IDIF) from ascending aorta (manually derived region of interest from dynamic PET series) was used for kinetic modelling of tissue specific glucose uptake.Tissue specific glucose uptake [µmol glucose/100 g tissue min] from PET was manually segmented from the fused MRI and PET-Patlak volumes. The M-value [mg/kg min] expressing the whole-body insulin sensitivity of the subject was determined during PET/MRI acquisition with the clamp-method, where a constant infusion of insulin (56 mU/m2/min) and variable infusion of glucose to the subject was set to maintain a steady state level of 5.6 mmol/l (plasma glucose) during imaging. The M-value was normalized to fat-free mass.

RESULTS

The M-value showed positive correlation with the fat fraction of the liver, whole body fat volume and the tissue specific uptake rate of 18F-FDG in skeletal muscle, subcutaneous adipose tissue and liver and a negative correlation in the brain. No correlation was seen for pancrea's fat fraction and the uptake rate of 18F-FDG in heart (left ventricle) and pancreas.

CONCLUSION

The applied whole-body FDG PET/MRI protocol, during euglycemic clamp, is feasible for studies of fat content and insulin sensitivity in various tissue, parameters relevant for development of T2D.

CLINICAL RELEVANCE/APPLICATION

FDG-PET/MR data generated at different stages of T2DM development, integrated with non-imaging data, can give important information for future more individualized therapy and improved outcomes.

SSJ14-02 Molecular MRI Targeting Myeloperoxidase Detects Inflammation in Human Non-Alcoholic Steatohepatitis

Tuesday, Nov. 29 3:10PM - 3:20PM Room: S504CD

Awards

Student Travel Stipend Award

Participants

Benjamin Pulli, MD, Boston, MA (*Presenter*) Nothing to Disclose Gregory R. Wojtkiewicz, MSc, Boston, MA (*Abstract Co-Author*) Nothing to Disclose Yoshiko Iwamoto, Boston, MA (*Abstract Co-Author*) Nothing to Disclose Muhammad Ali, MBBS, Boston, MA (*Abstract Co-Author*) Nothing to Disclose Matthias Zeller, MD, 02114, MA (*Abstract Co-Author*) Nothing to Disclose Lionel A. Bure, MD, Boston, MA (*Abstract Co-Author*) Nothing to Disclose Cuihua Wang, PhD, Boston, MA (*Abstract Co-Author*) Nothing to Disclose Yuri Choi, Boston, MA (*Abstract Co-Author*) Nothing to Disclose Ricard Masia, MD,PhD, Boston, MA (*Abstract Co-Author*) Nothing to Disclose Alexander R. Guimaraes, MD, PhD, Portland, OR (*Abstract Co-Author*) Speakers Bureau, Siemens AG; Kathleen Corey, MD, Boston, MA (*Abstract Co-Author*) Advisory Board, Gilead Sciences, Inc John W. Chen, MD, PhD, Boston, MA (*Abstract Co-Author*) Research Grant, Pfizer Inc

PURPOSE

Only a subset of patients with non-alcoholic fatty liver disease will progress to non-alcoholic steatohepatitis (NASH) and subsequently cirrhosis. Inflammation and oxidative stress are key facilitators for progression. Myeloperoxidase (MPO) is a proinflammatory and oxidative enzyme expressed by myeloid cells. We hypothesized that MPO-Gd, an MRI probe specific for MPO, could detect MPO activity in human biopsy samples.

METHOD AND MATERIALS

A total of 11 liver biopsy samples from obese patients undergoing clinical evaluation for NASH were obtained. A waiver was granted by our institution's IRB. Samples were incubated in cell culture medium, and T1 fat-sat pre-contrast MR imaging was performed on a 4.7 T MRI (Bruker). MPO-Gd (1 mg/ml) was added, and samples were incubated for 2 hours. Samples were washed. Post-contrast MR images were then acquired, and MPO-specific signal was calculated as CNRpost/CNRpre. After imaging, samples were cut to 5 μ m thickness, and stained with H&E and MPO for histopathological evaluation. The NAFLD activity score (NAS) was calculated; NASH was defined as NAS >5.

RESULTS

5 of 11 patients fulfilled criteria for NASH (NAS>5), the remaining 6 were used as controls. There was no difference in age (49.2 \pm 13.2 in NASH vs. 40.3 \pm 9.2 in control, P=0.35) or BMI (44.4 \pm 8.7 vs. 45.1 \pm 6.8, P=0.87). As expected, NASH patients had higher NAS sub-scores in steatosis (3 [interquartile range IQR 1.5-3], vs. 0 [0-0.5], inflammation (1 [1.5-3] vs. 0 [0-0]), fibrosis (1 [1-2] vs. 0 [0-0]), hepatocyte ballooning (2 [2-2] vs. 0 [0-0]), and a higher total NAS score (6 [5.5-6] vs. 0 [0-0.5]). Molecular MRI with MPO-Gd demonstrated an increase in CNR in samples from NASH patients (Fig., A) versus control (Fig., B) (CNRpost/CNRpre 2.61 \pm 0.91 vs. 1.29 \pm 0.22, P=0.004). Correlating with these results, we found more clusters of MPO-positive cells on histology in NASH versus control patients (Fig., C, 5.60 \pm 1.52 vs. 1.00 \pm 0.89, P=0.002).

CONCLUSION

In liver core biopsy samples of patients undergoing evaluation for NASH, MPO-Gd enhanced molecular MRI can reliably and noninvasively detect MPO activity in NASH patients.

CLINICAL RELEVANCE/APPLICATION

Molecular MRI with MPO-Gd could non-invasively assess for liver inflammation. This could allow for noninvasive identification of patients with NASH who are at high risk for developing cirrhosis.

SSJ14-03 Investigation of Aquaporin by DWI MRI with Multiple B Values in a Rat Model of Diabetic Nephropathy

Tuesday, Nov. 29 3:20PM - 3:30PM Room: S504CD

Participants

Yu Wang, BDS, Chengdu, China (*Presenter*) Nothing to Disclose Rongbo Liu, MD, Prof, Chendu, China (*Abstract Co-Author*) Nothing to Disclose Heng Zhang, BDS, Luzhou, China (*Abstract Co-Author*) Nothing to Disclose Ruzhi Zhang, BSC, Chengdu, China (*Abstract Co-Author*) Nothing to Disclose Zhoushe Zhao, Beijing, China (*Abstract Co-Author*) Nothing to Disclose Fabao Gao, MD, PhD, Chengdu, China (*Abstract Co-Author*) Nothing to Disclose Lei Wang, BA, Chengdu, China (*Abstract Co-Author*) Nothing to Disclose

PURPOSE

To assess the correlation between renal apparent diffusion coefficient (ADC) obtained from ultra-high b-values and the change of aquaporins (AQPs) in a rat model of type 2 diabetic nephropathy.

METHOD AND MATERIALS

Twenty-four male Sprague-Dawley rats were divided into 2 groups: (1) untreated controls, (2) diabetes (DM). Forty days after diabetes induction with streptozotocin, MR imaging was performed in a 7.0-T scanner.All rats received diffusion-weighted imaging (DWI) with 18 b-values (0–4500 s/mm2). Renal apparent diffusion coefficient values were calculated for each of the different anatomical layers of the kidney and maps of low ADC (ADCI) maps were calculated from low b-values(0-200),maps of standard ADC (ADCst) maps were calculated from standard b-values(300-1500) and maps of ultra-high ADC (ADCuh) were calculated from the ultra-high b-values (1700-4500). The expression of proteins involved in renal water transport in diabetic rats were then studied by immunohistochemistry microscopy and the mean value of integral optical density(IOD) of aquaporins positive signals were measured by applying immune tissue chemistry method. Imaging result, laboratory parameters of diabetic and kidney function, and renal histopathological changes were compared between groups.

RESULTS

All diabetic animals developed hyperglycemia. ultra-high ADC was significantly increased in DM animals in the cortex (CO) $(1.40\pm0.10\times10-3mm2/s; P<0.001)$, outer stripe of the outer medulla (OS) $(1.42\pm0.10\times10-3mm2/s; P<0.001)$, inner stripe of the outer medulla (IS) $(1.32\pm0.14\times10-3mm2/s; P=0.010)$ and inner medulla (IM) $(1.60\pm0.12\times10-3mm2/s; P=0.041)$ compared with control animals (CO, $1.20\pm0.14\times10-3mm2/s;$ OS, $1.22\pm0.14\times10-3mm2/s;$ IS, $1.19\pm0.41\times10-3mm2/s;$ IM, $1.51\pm0.15\times10-3mm2/s$). while, Between groups, ADCI and ADCst values were not different. DM rats had an increased IOD of AQP2 in the CO (0.035 ± 0.010 ; P=0.008), OS (0.06 ± 0.019 ; P=0.011), IM(0.058 ± 0.016 ; P=0.001), and IM (0.040 ± 0.012 ; P = 0.009) compared with control animals (CO, 0.023 ± 0.010 ; OS, 0.043 ± 0.009 ; IS , 0.036 ± 0.010 ; IM, 0.026 ± 0.011). In contrast, there were no major changes in the abundance of AQP1 and AQP4.

CONCLUSION

ADCub may be a useful measurement for peninyasiya avaluating kidnoy damage in dishetic penhropathy, and these changes in

ADCult may be a useful measurement for noninvasive evaluating kinney damage in diabetic nephropathy, and these changes in ADCuh may reflect function of the AQP.

CLINICAL RELEVANCE/APPLICATION

ADCuh may be a promising biomarker in differential diagnosis of diabetic nephropathy patients.

SSJ14-04 Facet Tropism and Facet Joint Orientation: Risk Factors For the Development of Early Biochemical Alterations of Lumbar Intervertebral Discs

Tuesday, Nov. 29 3:30PM - 3:40PM Room: S504CD

Awards

Student Travel Stipend Award

Participants

Christoph Schleich, MD, Dusseldorf, Germany (*Presenter*) Nothing to Disclose Anja Lutz, Dusseldorf, Germany (*Abstract Co-Author*) Nothing to Disclose Joel Aissa, Duesseldorf, Germany (*Abstract Co-Author*) Nothing to Disclose Benjamin Schmitt, Vienna, Austria (*Abstract Co-Author*) Nothing to Disclose Bernd Bittersohl, MD, Bern, Switzerland (*Abstract Co-Author*) Nothing to Disclose Gerald Antoch, MD, Duesseldorf, Germany (*Abstract Co-Author*) Nothing to Disclose Hans-Joerg Wittsack, PhD, Duesseldorf, Germany (*Abstract Co-Author*) Nothing to Disclose Johannes Boos, MD, Boston, MA (*Abstract Co-Author*) Nothing to Disclose Katrin S. Blum, MD, Dusseldorf, Germany (*Abstract Co-Author*) Nothing to Disclose Falk R. Miese, MD, Dusseldorf, Germany (*Abstract Co-Author*) Nothing to Disclose

PURPOSE

To assess the glycosaminoglycan (GAG) content of lumbar intervertebral discs (IVD) in healthy volunteers with facet tropism (FT) and sagittal facet joint (FJ) orientation using glycosaminoglycan chemical exchange saturation transfer imaging (gagCEST).

METHOD AND MATERIALS

Seventy-five lumbar IVDs of twenty-five young, healthy volunteers without any history of lumbar spine pathologies (13 female; 12 male; mean age: 28.0 ± 4.4 years; range: 21 - 35 years) were examined with a 3T MRI scanner. Orientation of FT and FJ were assessed for L3/4, L4/5 and L5/S1 using standard T2 weighted images. Biochemical gagCEST imaging was used to determine the GAG content of each nucleus pulposus (NP) and annulus fibrosus (AF).

RESULTS

Significantly higher gagCEST values of NP were found in volunteers without FT and normal FJ orientation compared to volunteers with FT and sagittal FJ orientation > 45° (p < 0.0001). GagCEST values were significantly higher in volunteers without FT compared to volunteers with moderate or severe FT (moderate FT: p < 0.0001; severe FT: p = 0.0033). Volunteers with normal FJ orientation showed significantly higher gagCEST values compared to those with sagittal FJ orientation > 45° (p < 0.001). We found a significant, negative correlation between gagCEST values and higher angels in sagittal FJ orientation (rho=-0.459; p < 0.0001).

CONCLUSION

GagCEST analysis demonstrated significantly lower GAG values of NP in young volunteers with FT and sagittal orientated FJ, indicating that FT and sagittal orientation of the FJ represent risk factors for the development of early biochemical alterations of lumbar IVDs.

CLINICAL RELEVANCE/APPLICATION

gagCEST imaging may be an additional feature in the evaluation of the biochemical composition in lumbar intervertebral discs on a clinical 3T MRI system and may be a powerful, non-invasive tool to investigate early disc degeneration processes.

SSJ14-05 Dynamic Creatine CEST MRI for Measuring Muscle Fatigability Post Exercise

Tuesday, Nov. 29 3:40PM - 3:50PM Room: S504CD

Participants

Alessandro Scotti, Chicago, IL (*Presenter*) Nothing to Disclose Rongwen Tain, PhD, Chicago, IL (*Abstract Co-Author*) Nothing to Disclose Xiaohong J. Zhou, PhD, Chicago, IL (*Abstract Co-Author*) Nothing to Disclose Kejia Cai, PhD, Chicago, IL (*Abstract Co-Author*) Nothing to Disclose

PURPOSE

Chronic fatigability is a pathological condition associated with abnormally fast exhaustion and slow energy restoration. Muscular fatigability prevents people from exercising, leading to obesity and progressive mobility impairment. Many studies investigated the rate of phosphocreatine (PCr) re-synthesis after exercise as a measure of energetic restoration rate. However, the detection of PCr by 31P-MRS is associated with long scan times and poor spatial resolution. Creatine (Cr), a key metabolites in cellular energy system, can be imaged with high resolution using an emerging method, Cr Chemical Exchange Saturation Transfer (CrCEST) MRI. Herein, we demonstrate a quantitative method for mapping energy restoration rate, an index for muscular fatigability, by fitting the post-exercise dynamic CrCEST data.

METHOD AND MATERIALS

Six healthy subjects underwent MRI at a 3T scanner while performing a physical exercise consisting of repeated pushes (1Hz rate) on a mildly loaded pedal (16 lbs) for 3 minutes. After B0 and B1 mapping, the calf muscles were imaged at rest and for 12 minutes following the workout by a series of fast CrCEST sequences with two pairs of offsets around 2ppm. Assuming a linear signal variation in the range between the two offsets, the B0-corrected CrCEST map at 2ppm was determined according to the deviation in the B0 map.

CrCEST maps were created at each time point, showing spatial variation in muscle activation. The time constant of the CrCEST contrast decay during the recovery phase was quantified pixelwise with a mono-exponential function. Our preliminary results demonstrate that subjects with high maximum voluntary strength showed much shorter energy restoration time (<5 minutes) compared to subjects with lower strength (>25 minutes) in the working muscles.

CONCLUSION

The design of the dynamic CEST sequence with only 2 offsets allows for fast acquisitions, and thus to distinguish Cr expression in different working muscles with unprecedented spatial and temporal resolution. Mapping the post-exercise energy restoration rate by our technique may have broad clinical impacts on the management of chronic fatigability.

CLINICAL RELEVANCE/APPLICATION

Dynamic bionergetic MRI based on creatine CEST contrast can have broad clinical impacts on the monitoring and management of chronic fatigability.

SSJ14-06 Non-Invasive Imaging of Human Intestinal Perfusion and Oxygenation of Hemoglobin in Patients with Crohn's Disease Using Multispectral Optoacoustic Tomography

Tuesday, Nov. 29 3:50PM - 4:00PM Room: S504CD

Participants

Ferdinand Knieling, Erlangen, Germany (*Presenter*) Nothing to Disclose Cornelia Egger, Erlangen, Germany (*Abstract Co-Author*) Nothing to Disclose Jing Claussen, Munich, Germany (*Abstract Co-Author*) Employee, iThera Medical GmbH Alexander Urich, Munchen, Germany (*Abstract Co-Author*) Nothing to Disclose Stefan Morscher, Munchen, Germany (*Abstract Co-Author*) Nothing to Disclose Stefan Morscher, Flangen, Germany (*Abstract Co-Author*) Nothing to Disclose Christian Kielisch, Erlangen, Germany (*Abstract Co-Author*) Nothing to Disclose Sarah Fischer, MD, Erlangen, Germany (*Abstract Co-Author*) Nothing to Disclose Alexander Hagel, Erlangen, Germany (*Abstract Co-Author*) Nothing to Disclose Rudiger Gortz, Erlangen, Germany (*Abstract Co-Author*) Nothing to Disclose Rudiger Gortz, Erlangen, Germany (*Abstract Co-Author*) Nothing to Disclose Rudiger Gortz, Erlangen, Germany (*Abstract Co-Author*) Nothing to Disclose Dane Wildner, Erlangen, Germany (*Abstract Co-Author*) Nothing to Disclose Date Wildner, Erlangen, Germany (*Abstract Co-Author*) Nothing to Disclose Date Wildner, Erlangen, Germany (*Abstract Co-Author*) Nothing to Disclose Date H. Strobel, MD, Erlangen, Germany (*Abstract Co-Author*) Nothing to Disclose Deike H. Strobel, MD, Erlangen, Germany (*Abstract Co-Author*) Nothing to Disclose Markus F. Neurath, Erlangen, Germany (*Abstract Co-Author*) Nothing to Disclose

PURPOSE

Multispectral Optoacoustic Tomography (MSOT) is a physical imaging approach to examine tissue by utilizing the photoacoustic effect to detect molecules based on their characteristic absorption spectra. The aim of the study was to non-invasively image human intestinal perfusion and oxygenation status of hemoglobin (hb) in patients with Crohn's disease (CD) and compare the results to clinical parameters of disease activity.

METHOD AND MATERIALS

The trial was registered (ClinicalTrails.gov ID: NCT02622139), ethical board approval was provided, and informed consent was obtained. n=60 patients ($32^{\circ}/28^{\circ}$) were included, mean age: 34.2 ± 13.5 ; n=27 in remission, n=15 with mild, and n=13 with moderate disease according to Harvey Bradshaw Index (HBI). The handheld optoacoustic detector (MSOT Acuity, iThera Medical GmbH, Munich, probe: 3-4MHz, 256 elements) was positioned on the skin of the abdomen. MSOT signals were aquired at 700/730/760/800/850/900nm. From all patients HBI, B-mode&Doppler ultrasound/endoscopic/histologic score, C-reactive protein and total leukocyte count was assessed and compared to MSOT signals.

METHOD AND MATERIALS

The clinical trial was registered (ClinicalTrails.gov Identifier: NCT02622139), ethical board approval was provided, and informed consent was obtained. n=60 patients (32/28) were included, mean age: 34.2 ± 13.5 ; n=27 in remission, n=15 with mild, and n=13 with moderate disease according to HBI. The used device (MSOT EIP 100, iThera Medical GmbH, Munich, probe: 4MHz, 256 elements) comprises as handheld detector that was positioned on the skin of the abdominal wall (Figure 1). Spectra were performed at 700, 730, 760, 800, 850, and 900nm. The region of interest was placed in the colon and 5mm above in the abdominal wall. From all patients Harvey Bradshaw Index (HBI) for disease activity, B-mode&Doppler ultrasound/endoscopic/histologic score, C-reactive protein and total leukocyte count was assessed and compared to MSOT signals.

RESULTS

Using B-Mode imaging, inflamed parts of the intestine were located and MSOT signals were acquired within only about 5 minutes per patient. Bowel wall thickness was 4.9 ± 2.7 mm, imaged at a depth of 19.1 ± 7.2 mm (terminal ileum) or 18.9mm ±6.9 mm (sigma). Using the MSOT system, deoxy- and oxyhemoglobin content in the intestinal wall could be quantified. An increase in oxygenated and deoxygenated hb from histologic grade 0 to 2 (oxy:15.5 ±3.8 vs. 23.8 ± 7.1 ; P =.03; deoxy: 19.9 ± 5.0 vs. 27.5 ± 3.6 ; P =.01) with a further rise in grade 3 (26.7 ± 5.1 ; P =.004; 26.3 ± 4.5 ; P =.02) was observed. Total hb increased from grade 0 to 2 (35.4 ± 6.6 vs. 51.3 ± 9.1 ; P =.005) also followed by a further rise in grade 3 (53.0 ± 9.0 ; P =.001). Ultrasound showed moderate correlation with histology (R^2 =.51, P<.0001); laboratory assessments did not show significant correlations with disease activity.

CONCLUSION

MSOT is a promising clinical translatable real-time, non-invasive modality to visualize inflammation in patients with CD. Further human studies are needed to define absolute cut-off parameters.

CLINICAL RELEVANCE/APPLICATION

This is a clinical feasibility study showing that MSOT enables physicians to quickly and non-invasivly assess the disease acitvity of CD in order to personalize therapeutic decisions.

Emerging Technologies: Prostate Cancer Imaging & Management

Tuesday, Nov. 29 4:30PM - 6:00PM Room: S505AB

GU MI MR NM

AMA PRA Category 1 Credits ™: 1.50 ARRT Category A+ Credits: 1.50

Participants

Peter L. Choyke, MD, Rockville, MD, (pchoyke@nih.gov) (*Moderator*) Researcher, Koninklijke Philips NV; Researcher, General Electric Company; Researcher, Siemens AG; Researcher, iCAD, Inc; Researcher, Aspyrian Therapeutics, Inc; Researcher, ImaginAb, Inc; Researcher, Aura Biosciences, Inc

LEARNING OBJECTIVES

1) Understand current issues in prostate cancer relevant to imaging. 2) Understand the role of emerging technologies in the imaging and management of prostate cancer.

ABSTRACT

Prostate cancer is a major health issue. Imaging has made great strides in the last decade including the use of multiparametric MRI, MR-ultrasound fusion biopsies and most recently PET scanning. This refresher course explores emerging technolgies in prostate cancer imaging and management.

Sub-Events

RC417A Introduction to Imaging in Prostate Cancer

Participants

Peter L. Choyke, MD, Rockville, MD, (pchoyke@nih.gov) (*Presenter*) Researcher, Koninklijke Philips NV; Researcher, General Electric Company; Researcher, Siemens AG; Researcher, iCAD, Inc; Researcher, Aspyrian Therapeutics, Inc; Researcher, ImaginAb, Inc; Researcher, Aura Biosciences, Inc

LEARNING OBJECTIVES

1) Understand the impact of new screening guidelines on imaging of prostate cancer. 2) Understand the issues facing clinicians treating prostate cancer.

ABSTRACT

This talk will review the current status of screening for prostate cancer and how stage migration is beginning to be seen. The problems of early detection, early recurrence and early metastases will be discussed. This talk will serve as a starting off point for the subsequent talks on new technologies.

RC417B Next Generation Prostate MRI

Participants

Baris Turkbey, MD, Bethesda, MD, (turkbeyi@mail.nih.gov) (Presenter) Nothing to Disclose

LEARNING OBJECTIVES

1) Understand current status and uses of multi-parametric MRI. 2) Understand role of MRI in assessment of prostate cancer agressiveness and tumor heterogeneity. 3) Understand role of computer aided diagnosis systems in evaluation of prostate cancer agressiveness and tumor heterogeneity.

ABSTRACT

RC417C Molecular Prostate Imaging: Chemistry to Clinic

Participants

Martin G. Pomper, MD, PhD, Baltimore, MD (*Presenter*) Shareholder, CTS, Inc; Board Member, CTS, Inc; Research Grant, CTS, Inc; Advisor, CTS, Inc; Institutional license agreement, Progenics Pharmaceuticals, Inc; Institutional license agreement, Advanced Accelerator Applications SA; Institutional license agreement, LI-COR, Inc; Institutional license agreement, BIND Therapeutics, Inc

LEARNING OBJECTIVES

View learning objectives under the main course title.

RC417D PET/MRI: Is Prostate Cancer a Perfect Fit?

Participants

Peter L. Choyke, MD, Rockville, MD, (pchoyke@nih.gov) (*Presenter*) Researcher, Koninklijke Philips NV; Researcher, General Electric Company; Researcher, Siemens AG; Researcher, iCAD, Inc; Researcher, Aspyrian Therapeutics, Inc; Researcher, ImaginAb, Inc; Researcher, Aura Biosciences, Inc

LEARNING OBJECTIVES

1) Understand the potential value of PET/MRI in prostate cancer.

ABSTRACT

PET/MRI offers the sensitivity and specificity of PET with the high contrast resolution of MRI. In the prostate this can be very useful in identifying prostate cancers and recurrent disease after treatment. This talk will review the various features of PET/MRI that make prostate cancer a "perfect fit" for it.

RC417E Hyperpolarized C-13 MR Molecular Imaging of Prostate Cancer

Participants

Daniel B. Vigneron, PhD, San Francisco, CA (Presenter) Research Grant, General Electric Company; Research Grant, GlaxoSmithKline

LEARNING OBJECTIVES

View learning objectives under the main course title.

Deconstructing Tumors with Imaging

Tuesday, Nov. 29 4:30PM - 6:00PM Room: S404AB

MI OI

AMA PRA Category 1 Credits ™: 1.50 ARRT Category A+ Credits: 1.50

FDA Discussions may include off-label uses.

Participants

Sub-Events

RC418A Imaging Proteomics Genomics Interaction - New Frontiers Ahead

Participants

Evis Sala, MD, PhD, New York, NY, (salae@mskcc.org) (Presenter) Nothing to Disclose

LEARNING OBJECTIVES

1) Learn the major differences between proteome and genome data. 2) Discuss how the proteome signal might be correlated with imaging features. 3) Provide insights into imaging of proteomics-genomics interaction.

ABSTRACT

Honored Educators

Presenters or authors on this event have been recognized as RSNA Honored Educators for participating in multiple qualifying educational activities. Honored Educators are invested in furthering the profession of radiology by delivering high-quality educational content in their field of study. Learn how you can become an honored educator by visiting the website at: https://www.rsna.org/Honored-Educator-Award/

Evis Sala, MD, PhD - 2013 Honored Educator

RC418B Imaging of Angiogenesis: What Do Vessels Tell Us about Tumors?

Participants

Roberto Garcia Figueiras, MD, PhD, Santiago de Compostela, Spain, (roberto.garcia.figueiras@sergas.es) (*Presenter*) Nothing to Disclose

LEARNING OBJECTIVES

1) Improve basic knowledge and skills relevant to the evaluation of angiogenesis in clinical practice.2) Get an overview of the most relevant functional imaging modalities that are available.3) Apply the most appropriate imaging technique for evaluating tumor angiogenic phenotype and tumor response.4) Understand imaging limitations and technical requirements.

ABSTRACT

Tumor angiogenesis is the process whereby new blood vessels are formed in order to supply nutrients and oxygen to support the growth of tumors. Angiogenesis is a key cancer hallmark and an important target for cancer therapy. This lecture reviews the biological basis behind imaging features and the different imaging modalities used to assess the status of tumor neovasculature in vivo and tumor vascular changes secondary to different therapies.

Handout:Roberto Garcia Figueiras

http://abstract.rsna.org/uploads/2016/16000386/HANDOUT RC418B.pdf

RC418C Multiparametric Imaging of Bone Marrow Metastatic Disease

Participants

Anwar R. Padhani, MD, FRCR, Northwood, United Kingdom, (anwar.padhani@stricklandscanner.org.uk) (*Presenter*) Advisory Board, Siemens AG; Speakers Bureau, Siemens AG; Researcher, Siemens AG; Speakers Bureau, Johnson & Johnson

LEARNING OBJECTIVES

1) To become familiar with the normal appearances of bone marrow on PET/MRI/CT scans and how these reflect underlying biologic properties. 2) To understand the biologic mechanisms responsible for osteoblastic and osteolytic lesions in malignancy settings. 3) To explain how imaging appearances of normal and pathologic bone marrow reflect therapy impacts. 4) To innumerate the professional challenges for implementing multiparametric imaging in bone therapy monitoring.

ABSTRACT

Honored Educators

Presenters or authors on this event have been recognized as RSNA Honored Educators for participating in multiple qualifying educational activities. Honored Educators are invested in furthering the profession of radiology by delivering high-quality educational content in their field of study. Learn how you can become an honored educator by visiting the website at: https://www.rsna.org/Honored-Educator-Award/

Anwar R. Padhani, MD, FRCR - 2012 Honored Educator

RC418D Imaging Tumor Metabolism with Hyperpolarized MRI

Participants

Kayvan Keshari, PhD, New York, NY (Presenter) Nothing to Disclose

LEARNING OBJECTIVES

1) Comprehend the basic principles of hyperpolarized MRS. 2) Assess the potential of using hyperpolarized probes to study cancer metabolism. 3) Assess the changes in cancer metabolism across multiple tumor types.

ABSTRACT

Oncogenic transformation has been shown to have a dramatic impact on the metabolic state of the cell. Recent work has shown that hyperpolarization of endogenous substrates can be used to trace metabolism in the setting of cancer, non-invasively in vivo. In this this educational lecture, we will discuss the use of hyperpolarized 13C molecules in the setting of cancer imaging, spanning a number of molecules, which have been used preclinically as well as hyperpolarized pyruvate which has recently been used in the clinic.

Molecular Imaging Wednesday Case of the Day

Wednesday, Nov. 30 7:00AM - 11:59PM Room: Case of Day, Learning Center

MI

AMA PRA Category 1 Credit ™: .50

Participants

Jonathan E. McConathy, MD, PhD, Birmingham, AL (Presenter) Research Consultant, Eli Lilly and Company; Research Consultant, Blue Earth Diagnostics Ltd; Research Consultant, Siemens AG; Research Consultant, General Electric Company; Suzanne E. Lapi, PhD, Birmingham, AL (Presenter) Research Grant, AbbVie Inc; Spouse, Consultant, General Electric Company; Consultant, Siemens AG; Consultant, Blue Earth Diagnostics Ltd; Consultant, Eli Lilly and Company Matthias J. Eiber, MD, Muenchen, Germany (Abstract Co-Author) Nothing to Disclose Thomas A. Hope, MD, San Francisco, CA (Abstract Co-Author) Research Grant, Consultant, GE Healtcare Robert R. Flavell, MD, PhD, San Francisco, CA (Abstract Co-Author) Nothing to Disclose Samuel J. Galgano, MD, Birmingham, AL (Abstract Co-Author) Nothing to Disclose Asim K. Bag, MD, Birmingham, AL (Abstract Co-Author) Nothing to Disclose David M. Schuster, MD, Atlanta, GA (Abstract Co-Author) Institutional Research Grant, Nihon Medi-Physics Co, Ltd; Institutional Research Grant, Blue Earth Diagnostics Ltd; Consultant, WellPoint, Inc; ; Ephraim E. Parent, MD, PhD, Saint Louis, MO (Abstract Co-Author) Nothing to Disclose Bital Savir-Baruch, MD, Maywood, IL (Abstract Co-Author) Nothing to Disclose Pamela K. Woodard, MD, Saint Louis, MO (Abstract Co-Author) Research Grant, Astellas Group; Research Grant, Bayer AG; Research agreement, Siemens AG; ; ; ; Sebastian R. McWilliams, MBBCh, Saint Louis, MO (Abstract Co-Author) Nothing to Disclose Amir K. Durrani, MD, St Louis, MO (Abstract Co-Author) Nothing to Disclose Robert J. Gropler, MD, Saint Louis, MO (Abstract Co-Author) Nothing to Disclose Michael Hofman, PhD, San Francisco, CA (Abstract Co-Author) Nothing to Disclose Man Chun Jeffrey Lau, MD, PhD, Saint Louis, MO (Abstract Co-Author) Nothing to Disclose Richard Laforest, PhD, Saint Louis, MO (Abstract Co-Author) Nothing to Disclose

TEACHING POINTS

1) Interpret amyloid-PET scans as positive or negative. 2) Apply appropriate use criteria for selecting patients for amyloid-PET study. 3) Understand the goals of the IDEAS study as it relates to coverage with evidence development for clinical amyloid-PET scans.

RC523

Molecular Imaging Mini-Course: Clinical Applications of Molecular Imaging-Oncology

Wednesday, Nov. 30 8:30AM - 10:00AM Room: S403A

MI OI PH

AMA PRA Category 1 Credits ™: 1.50 ARRT Category A+ Credits: 1.50

FDA Discussions may include off-label uses.

Participants

Sub-Events

RC523A Diagnosis

Participants

Terence Z. Wong, MD, PhD, Chapel Hill, NC, (tzwong@med.unc.edu) (Presenter) Nothing to Disclose

LEARNING OBJECTIVES

1) Discuss the value of combined FDG-PET and CT for diagnosing malignant disease.2) Discuss selection of PET radiotracers the potential role of non-FDG PET tracers in managing patients with cancer.

RC523B Staging

Participants

Dominique Delbeke, MD, PhD, Nashville, TN, (dominique.delbeke@vanderbilt.edu) (*Presenter*) Nothing to Disclose

LEARNING OBJECTIVES

1) The potential clinical indications of PET and PET/CT in the evaluation of patients with malignancies. 2) The impact on patient care. 3) Recommendations for PET/CT in the NCCN guidelines.

Active Handout:Dominique Delbeke

http://abstract.rsna.org/uploads/2016/15002834/Handout NCCN.pdf

RC523C Evaluation of Treatment

Participants

David A. Mankoff, MD, PhD, Philadelphia, PA, (david.mankoff@uphs.upenn.edu) (*Presenter*) Speaker, Koninklijke Philips NV; Consultant, General Electric Company; Advisory Board, RefleXion Medical Inc

LEARNING OBJECTIVES

1) List applications of quantitative imaigng for clinical trials. 2) Describe the approach to the design of cancer imaging trials. 3) Discuss biomarkers application for for cancer imaging.

Honored Educators

Presenters or authors on this event have been recognized as RSNA Honored Educators for participating in multiple qualifying educational activities. Honored Educators are invested in furthering the profession of radiology by delivering high-quality educational content in their field of study. Learn how you can become an honored educator by visiting the website at: https://www.rsna.org/Honored-Educator-Award/

David A. Mankoff, MD, PhD - 2013 Honored Educator

Molecular Imaging (Oncology)

Wednesday, Nov. 30 10:30AM - 12:00PM Room: S504CD

MI RO

AMA PRA Category 1 Credits ™: 1.50 ARRT Category A+ Credits: 1.50

FDA Discussions may include off-label uses.

Participants

Umar Mahmood, MD, PhD, Charlestown, MA (*Moderator*) Research Grant, Sabik Medical Inc; Advisory Board, Blue Earth Diagnostics Ltd;

Yasuhisa Fujibayashi, PhD, Fukui, Japan (Moderator) Nothing to Disclose

Sub-Events

SSK11-01 A Dual-Labeled Anti-CD 146 Monoclonal Antibody for PET/NIRF Detection of Liver Malignancies

Awards

Student Travel Stipend Award

Participants

Emily B. Ehlerding, Madison, WI (*Presenter*) Nothing to Disclose Reinier Hernandez, MSc, Madison, WI (*Abstract Co-Author*) Nothing to Disclose Haiyan Sun, Madison, WI (*Abstract Co-Author*) Nothing to Disclose Yunan Yang, Madison, WI (*Abstract Co-Author*) Nothing to Disclose Christopher England, PhD, Madison, WI (*Abstract Co-Author*) Nothing to Disclose Todd Barnhart, Madison, WI (*Abstract Co-Author*) Nothing to Disclose Weibo Cai, PhD, Palo Alto, CA (*Abstract Co-Author*) Nothing to Disclose

PURPOSE

Due to hepatic clearance of the majority of contrast agents, molecular imaging of liver malignancies is challenging. However, overexpression of CD146 has been associated with aggressiveness and metastatic potential in liver cancer. Herein we develop a CD146-targeted probe for high contrast positron emission tomography (PET) and nearinfared fluorescence (NIRF) imaging of liver cancer.

METHOD AND MATERIALS

In vitro expression levels of CD146 were characterized in the liver cancer cell lines HepG2 (+) and Huh7 (-) via several in situ methods. YY146, an anti-CD146 monoclonal antibody, was conjugated to the NIRF dye ZW800-1 and to deferoxamine (Df) for radiolabeling with 89Zr. Sequential PET and NIRF imaging were performed after intravenous injection of 3.7 – 7.4 MBq of 89Zr-Df-YY146-ZW800 in athymic nude mice bearing HepG2 or Huh7 subcutaneous (s.c.) xenografts. Orthotopic tumors were generated by injection of luciferase-transfected HepG2 cells into the liver, allowing progression monitoring by bioluminescent imaging. Multimodality imaging was carried out in mice with confirmed orthotopic liver tumors as described for s.c. tumors. At 168 h p.i., tissues were collected for ex vivo NIRF imaging, biodistribution, and histological studies.

RESULTS

PET and NIRF imaging unveiled a prominent and persistent uptake of 89Zr-Df-YY146-ZW800 in HepG2 tumors that peaked at 31.7±7.2 %ID/g 72 h p.i. Owing to such marked accumulation, the detection of orthotopic HepG2 tumors was successful despite the relatively high liver background. CD146-negative Huh7 and CD146-blocked HepG2 tumors exhibited significantly lower 89Zr-Df-YY146-ZW800 accretion (6.1±0.5 and 8.1±1.0 %ID/g at 72 h p.i., respectively), demonstrating the CD146-specificity of the tracer in vivo. Ex vivo studies verified the accuracy of the imaging data and correlated 89Zr-Df-YY146-ZW800 uptake with in situ CD146 expression.

CONCLUSION

Overall, 89Zr-Df-YY146-ZW800 showed excellent properties as a PET/NIRF imaging agent, including high specificity for CD146expressing liver cancer. Molecular imaging using dual-labeled YY146 had great potential for noninvasive detection and image-guided resection of liver malignancies.

CLINICAL RELEVANCE/APPLICATION

Liver malignancies are often difficult to distinguish from background tissue. Thus, we present a dual nearinfared- and radio-labeled antibody targeting CD146 for detection of these malignancies.

SSK11-02 Role of 11C-Acetate and 18F FDG Dual Tracer PET-CT Scan for Detection of Hepatocellular Carcinoma

Wednesday, Nov. 30 10:40AM - 10:50AM Room: S504CD

Participants

Wan Hang K. Chiu, MBBCh, FRCR, Hong Kong, Hong Kong (*Presenter*) Nothing to Disclose Pek Lan Khong, MBBS, FRCR, Hong Kong, Hong Kong (*Abstract Co-Author*) Nothing to Disclose Tony Kwok Loon Loke, MBBS, FRCR, Hong Kong, Hong Kong (*Abstract Co-Author*) Nothing to Disclose Joseph K. Lee, MD, Singapore, Singapore (*Abstract Co-Author*) Nothing to Disclose

PURPOSE

Up to 45% of Hepatocellular Carcinoma (HCC) show atypical contrast enhancement (CE) pattern on CT/MR, thereby requiring

histologic confirmation. The aim of this study is to evaluate the additional value of Dual Tracer (DT) PET with 11C Acetate (Ac) and 18F FDG for detection and characterization of HCC.

METHOD AND MATERIALS

Consecutive patients who had histological confirmation of HCC and underwent CT/MR and DT in our centres from 2014-16 were identified. CE and PET uptake patterns were reviewed. Typical CE pattern on CT/MR was arterial hyperenhancement followed by portovenous/delayed phase washout. All other CE patterns were considered atypical. On PET, a lesion was deemed positive by visual inspection of lesion above background liver uptake on Ac and/or FDG. Results were compared with tumor size and grade on histology. Tumour size were separated into <3 cm, 3-5 cm and >5 cm groups as each has different treatment option. Grading was based on Edmondson and Steiner system. Pearson's Chi-Square tests were applied to compare the sensitivities and ANOVA-test for subgroup analysis.

RESULTS

Thirty-two HCC lesions from 24 patients were identified (mean size \pm SD 34 \pm 27 mm). The sensitivity of CT/MR by CE pattern was 53%, FDG alone 56%, Ac alone 94%, DT 97% and combined CT/MR with DT 100% (p<0.0001).Two lesions were non-Ac avid. Enhancement pattern were not affected by tumour size whereas FDG sensitivities increase with tumour size from 39% to 67% and 75% for lesions <3 cm, 3-5 cm and >5cm respectively.Histological grade available in 30 lesions were well differentiated HCC (n=7), moderately-differentiated HCC (n=22) and poorly differentiated HCC (n=1). Atypical enhancement pattern was more common in well-differentiated compared to moderately-differentiated lesions (71% vs 45%). No trend was observed for tracer avidities in different grades of HCC.

CONCLUSION

DT combined with CT/MR increases the sensitivity of HCC detection compared to CT/MR alone, providing 100% sensitivity and hence, being most helpful in equivocal liver lesions with atypical contrast enhancement.

CLINICAL RELEVANCE/APPLICATION

The use of DT obviates tissue sampling for diagnosing HCC in patients with liver lesions with atypical CT/MR contrast enhancement.

SSK11-03 64Cu-Labeled Ipilimumab for Determination of CTLA-4 Levels in Lung Cancer

Wednesday, Nov. 30 10:50AM - 11:00AM Room: S504CD

Participants

Emily B. Ehlerding, Madison, WI (*Presenter*) Nothing to Disclose Christopher England, PhD, Madison, WI (*Abstract Co-Author*) Nothing to Disclose Stephen Graves, Madison, WI (*Abstract Co-Author*) Nothing to Disclose Glenn Liu, Madison, WI (*Abstract Co-Author*) Nothing to Disclose Robert J. Nickles, PhD, Madison, WI (*Abstract Co-Author*) Nothing to Disclose Weibo Cai, PhD, Palo Alto, CA (*Abstract Co-Author*) Nothing to Disclose

PURPOSE

CTLA-4 is expressed on the surface of activated T cells and some cancer cells, and is the target of the clinically-approved monoclonal antibody Ipilimumab. Ipilimumab is only successful in a small subset of patients, making neoadjuvant patient selection crucial. In this study, we employ radiolabeled 64Cu-DOTA-Ipilimumab to monitor CTLA-4 expression levels in subcutaneous (s.c.) lung cancer xenografts using positron emission tomography (PET).

METHOD AND MATERIALS

Ipilimumab was conjugated with the chelator 1,4,7,10-tetraazacyclododecane-1,4,7,10-tetraacetic acid (DOTA) for radiolabeling with 64Cu (t1/2 = 12.7 h). Western blot, ELISA, flow cytometry, and live cell imaging were employed to determine the CTLA-4 expression levels of three lung cancer cell lines: A549, H460, and H358. Longitudinal PET studies following intravenous injection of 64Cu-DOTA-Ipilimumab into mice bearing s.c. xenografts of the aforementioned lung cancer cells allowed for tracer uptake to be quantified up to 48 h p.i. Ex vivo biodistribution and histological studies were employed to verify PET results.

RESULTS

By in situ analysis, A549 was found to have the highest CTLA-4 expression level, and H358 the lowest. PET quantification verified these results, with A549 tumor uptake peaking at $13.1 \pm 3.9 \text{ }\%\text{ID/g}$, H460 at $10.5 \pm 1.9 \text{ }\%\text{ID/g}$, and H358 at $8.3 \pm 1.3 \text{ }\%\text{ID/g}$, 48 h p.i. A549-blocked mice also displayed decreased tracer uptake values at $8.1 \pm 1.0 \text{ }\%\text{ID/g}$. Ex vivo analysis following the terminal imaging timepoint also corroborated these findings.

CONCLUSION

Radiolabeled 64Cu-DOTA-Ipilimumab is able to differentiate tumors based on their CTLA-4 expression levels noninvasively using PET. Thus, this antibody holds promise to be employed in small doses prior to immunotherapy treatment to predict the success of such anti-CTLA-4 therapy and aid in patient selection.

CLINICAL RELEVANCE/APPLICATION

Anti-CTLA-4 immunotherapies are effective in a small subset of patients. Thus, we use 64Cu-DOTA-Ipilimumab to determine tumors which have high expression levels and may respond well to such therapy.

SSK11-04 Molecular Optical Imaging in Radiofrequency Heating-Enhanced Direct Intratumoral HSV-TK Gene Therapy of Cholangiocarcinoma

Wednesday, Nov. 30 11:00AM - 11:10AM Room: S504CD

Participants Yin Jin, MD, Seattle, WA (*Presenter*) Nothing to Disclose Feng Zhang, MD, Seattle, WA (*Abstract Co-Author*) Nothing to Disclose

Jun Gao, MD, PhD, Seattle, WA (Abstract Co-Author) Nothing to Disclose

Xiaoming Yang, MD, PhD, Seattle, WA (Abstract Co-Author) Nothing to Disclose

PURPOSE

To validate the feasibility of using molecular optical imaging to monitor radiofrequency heating (RFH)-enhanced herpes simplex virus thymidine kinase (HSV-TK)/ganciclovir (GCV) therapy of cholangiocarcinomas.

METHOD AND MATERIALS

This study included in-vitro confirmation experiments with luciferase/mCherry-labelled human cholangiocarcinoma cells (Mz-Cha-1) and in-vivo validation experiments using mouse models with luciferase/mCherry-cholangiocarcimonas. Both in-vitro and in-vivo experiments were divided into four groups with treatments of: (i) combination therapy (green fluorescent protein (GFP)/HSV-TK/plasmid gene transfection plus RFH at 42°C, and followed by ganciclovir administration; (ii) gene therapy alone; (iii) RFH alone; and (iv) saline. GFP optical imaging was first performed to detect successful expression of GFP/HSV-TK genes, while bioluminescent optical imaging used to follow up tumor responses to various treatments among different groups, which were correlated with subsequent histologic confirmation.

RESULTS

Of in-vitro experiments, MTS assay demonstrated the lowest cell proliferation in combination therapy compared with three control groups ($24.1\pm7.2\%$ vs $41.6\pm4.9\%$ vs $72.3\pm7.9\%$ vs 100%, p<0.05). Of in-vivo experiments, GFP optical imaging detected greater green fluorescent signal from GFP/HSV-TK/plasmid-transfected tumors than non-gene transfected tumors (200.73 ± 37.85 VS 52.80 ± 17.36 , p<0.05), which indicated successful expression of GFP/HSV-TK genes. Bioluminescent optical imaging demonstrated decreases of both bioluminescence signals and tumor sizes in combination therapy, compared to other control groups (0.68 ± 0.11 vs 1.47 ± 0.19 vs 2.01 ± 0.33 vs 2.33 ± 0.41 , p<0.05), which were confirmed by histologic correlation (Figure).

CONCLUSION

We have established the "proof-of-principle" of using molecular optical imaging to monitor RFH-enhanced GFP/HSV-TK/plasmid gene expression and HSV-TK/GCV gene therapy of cholangiocarcinoma. This concept may pave a new avenue for management of pancreatobiliary malignancies by simultaneous integration of molecular optical imaging, radiofrequency technology, interventional oncology, and direct intratumoral gene therapy.

CLINICAL RELEVANCE/APPLICATION

This concept may pave a new avenue for management of cholangiocarcinoma by simultaneous integration of molecular optical imaging, radiofrequency technology, interventional oncology, and gene therapy.

SSK11-05 89Zr-Labeled Pembrolizumab for Neoadjuvant Imaging and Human Dosimetry Estimation

Wednesday, Nov. 30 11:10AM - 11:20AM Room: S504CD

Participants

Emily B. Ehlerding, Madison, WI (*Presenter*) Nothing to Disclose Christopher England, PhD, Madison, WI (*Abstract Co-Author*) Nothing to Disclose Reinier Hernandez, MSc, Madison, WI (*Abstract Co-Author*) Nothing to Disclose Stephen Graves, Madison, WI (*Abstract Co-Author*) Nothing to Disclose Todd Barnhart, Madison, WI (*Abstract Co-Author*) Nothing to Disclose Weibo Cai, PhD, Palo Alto, CA (*Abstract Co-Author*) Nothing to Disclose

PURPOSE

Pembrolizumab is a clinically-available humanized monoclonal antibody that targets programmed cell death protein (PD-1) on the surface of activated T and B cells. In order to potentially identify patients who would benefit from such therapy, herein we evaluate the pharmacokinetics, biodistribution, and dosimetry of 89Zr-labeled pembrolizumab in vivo using positron emission tomography (PET).

METHOD AND MATERIALS

Pembrolizumab was conjugated with the chelator desferrioxamine (Df) for radiolabeling with 89Zr (t1/2 = 3.3 days). Whole-body tracking of the radiolabeled antibody was compared in two murine models, including NSG and PBL mice (NSG mice reconstituted with human peripheral blood mononuclear cells). Mice were injected with 5-10 MBq of radiolabeled antibody. Timepoints from 0.5 h to 168 h p.i. were utilized in the PET study to fully capture the pharmacokinetics of Pembrolizumab. Biodistribution data obtained from PET scans were extrapolated to predict radiation dose estimates in humans.

RESULTS

In all groups, 89Zr-Df-Pembrolizumab stayed in circulation throughout the study and accumulated greatest in liver and spleen. Notable biodistribution differences between PBL and NSG mice included significant uptake in salivary glands in PBL mice, indicating the specificity of Pembrolizumab for human T-cells, which localize here following an autoimmune response. Peak uptake values for the liver of $14.40 \pm 1.55 \text{ }\%\text{ID/g}$ for PBL and $12.93 \pm 1.96 \text{ }\%\text{ID/g}$ for NSG mice, and for the spleen of $7.33 \pm 1.53 \text{ }\%\text{ID/g}$ for PBL and $5.48 \pm 0.71 \text{ }\%\text{ID/g}$ for NSG were found 0.5 h p.i. with values steadily declining thereafter. Even with relatively high uptake in these clearance organs, the estimated doses remained well within safe limits, with a total body effective dose of $0.515 \pm 0.005 \text{ mGy/MBq}$ calculated.

CONCLUSION

The low total body and major organ doses found in this study indicate the potential use of 89Zr-Df-Pembrolizumab for the clinical selection of patients that may benefit from anti-PD-1 therapy. The techniques in this study may be further applied to other antibodies for better understanding of the pharmacokinetics, biodistribution, and dosimetry for future clinical applications.

CLINICAL RELEVANCE/APPLICATION

Herein we evaluate a radiolabeled, clinically-approved antibody, 89Zr-Df-Pembrolizumab, targeting PD-1, that could potentially screen for patients who would respond to such anti-PD-1 immunotherapy.

SSK11-06 Prolactin Receptor-Mediated Internalization of Imaging Agents Detects Epithelial Ovarian Cancer with

Enhanced Sensitivity and Specificity

Wednesday, Nov. 30 11:20AM - 11:30AM Room: S504CD

Participants

Karthik M. Sundaram, MD, PhD, Nashville, TN (*Presenter*) Nothing to Disclose Yilin Zhang, PhD, Chicago, IL (*Abstract Co-Author*) Nothing to Disclose Brian B. Roman, PhD, Chicago, IL (*Abstract Co-Author*) Nothing to Disclose Joseph A. Piccirilli, PhD, Chicago, IL (*Abstract Co-Author*) Nothing to Disclose Ernst Lengyel, MD,PhD, Chicago, IL (*Abstract Co-Author*) Nothing to Disclose

PURPOSE

To develop a highly sensitive, specific, and clinically amenable molecular imaging agent for ovarian cancer diagnosis that enables (i) detection of tumors when they are still small, confined to the pelvis, and curable and (ii) differentiation between benign and malignant ovarian tumors.

METHOD AND MATERIALS

We used tissue microarray analysis to identify the prolactin receptor (PRLR) as a high specificity biomarker for malignant OvCa. We conjugated gadolinium-chelates and near-infrared fluorescence imaging probes to human placental lactogen (hPL), a specific and high affinity PRLR ligand, and evaluated internalization by PRLR (+) and PRLR (-) ovarian cancer cells. We further evaluated that capacity of hPL-conjugates and reduced binding hPL analog conjugates to imaging mouse xenografts of human ovarian cancer by magnetic resonance imaging and near-infrared fluorescence imaging.

RESULTS

Our results indicate that > 98% of OvCas over-express PRLR regardless of stage, grade, and type. Furthermore, we show both hPLgadolinium conjugates and hPL-near-infrared probes conjugates internalize specifically and efficiently into PRLR (+) cancer cells in OvCa mouse models. This enables detection of xenograft PRLR (+) tumors in mice with substantially greater specificity and sensitivity than currently used clinical contrast agents.

CONCLUSION

Using prolactin receptor-mediated internalization, hPL-conjugates demonstrate the specificity to distinguish PRLR (+) from PRLR (-) tumors in mouse models of ovarian cancer. Given that > 98% of OvCas over-express PRLR, we believe our ability to image PRLR will enhance specificity and sensitivity of ovarian cancer diagnosis.

CLINICAL RELEVANCE/APPLICATION

Given the difficulties of currently used methods for ovarian cancer diagnosis, we believe molecular PRLR imaging using hPLconjugates will engender a new paradigm for targeted molecular imaging of OvCa. Coupled with magnetic resonance imaging, molecular PRLR imaging holds the potential to achieve a more precise and earlier diagnosis of OvCa, thereby reducing the number of unnecessary surgeries and increasing patient survival.

SSK11-07 Designed Multifunctional Gold Nanocomposites for Targeted Tri-Mode CT/MR/ Optical Imaging of Human Non-Small Cell Lung Cancer Cells

Wednesday, Nov. 30 11:30AM - 11:40AM Room: S504CD

Participants

Jingwen Chen, Shanghai, China (*Presenter*) Nothing to Disclose Qian Chen, Shanghai, China (*Abstract Co-Author*) Nothing to Disclose Gui-Xiang Zhang, MD, Shanghai, China (*Abstract Co-Author*) Nothing to Disclose Xiang-Yang Shi, Shanghai, China (*Abstract Co-Author*) Nothing to Disclose Han Wang, MD, PhD, Shanghai, China (*Abstract Co-Author*) Nothing to Disclose

PURPOSE

The high incidence and mortality rate of non-small cell lung cancer (NSCLC) prompts exhaustive efforts to develop new effective methods for its diagnosis at the early-stage to improve the survival rate. We are developing multifuctional gold nanocomposites to use as the nanoprobes for targeted tri-mode CT / MR / optical imaging of human non-small cell cancer cells both in vitro and in vivo.

METHOD AND MATERIALS

Amine-terminated generation 5 poly(amidoamine) dendrimers were used as a nanoplatform to be covalently modified with Gd chelator, Cy5.5, and FA. Then the multifunctional dendrimers were used as templates to entrap gold nanoparticles, followed by chelating Gd(III) ions and acetylation of the remaining dendrimer terminal amines. The thus-formed multifunctional Au DENPs (in short, Cy5.5-Gd-Au DENPs-FA) were characterized via different techniques, and then were used for both in vitro and in vivo targeted CT/ MR/ NIR optical tri-mode imaging of human NSCLC cells (NCI-H460 cells) and the xenograft tumor model.

RESULTS

CT/MR/optical images show that NCI-H460 cells can be detected after incubation with the Cy5.5-Gd-Au DENPs-FA in vitro and the xenograft tumor model can be imaged after intravenous administration of the particles. Combine the inductively coupled plasmaatomic emission spectroscopy (ICP-AES) measurements with the transmission electron microscopy (TEM) data confirm that the Cy5.5-Gd-Au DENPs-FA is able to be uptaken by the treated cells. MTT (3-(4,5-dimethylthiazol-2-yl)-2,5-diphenyltetrazolium bromide) assay show that the Cy5.5-Gd-Au DENPs-FA has a good biocompatibility at the given concentration range.

CONCLUSION

The findings of this study suggest that the developed Cy5.5-Gd-Au DENPs-FA may be used as a promising tri-mode nanoprobe for targeted CT/MR/opticl imaging of human NSCLC and other folate receptor (FR) over-expressing cancers.

CLINICAL RELEVANCE/APPLICATION

In consideration of the special structural characteristic, the dendrimer based nanocomposites may be further modified with therapeutic antibodies or small interfering RNA (siRNA) to be expectably developed for the personalized theranostics of cancers at early-stage with the high accuracy and sensitivity.

SSK11-08 Differential Uptake of CD146-Specific Antibody in Solid Lung Malignancies

Wednesday, Nov. 30 11:40AM - 11:50AM Room: S504CD

Participants

Christopher England, PhD, Madison, WI (*Presenter*) Nothing to Disclose Haiyan Sun, Da Lian, China (*Abstract Co-Author*) Nothing to Disclose Reinier Hernandez, MSc, Madison, WI (*Abstract Co-Author*) Nothing to Disclose Yunan Yang, Madison, WI (*Abstract Co-Author*) Nothing to Disclose Todd Barnhart, Madison, WI (*Abstract Co-Author*) Nothing to Disclose Weibo Cai, PhD, Palo Alto, CA (*Abstract Co-Author*) Nothing to Disclose

PURPOSE

Recent studies have revealed that a cell surface protein called CD146 is a marker of epithelial-to-mesenchymal transition (EMT) in cancer cells whose overexpression has also been found to correlate with cancer progression, invasion, and metastasis. Additionally, CD146 has low background levels in normal tissue as well as differential expression in metastases and advanced primary tumors, showing its significant potential in cancer therapies. This study evaluates the utilization of YY146, an anti-CD146 monoclonal antibody, for molecular imaging of solid lung malignancies.

METHOD AND MATERIALS

The anti-CD146 antibody (YY146) was conjugated to 1,4,7-triazacyclononane-triacetic acid (NOTA) and radiolabeled with 64Cu. CD146 expression was evaluated in six human lung cancer cell lines (A549, NCI-H358, NCI-H522, HCC4006, H23, and NCI-H460) by flow cytometry and quantitative Western blot studies. The biodistribution and tumor uptake of 64Cu-NOTA-YY146 was assessed by sequential PET imaging in athymic nude mice bearing subcutaneous lung cancer xenografts. The correlation between CD146 expression and tumor uptake of 64Cu-NOTA-YY146 was evaluated by graphical software while ex vivo biodistribution and immunohistochemistry studies were performed to validate the accuracy of PET data and spatial expression of CD146.

RESULTS

Flow cytometry and Western blot studies showed similar findings with H460 and H23 cells highly expressing CD146. Small differences in CD146 expression levels were found between A549, H4006, H522, and H358 cells. Tumor uptake of 64Cu-NOTA-YY146 was highest in CD146-expressing H460 and H23 tumors, peaking at 20.1 ± 2.86 and 11.6 ± 2.34 %ID/g at 48 h post-injection (n=4). Tumor uptake was lowest in the H522 model (4.1 ± 0.98 %ID/g at 48 h post-injection; n=4), while H4006, A549 and H358 exhibited similar uptake of 64Cu-NOTA-YY146. A positive correlation was found between tumor uptake of 64Cu-NOTA-YY146 (%ID/g) and relative CD146 expression (r2=0.98, p<0.01). Ex vivo biodistribution corroborated the accuracy of PET data.

CONCLUSION

The strong correlation between tumor uptake of 64Cu-NOTA-YY146 and CD146 expression demonstrates the potential use of this radiotracer for imaging tumors that elicit varying levels of CD146.

CLINICAL RELEVANCE/APPLICATION

This imaging tracer may promote enhanced monitoring of therapeutic response and improved patient stratification.

SSK11-09 Smartphone based Diagnostics (D3) Enable Molecular Characterization of Lymphoma in Resourcelimited Countries

Wednesday, Nov. 30 11:50AM - 12:00PM Room: S504CD

Awards

Student Travel Stipend Award

Participants

Aoife Kilcoyne, MBBCh, Boston, MA (*Presenter*) Nothing to Disclose Divya Pathania, Boston, MA (*Abstract Co-Author*) Nothing to Disclose Hyungsoon Im, Boston, MA (*Abstract Co-Author*) Nothing to Disclose Hakho Lee, PhD, Boston, MA (*Abstract Co-Author*) Nothing to Disclose Cesar Castro, Boston, MA (*Abstract Co-Author*) Nothing to Disclose Ralph Weissleder, MD, PhD, Boston, MA (*Abstract Co-Author*) Investor, T2 Biosystems, Inc

PURPOSE

A major hurdle in cancer therapy is it's timely diagnosis and treatment. This is of particular concern in resource-limited settings. For example, aggressive forms of non-Hodgkins lymphoma are major health concerns in sub-Saharan Africa. A substantial number of cases evade comprehensive evaluation and are not appropriately classified due to the lack of proper tissue specimens, diagnostic reagents and specialists. Although a good proportion of cases are curable even in low and middle income countries, windows of therapuetic opportunity are often missed due to delay in diagnosis. This necessitates the need for a low-cost, rapid and accurate detection technology to expedite the diagnosis of aggressive lymphomas (and other prevalent cancers) in the resource-limited environment.

METHOD AND MATERIALS

We have developed a digital diffraction diagnostic (D3) platform that allows modern smartphones to be used for molecular cancer diagnostics of scant clinical samples (fine needle aspirates). Fine Needle Aspirate (FNA) samples are immunolabeled with microbeads in a microfluidic module and then holographically detected by the smartphone camera.

RESULTS

Diffraction patterns generated by the antibody-microbeads were detected with the smartphone camera using bright-field settings.

Digital signal processing was used to reconstruct images to count bead-bound cells. We optimized the assay so that thousands of cells could be analyzed without washing steps in near real-time. The D3 profiling results on lymphoma cell lines demonstrated excellent agreement with those by flow cytometry (gold standard). We further analyzed scant clinical samples (FNAs) from 8 patients. The D3 assay generated readouts within an hour and demonstrated agreement (100%) with standard pathology.

CONCLUSION

The D3 approach of molecular analysis could have far reaching applications. The major advantages are the simplicity of the method, the accuracy and it's ability to be used in resource-limited settings.

CLINICAL RELEVANCE/APPLICATION

Leveraging smartphones as a mobile diagnostic terminal could empower resource-poor communities with complex laboratory tests. This work addresses the practical diagnostic needs of low and middle income countries and reflects the type of technologies that may gain sustainable traction in such settings.

Molecular Imaging Wednesday Poster Discussions

Wednesday, Nov. 30 12:15PM - 12:45PM Room: S503AB

MI

AMA PRA Category 1 Credit ™: .50

FDA Discussions may include off-label uses.

Participants

Homer A. Macapinlac, MD, Houston, TX (Moderator) Nothing to Disclose

Sub-Events

MI220-SD-WEA1 Development of a Patient Derived Xenograft Model for Ultrasound Molecular Imaging Applications in Regnal Cell Carcinoma

Station #1

Participants

Ingrid Leguerney, Villejuif, France (*Abstract Co-Author*) Nothing to Disclose Alexandre Ingels, MD, Villejuif, France (*Presenter*) Nothing to Disclose Catherine Sebrie, Orsay, France (*Abstract Co-Author*) Nothing to Disclose Laurene Jourdain, Orsay, France (*Abstract Co-Author*) Nothing to Disclose Jean-Jacques Patard, Le Kremlin-Bicetre, France (*Abstract Co-Author*) Nothing to Disclose Nathalie B. Lassau, MD, PhD, Villejuif, France (*Abstract Co-Author*) Speaker, Toshiba Corporation; Speaker, Bracco Group

PURPOSE

To develop a reliable in vivo model to assess by ultrasound and MRI imaging techniques tumor development and local molecular expressions

METHOD AND MATERIALS

The model used is a patient derived xenograft: a 8 mm tumor core is gathered from a fresh renal cell carcinoma (RCC) at time of surgery. The tissue core is cut in homogenous 300 µm slices with a dedicated device (Krumdieck, Alabama Research & Development). Each slice is engrafted under renal capsula of RAG2-/-Yc-/- immunocompromised mice in order to develop a cohort with the same tumor. The tumor engrafted is routinely followed-up with ultrasound (US) imaging (Aplio, Toshiba and VEVO2100, Visualsonics). Once the tumor is detected, a first 7T MRI (Bruker spectrometer) is performed in order to measure precisely the tumor volume and series of US molecular imaging are performed.US molecular imaging is based on microbubble contrast agents linked with antibodies through (MicroMarker™, Visualsonics). The antibodies selected for our RCC study are VEGFR1 and 2 and FSHR. The targeted signal enhancement is quantified and compared with the untargeted microbubble signal 10 minutes after injection. Imaging is performed. The specific targeted US imaging signal is compared with the MRI specific growth rate (ln(V2/V1)/(t2-t1)) through a Spearman's correlation index to search for a correlation. The targeted US imaging signal at 1 month is compared with the same antibody immunohistochemistry expression from the paraffin embedded graft.

RESULTS

At this stage, seven tumors have been gathered and implanted. Tumor volumes measured by MRI on the 1rst cohort of mice (n=7) ranged between 118.39 and 390.40 mm3. We performed a first US molecular imaging session using VEGFR2 targeting versus non-targeted contrast agents. We observed a difference in expression between targeted and non-targeted microbubbles by a factor of about 3.5. Initial analyzes indicate that the expression of VEGFR2 marking is correlated with tumor volume.

CONCLUSION

The patient derived xenograft is a feasible model for molecular imaging studies. These preliminary results are encouraging to follow up the molecular imaging with the other markers (VEGFR1 and FSHR).

CLINICAL RELEVANCE/APPLICATION

Good pre-clinical models are paramount to better tailored clinical trials in molecular imaging

MI221-SD- Designed Multifunctional Gold Nanocomposites for Targeted Tri-mode CT/ MR/ Optical Imaging of WEA2 Human Non-small Cell Lung Cancer Cells

Station #2

Awards

Trainee Research Prize - Medical Student

Participants

Jingwen Chen, Shanghai, China (*Presenter*) Nothing to Disclose Qian Chen, Shanghai, China (*Abstract Co-Author*) Nothing to Disclose Gui-Xiang Zhang, MD, Shanghai, China (*Abstract Co-Author*) Nothing to Disclose Xiang-Yang Shi, Shanghai, China (*Abstract Co-Author*) Nothing to Disclose Han Wang, MD, PhD, Shanghai, China (*Abstract Co-Author*) Nothing to Disclose

PURPOSE

The high incidence and mortality rate of non-small cell lung cancer (NSCLC) prompts exhaustive efforts to develop new effective methods for its diagnosis at the early-stage to improve the survival rate. We are developing multifuctional gold nanocomposites to

use as the nanoprobes for targeted tri-mode CT / MR / optical imaging of human non-small cell cancer cells both in vitro and in vivo.

METHOD AND MATERIALS

Amine-terminated generation 5 poly(amidoamine) dendrimers were used as a nanoplatform to be covalently modified with Gd chelator, Cy5.5, and FA. Then the multifunctional dendrimers were used as templates to entrap gold nanoparticles, followed by chelating Gd(III) ions and acetylation of the remaining dendrimer terminal amines. The thus-formed multifunctional Au DENPs (in short, Cy5.5-Gd-Au DENPs-FA) were characterized via different techniques, and then were used for both in vitro and in vivo targeted CT/ MR/ NIR optical tri-mode imaging of human NSCLC cells (NCI-H460 cells) and the xenograft tumor model.

RESULTS

CT/MR/optical images show that NCI-H460 cells can be detected after incubation with the Cy5.5-Gd-Au DENPs-FA in vitro and the xenograft tumor model can be imaged after intravenous administration of the particles. Combine the inductively coupled plasmaatomic emission spectroscopy (ICP-AES) measurements with the transmission electron microscopy (TEM) data confirm that the Cy5.5-Gd-Au DENPs-FA is able to be uptaken by the treated cells. MTT (3-(4,5-dimethylthiazol-2-yl)-2,5-diphenyltetrazolium bromide) assay show that the Cy5.5-Gd-Au DENPs-FA has a good biocompatibility at the given concentration range.

CONCLUSION

The findings of this study suggest that the developed Cy5.5-Gd-Au DENPs-FA may be used as a promising tri-mode nanoprobe for targeted CT/MR/opticl imaging of human NSCLC and other folate receptor (FR) over-expressing cancers.

CLINICAL RELEVANCE/APPLICATION

In consideration of the special structural characteristic, the dendrimer based nanocomposites may be further modified with therapeutic antibodies or small interfering RNA (siRNA) to be expectably developed for the personalized theranostics of cancers at early-stage with the high accuracy and sensitivity.

Molecular Imaging Wednesday Poster Discussions

Wednesday, Nov. 30 12:45PM - 1:15PM Room: S503AB

MI

AMA PRA Category 1 Credit [™]: .50

FDA Discussions may include off-label uses.

Participants

Homer A. Macapinlac, MD, Houston, TX (Moderator) Nothing to Disclose

Sub-Events

MI222-SD-WEB1 Accuracy of the of NO Nodal Staging of the High-risk Prostatic Carcinoma based on18F-fluorocholine-PET/MRI, Comparison with Surgical Findings

Station #1

Participants

Jiri Ferda, MD, PhD, Plzen, Czech Republic (*Presenter*) Nothing to Disclose Eva Ferdova, MD, Plzen, Czech Republic (*Abstract Co-Author*) Nothing to Disclose Jan Baxa, MD, PhD, Plzen, Czech Republic (*Abstract Co-Author*) Nothing to Disclose Milan Hora, Plzen, Czech Republic (*Abstract Co-Author*) Nothing to Disclose Ondrej Hes, MD, PhD, Plzen, Czech Republic (*Abstract Co-Author*) Nothing to Disclose

PURPOSE

To evaluate the possibilities of pelvic nodal-staging assessment of the high-risk prostatic carcinoma using 18F-fluorocholine-PET/MRI and to compare findings with surgery.

METHOD AND MATERIALS

25 men (mean age 66,8 years, range 59 - 78) with by biopsy confirmed prostatic carcinoma with Gleason score 8 and more were examined before surgery using 18F-fluorocholine-PET/MRI and with finding of no positive node (N0 N-stage based on PET/MRI) were recommended to radical prostatectomy. All examination were delayed 15 min after intravenous application of 18F-fluorocholine in the dose 1,25 MBq per kilogram of body weight. The imaging included T2 STIR, DWI and dynamic gadolinium enhanced GRE T1 imaging, the PET acquisition last 15 min. All examinations were completed with whole trunk PET/MRI acquisition. The TNM staging was evaluated. In all men, the radical surgery was performed including pelvic lymph node resection. The comparison of the histopathological results were compared with those obtained by PET/MRI according nodal staging and according local T-staging.

RESULTS

25 surgeries were performed. There were found 22 true negative findings, and three false negative findings including one micrometastase. The negative predictive value of pelvic lymph node metastase reached 88,0 %(22/25) excluding micrometastase, NPV rised to 92,0% (23/25). One deviation between T2 or T3 size was noted after histopathological evaluation, one case was evaluated as T3B by PET/MRI, after histopathological evaluation the stage was set as T2C; in one case, the T2b based on PET/MRI was evaluated as T2C, no other deviation was noted nor between T2 or T3 subcathegories, nor in T3A subcathegory. It results in 92% (23/25) accuracy in local staging.

CONCLUSION

The 18F-fluorocholine PET/MRI derived pelvic lymph N-staging N0 and T-stage in prostatic carcinoma reaches sufficien results and provides sufficient information in the treatment decisions.

CLINICAL RELEVANCE/APPLICATION

In prostatic carcinoma, the negative pelvic nodal staging and T-staging using 18F-fluorocholine PET/MRI exhibits sufficient clinical value in the decisions to perform radical prostate surgery.

MI223-SD- Molecular Imaging of Metastasis From Pancreatic Cancer in Patient-Derived Xenograft Models Using WEB2 uPAR-Targeted Multifunctional Nanoparticles

Station #2

Participants Kai Cao, MD, PhD, ShangHai, China (*Presenter*) Nothing to Disclose

PURPOSE

Lymphatic metastasis is an important prognostic factor regarding long-term survival rate of pancreatic cancer (PC) patients. Pretreatment knowledge of lymph node status is extremely helpful for planning treatment and prognosis. However, to date, no imaging method has been demonstrated to be effective for detecting lymphatic metastasis in PC. Molecular imaging probes based on upconversion nanoparticles with unique optical and magnetic properties have provided great hope for early tumor detection. Herein we report highly sensitive detection of lymphatic spread using core@shell structured NaGdF4:Yb,Er@NaGdF4 upconversion nanoparticles coated with polyethylene glycol (PEG).

METHOD AND MATERIALS

The orthotopic patient-derived xenograft model, which can better retained the human pancreatic cancer morphology and genetic stability, was built upon engraftment of pancreatic cancer specimens in nude mice and the tumor development was carefully monitored through histopathological and immunohistochemical analyses to reveal the pathophysiological processes and molecular

features of the cancer microenvironment. A PC-speific probe was constructed through "click" reaction between the maleimide moiety of PEG ligand and the thiol group from conjugating amino-terminal fragment of the receptor binding domain of human urokinase plasminogen activator(uPA), whose receptor(uPAR) is highly expressed in the pancreatic cancer.

RESULTS

Upon 980nm laser excitation, the primary tumor and adjacent lymphatic metastasis site were clearly differentiated owing to the ultralow background of the upconversion luminescence after the uPAR-specific probe was delivered through tail vein injection into tumor-bearing nude mice. Target specificity of nanoparticles is further confirmed by a clinical MRI scanner at a field strength of 3 Tesla.

CONCLUSION

Our results revealed that the probe could be useful for not only tiny tumor lesion diagnosis but also for lymphatic metastasis detections, indicating potential clinical applications in the early pancreatic cancer diagnosis and lymph node status evaluation.

CLINICAL RELEVANCE/APPLICATION

We believe that the current studies provide a highly effective and potential approach for pancreatic cancer surgical navigation.

Molecular Imaging (Urology/Prostate)

Wednesday, Nov. 30 3:00PM - 4:00PM Room: S504CD

GU CT MI MR

AMA PRA Category 1 Credit ™: 1.00 ARRT Category A+ Credit: 1.00

FDA Discussions may include off-label uses.

Participants

Peter L. Choyke, MD, Rockville, MD (*Moderator*) Researcher, Koninklijke Philips NV; Researcher, General Electric Company; Researcher, Siemens AG; Researcher, iCAD, Inc; Researcher, Aspyrian Therapeutics, Inc; Researcher, ImaginAb, Inc; Researcher, Aura Biosciences, Inc

Steven P. Rowe, MD, PhD, Parkville, MD (Moderator) Nothing to Disclose

Sub-Events

SSM13-01 68Ga-RM2 PET/MRI in Biochemically Recurrent Prostate Cancer: A Comparison with Conventional Imaging

Wednesday, Nov. 30 3:00PM - 3:10PM Room: S504CD

Participants

Ida Sonni, MD, Stanford, CA (*Presenter*) Nothing to Disclose Ryogo Minamimoto, MD, PhD, Tokyo, Japan (*Abstract Co-Author*) Nothing to Disclose Andreas M. Loening, MD, PhD, San Francisco, CA (*Abstract Co-Author*) Nothing to Disclose Shreyas S. Vasanawala, MD, PhD, Stanford, CA (*Abstract Co-Author*) Research collaboration, General Electric Company; Consultant, Arterys Inc; Research Grant, Bayer AG; Andrei Iagaru, MD, Stanford, CA (*Abstract Co-Author*) Research Grant, General Electric Company; Research Grant, Bayer AG; Research Grant, The Piramal Group

PURPOSE

68Ga-RM2 (formerly known as 68Ga-Bombesin or BAY86-7548) is a synthetic bombesin receptor antagonist that targets gastrinreleasing peptide receptors (GRPr). GRPr are highly overexpressed in prostate cancer (PC). Because of their low expression in BPH and inflammatory prostatic tissues, imaging GRPr has potential advantages over current choline- and acetate-based radiotracers. We now present data on the use of 68Ga-RM2 PET/MRI in patients with biochemically recurrent prostate cancer (BCR PC) and noncontributory conventional imaging (CI).

METHOD AND MATERIALS

We enrolled 27 men with BCR PC, 59-83 year-old (mean±SD: 68.4±6.8) in an IRB-approved prospective study. Imaging started at 40-69 minutes (mean±SD: 49.9±7.2) after injection of 3.6-4.1 mCi (mean±SD: 3.8±0.2) of 68Ga-RM2 using a TOF-enabled simultaneous PET/MRI scanner. MRI included T1-weighted, T2-weighted and DWI. SUVmax and SUVmean measurements were recorded in normal tissues and areas of uptake outside the expected physiologic biodistribution.

RESULTS

PSA ranged 0.3-36.4 ng/mL (mean±SD: 7.2 \pm 7.9). CT, MRI, 99mTc MDP bone scan were negative. 68Ga-RM2 uptake had the highest value in the pancreas and bladder, while moderate uptake was noted in the esophagus, kidneys, blood pool, stomach, small bowel and colon. High 68Ga-RM2 uptake (SUVmax: 12.7 \pm 7.8 [range: 2.6 – 33.5], SUVmean: 5.7 \pm 2.5 [range: 1.7 – 10.8]) corresponded to pelvic lymph nodes (7 patients), retroperitoneal lymph nodes (5 patients), prostate bed (3 patients), seminal vesicle (2 patients), supraclavicular lymph node (2 patients), mesenteric lymph nodes (1 patient), mediastinal lymph node (1 patient), liver (1 patient), lung (1 patient) and bone marrow (1 patient). 68Ga-RM2 PET findings were compatible with recurrent prostate cancer in 19 of the 27 participants. MRI identified findings compatible with recurrent prostate cancer in 8 of the 27 patients, prostate bed in 1 patient, lung in 1 patient and bone marrow in 1 patient).

CONCLUSION

68Ga-RM2 produces high quality PET images for assessment of GRPr expression in patients with BCR PC. High uptake in multiple areas compatible with cancer lesiosn suggests that 68Ga-RM2 is a promising PET radiopharmaceutical for localization of disease in participants with BCR PC and non-contributory conventional imaging.

CLINICAL RELEVANCE/APPLICATION

68Ga-RM2 produces high quality PET images for assessment of GRPr expression in patients with BCR PC.

SSM13-02 18F-Fluoromethycholine Dynamic PET with Multiparameteric MR Imaging in Patients with High Risk Prostate Cancer

Wednesday, Nov. 30 3:10PM - 3:20PM Room: S504CD

Participants

Ur Metser, MD, FRCPC, Toronto, ON (*Presenter*) Consultant, AbbVie Inc Lisa P. Lavelle, MBBCh, FFR(RCSI), Toronto, ON (*Abstract Co-Author*) Nothing to Disclose Douglas Hussey, BSC,RT, Toronto, ON (*Abstract Co-Author*) Nothing to Disclose Kartik S. Jhaveri, MD, Toronto, ON (*Abstract Co-Author*) Speaker, Bayer AG; Speaker, Siemens AG Sangeet Ghai, MD, Toronto, ON (*Abstract Co-Author*) Nothing to Disclose Jaydeep A. Halankar, MD, DMRD, Toronto, ON (*Abstract Co-Author*) Nothing to Disclose To investigate the qualitative and quantitative parameters of dynamic 18F-Fluoromethylcholine (FCH) PET (dPET) in patients with high risk primary prostate cancer, and correlate these with multiparametric MR (mpMR) of the prostate.

METHOD AND MATERIALS

Twenty patients with biopsy-proven hrPCa were included (age 50-82 yrs, median, 70; Gleason score 7-9, median 8; serum PSA 3-90 ng/mL, median, 18.5). All patients underwent FCH-dPET (10 min) of the pelvis prior to a whole body scan and 3T mpMR of the prostate including high resolution T2-weighted, diffusion weighted, and dynamic contrast enhanced imaging. All primary tumor sites on mpMR and FCH-PET were recorded separately by an experienced prostate MR and PET reader, respectively, noting lesion location and degree of certainty (definite tumor or equivocal lesion). On PET, SUV was measured on static images, and time activity curves (TAC) were generated from dPET data. Quantitative dPET analysis was based on a two-tissue compartment model with image-derived arterial input.

RESULTS

Twenty one tumors in 20 patients were identified on mpMR (peripheral zone, n=20). All tumors on mpMR were also identified on PET. One additional lesion considered equivocal on mpMR did not show focal FCH uptake. Ten additional foci of FCH uptake in 8 patients were identified on PET (peripheral zone, n=5), with no mpMR correlate. Median SUVmax for MR-confirmed and non-MR confirmed lesions was 7.2 ± 2.2 , and 5.7 ± 2.6 , respectively. Median dPET parameters for MR-confirmed and non-MR confirmed lesions (1/min) were K1=0.73 \pm 0.31 and 0.56 \pm 0.18 (p=0.04); K3=0.24 \pm 0.17 and 0.24 \pm 0.14 (p=0.91); Ki=0.28 \pm 0.14 and 0.27 \pm 0.08 (p=0.31), respectively.

CONCLUSION

There is discordance in lesions identified in the prostate on mpMR and FCH-PET in patients with high-risk prostate cancer, with PET identifying >30% additional lesions. Furthermore, K1 values for MR-confirmed tumors were different from those derived from non-MR confirmed cohort of lesions. Further prospective studies with PET/MR-Ultrasound fusion biopsies of all PET and MR detected lesions are warranted.

CLINICAL RELEVANCE/APPLICATION

This study provides insight on the performance of FCH-PET in the detection of primary prostate cancer, as it correlates with multiparametric MR, along with quantitative dynamic FCH-PET data.

SSM13-03 PET/CT Imaging with 68Ga-labelled Prostate Specific Membrane Antigen-ligands in Restaging of Prostate Cancer: A Meta-analysis

Wednesday, Nov. 30 3:20PM - 3:30PM Room: S504CD

Awards

Student Travel Stipend Award

Participants

Sara Sheikhbahaei, MD, MPH, Baltimore, MD (*Presenter*) Nothing to Disclose Lilja B. Solnes, MD, MBA, Baltimore, MD (*Abstract Co-Author*) Nothing to Disclose Ali Afshar-Oromieh, Heidelberg, Germany (*Abstract Co-Author*) Nothing to Disclose Esther Mena, MD, Bethesda, MD (*Abstract Co-Author*) Nothing to Disclose Mehdi Taghipour, MD, BOSTON, MA (*Abstract Co-Author*) Nothing to Disclose Rathan M. Subramaniam, MD, PhD, Dallas, TX (*Abstract Co-Author*) Nothing to Disclose

PURPOSE

The PSMA has emerged as a promising target for PET-imaging of patients with recurrent prostate cancer (PCa) with higher rate of tumor detection in different studies. Given the relatively small patient population in most of these studies, in this meta-analysis we aim to establish the summary estimates of the performance of 68Ga-PSMA PET/CT imaging in relation to PSA values. The lesion-based diagnostic values of 68Ga-PSMA-ligands were also evaluated where possible.

METHOD AND MATERIALS

Systematic search were performed in PubMed and EMBASE (last updated in Feb 2016). Studies investigating the performance of 68Ga-PSMA-ligands PET/CT in patients with recurrent PCa were eligible for inclusion. When the individual patient data on rate of lesion detection in relation to PSA level were not extractable, the study authors were contacted seeking for additional information. Studies with patient overlap were excluded. Studies with histopathology reference standard were included in the diagnostic accuracy analysis. The pooled results were reported along with its 95% CI.

RESULTS

A total of 8 studies including 850 patients (788 patients suspected of recurrence, 62 patients with newly diagnosed PCa to exclude metastases) who were referred to 68Ga-PSMA-ligands PET/CT were included in this individual patient data meta-analysis. At least one lesion was identified on 68Ga-PSMA-ligands PET/CT in 52%(41-62%) of patients with PSA (ng/dl) of ≤ 0.5 ng/ml (n=89), 58% (46-69%) of patients with PSA of 0.5-1 ng/ml (n=82), 80% (71-86%) of patients with PSA of 1-2 ng/ml (n=149) and 91% (88-93%) of patients with PSA≥2 ng/ml (n= 535). Three studies provided the lesion-based accuracy information (967 lesions). The pooled per-lesion accuracy analysis revealed the sensitivity of 0.84 (0.71-0.91), specificity of 0.98 (0.90-1.0), negative predictive value of 0.96 (0.89-0.99) and positive predictive value of 0.92 (0.64-0.98).

CONCLUSION

Analysis of the available studies indicates that 68Ga-PSMA-ligands PET/CT are highly specific for lesions of PCa. There is a significant trend in tumor detection, from 52% to 91%, in association with PSA level ranging from <0.5 to >2 ng/dl.

CLINICAL RELEVANCE/APPLICATION

68Ga-PSMA-PET/CT is a valuable imaging with substantial diagnostic performance and high tumor detection rate even in clinically important range of low PSA levels (PSA< 0.5 ng/dl) which support its use in clinical practice in restaging of PCa with suspected recurrence.

SSM13-04 Nypedspolarized 13C-Tert-Butanol MRI Perfusion Mapping and Microvessel Density in Sunitnib-Treated Renal Cell Carcinoma Xenografts: Rad-Path Correlation in the Characterization of Intratumoral Heterogeneity and Pre- and Post-Treatment Change

Wednesday, Nov. 30 3:30PM - 3:40PM Room: S504CD

Student Travel Stipend Award

Participants

Patricia Coutinho De Souza, DVM, PhD, Boston, MA (*Presenter*) Nothing to Disclose Aaron K. Grant, PhD, Boston, MA (*Abstract Co-Author*) Nothing to Disclose Xiaoen Wang, MD, Boston, MA (*Abstract Co-Author*) Nothing to Disclose Rupal Bhatt, Boston, MA (*Abstract Co-Author*) Nothing to Disclose Gopal Varma, PhD, Boston, MA (*Abstract Co-Author*) Nothing to Disclose David C. Alsop, PhD, Boston, MA (*Abstract Co-Author*) Nothing to Disclose David C. Alsop, PhD, Boston, MA (*Abstract Co-Author*) Research support, General Electric Company Leo L. Tsai, MD, PhD, Boston, MA (*Abstract Co-Author*) Co-founder, Agile Devices Inc; Stockholder, Agile Devices Inc; Research Consultant, Agile Devices Inc;

PURPOSE

Hyperpolarized 13C-tert-butanol (h13C-TB) is a freely-diffusible novel MRI tracer that provides high-SNR tissue perfusion mapping. We use h13C-TB MRI to quantify perfusion within and between untreated (UT) and sunitinib resistant (SR) renal cell carcinoma mouse xenografts. Our goal was to determine if regional perfusion measured with h13C-TB correlated with local CD34 expression and microvessel density (MVD) in these tumors.

METHOD AND MATERIALS

8 mice were implanted with A498 RCC tumors. 4 (SR) were treated with sunitinib daily; the other 4 were UT. SR mice were imaged at resistance (when regrowth was seen, 14–54 days). UT mice were imaged when tumors reached 20 mm in size. MRI was performed at 4.7 T using: (1) Anatomical 1H-T2-weighed images using rapid acquisition with refocused echoes, TR/TE=3000/80ms, 128x128 matrix, 2mm slice, 3.5cm FOV, (2) h13C-TB perfusion maps using 2D balanced steady state free precession, 128x128 matrix, 8.5cm FOV, 3.3mm slice, 512ms/frame, 100 frames. Tumors were sectioned along the imaging plane, stained with immunofluorescent-labeled CD34, and scanned into virtual slides. 75 ROI (0.25mm2) were selected for each MR perfusion map (Fig B and F) and the MVD of each matching location was determined in the pathologic specimen (Fig C and G).

RESULTS

1H images of UT and SR tumors are shown in Figures A and B, respectively (outlined in blue). Superimposed perfusion maps from h13C-TB MRI (green) is shown in example UT (Fig B) and SR (Fig F) tumors. Figures C-D and G-H show CD34 expression, showing qualitative similarity to respective MR perfusion maps. Measured perfusion was greater in UT relative to SR tumors (p < 0.05, Fig I), but the average MVD was lower (p < 0.05) (Fig. J). However, within each UT or SR tumor the local MVD correlated with local perfusion (Fig K-L).

CONCLUSION

h13C-TB MRI provides high-SNR perfusion mapping even in low flow areas. There is significant correlation between local perfusion and MVD within each tumor. However, resistance tumors demonstrate lower perfusion and greater MVD relative to untreated tumors, suggesting that MVD alone is not predictive of perfusion when assessing antiangiogenic response.

CLINICAL RELEVANCE/APPLICATION

h13C-tert-butanol provides noninvasive high-SNR quantitative perfusion mapping even in treated tumors with low flow. Improved radiologic-pathologic correlation is necessary to increase our accuracy in predicting therapeutic response and resistance.

SSM13-05 Added Value of CT Textural Analysis Compared to PET-CT alone in Differentiating Benign from Malignant Adrenal Lesions?

Wednesday, Nov. 30 3:40PM - 3:50PM Room: S504CD

Participants

Shaunagh McDermott, FFR(RCSI), Boston, MA (*Presenter*) Nothing to Disclose Leslie K. Lee, MD, Boston, MA (*Abstract Co-Author*) Nothing to Disclose Rodrigo Canellas, MD, Cambridge, MA (*Abstract Co-Author*) Nothing to Disclose Hei Shun Yu, MD, Boston, MA (*Abstract Co-Author*) Nothing to Disclose Michael S. Gee, MD, PhD, Jamaica Plain, MA (*Abstract Co-Author*) Nothing to Disclose Michael A. Blake, MBBCh, Boston, MA (*Abstract Co-Author*) Editor with royalties, Springer Science+Business Media Deutschland GmbH

PURPOSE

To assess the added value of CT textural analysis to contrast-enhanced PET-CT in differentiating benign from malignant adrenal lesions.

METHOD AND MATERIALS

We retrospectively assessed a series of 45 consecutive patients who had undergone contrast-enhanced PET-CT scan prior to a percutaneous biopsy of an adrenal lesion over a 10 year period. Final diagnosis was based on pathology or stability on imaging for at least one year. CT textural analysis (CTTA) was assessed using a commercially available research software program (TexRAD) that applies a filtration-histogram technique for characterizing tumor heterogeneity. Filtration step selectively filters and extracts texture features at different anatomical scales varying from 2mm (fine features) to 6mm (coarse features). Receiver operating characteristics (ROC) was performed to assess sensitivity and specificity for differentiating between the benign and malignant adrenal lesions. The PET scan was considered positive if the adrenal lesion qualitatively showed greater FDG uptake than the reference hepatic uptake.

RESULTS

The final diagnosis was benign in 16 cases and malignant in 29 cases. The mean gray level intensity for medium filter (SSF 4) was significantly higher for benign compared to malignant adrenal lesions (4.7 vs. -8.6)(p < 0.005). Using a mean gray level intensity cutoff of -2 on SSF 4, the sensitivity was 75% and specificity was 69% for the detection of a malignant adrenal lesion (AUC 0.76). The sensitivity and specificity for PET was 69% and 100%, respectively. Using a combined approach, if a mean gray level signal intensity cutoff of -2 was utilized in patients with an adrenal that showed greater than hepatic FDG uptake, then the overall sensitivity was 90% and the specificity was 100%.

CONCLUSION

Performing CT textural analysis on PET positive adrenal nodules increases the sensitivity of the study.

CLINICAL RELEVANCE/APPLICATION

Many patients being worked up for malignancy now undergo a PET-CT scan and the addition of CT textural analysis may increase the study's diagnostic accuracy and reduce the need for further imaging or tissue sampling.

SSM13-06 Accuracy of the of NO Nodal Staging of the High-risk Prostatic Carcinoma based on18F-fluorocholine-PET/MRI, Comparison with Surgical Findings

Wednesday, Nov. 30 3:50PM - 4:00PM Room: S504CD

Participants

Jiri Ferda, MD, PhD, Plzen, Czech Republic (*Presenter*) Nothing to Disclose Eva Ferdova, MD, Plzen, Czech Republic (*Abstract Co-Author*) Nothing to Disclose Jan Baxa, MD, PhD, Plzen, Czech Republic (*Abstract Co-Author*) Nothing to Disclose Milan Hora, Plzen, Czech Republic (*Abstract Co-Author*) Nothing to Disclose Ondrej Hes, MD, PhD, Plzen, Czech Republic (*Abstract Co-Author*) Nothing to Disclose

PURPOSE

To evaluate the possibilities of pelvic nodal-staging assessment of the high-risk prostatic carcinoma using 18F-fluorocholine-PET/MRI and to compare findings with surgery.

METHOD AND MATERIALS

25 men (mean age 66,8 years, range 59 - 78) with by biopsy confirmed prostatic carcinoma with Gleason score 8 and more were examined before surgery using 18F-fluorocholine-PET/MRI and with finding of no positive node (N0 N-stage based on PET/MRI) were recommended to radical prostatectomy. All examination were delayed 15 min after intravenous application of 18F-fluorocholine in the dose 1,25 MBq per kilogram of body weight. The imaging included T2 STIR, DWI and dynamic gadolinium enhanced GRE T1 imaging, the PET acquisition last 15 min. All examinations were completed with whole trunk PET/MRI acquisition. The TNM staging was evaluated. In all men, the radical surgery was performed including pelvic lymph node resection. The comparison of the histopathological results were compared with those obtained by PET/MRI according nodal staging and according local T-staging.

RESULTS

25 surgeries were performed. There were found 22 true negative findings, and three false negative findings including one micrometastase. The negative predictive value of pelvic lymph node metastase reached 88,0 %(22/25) excluding micrometastase, NPV rised to 92,0% (23/25). One deviation between T2 or T3 size was noted after histopathological evaluation, one case was evaluated as T3B by PET/MRI, after histopathological evaluation the stage was set as T2C; in one case, the T2b based on PET/MRI was evaluated as T2C, no other deviation was noted nor between T2 or T3 subcathegories, nor in T3A subcathegory. It results in 92% (23/25) accuracy in local staging.

CONCLUSION

The 18F-fluorocholine PET/MRI derived pelvic lymph N-staging N0 and T-stage in prostatic carcinoma reaches sufficien results and provides sufficient information in the treatment decisions.

CLINICAL RELEVANCE/APPLICATION

In prostatic carcinoma, the negative pelvic nodal staging and T-staging using 18F-fluorocholine PET/MRI exhibits sufficient clinical value in the decisions to perform radical prostate surgery.

Molecular Imaging Thursday Case of the Day

Thursday, Dec. 1 7:00AM - 11:59PM Room: Case of Day, Learning Center

MI

AMA PRA Category 1 Credit ™: .50

Participants

Jonathan E. McConathy, MD, PhD, Birmingham, AL (Presenter) Research Consultant, Eli Lilly and Company; Research Consultant, Blue Earth Diagnostics Ltd; Research Consultant, Siemens AG; Research Consultant, General Electric Company; Suzanne E. Lapi, PhD, Birmingham, AL (Presenter) Research Grant, AbbVie Inc; Spouse, Consultant, General Electric Company; Consultant, Siemens AG; Consultant, Blue Earth Diagnostics Ltd; Consultant, Eli Lilly and Company Matthias J. Eiber, MD, Muenchen, Germany (Abstract Co-Author) Nothing to Disclose Thomas A. Hope, MD, San Francisco, CA (Abstract Co-Author) Research Grant, Consultant, GE Healtcare Robert R. Flavell, MD, PhD, San Francisco, CA (Abstract Co-Author) Nothing to Disclose Samuel J. Galgano, MD, Birmingham, AL (Abstract Co-Author) Nothing to Disclose Asim K. Bag, MD, Birmingham, AL (Abstract Co-Author) Nothing to Disclose David M. Schuster, MD, Atlanta, GA (Abstract Co-Author) Institutional Research Grant, Nihon Medi-Physics Co, Ltd; Institutional Research Grant, Blue Earth Diagnostics Ltd; Consultant, WellPoint, Inc; ; Ephraim E. Parent, MD, PhD, Saint Louis, MO (Abstract Co-Author) Nothing to Disclose Bital Savir-Baruch, MD, Maywood, IL (Abstract Co-Author) Nothing to Disclose Pamela K. Woodard, MD, Saint Louis, MO (Abstract Co-Author) Research Grant, Astellas Group; Research Grant, Bayer AG; Research agreement, Siemens AG; ; ; ; ; Sebastian R. McWilliams, MBBCh, Saint Louis, MO (Abstract Co-Author) Nothing to Disclose Amir K. Durrani, MD, St Louis, MO (Abstract Co-Author) Nothing to Disclose Robert J. Gropler, MD, Saint Louis, MO (Abstract Co-Author) Nothing to Disclose Michael Hofman, PhD, San Francisco, CA (Abstract Co-Author) Nothing to Disclose

Miguel Pampaloni, MD, San Francisco, CA (Abstract Co-Author) Nothing to Disclose

TEACHING POINTS

1) Interpret amyloid-PET scans as positive or negative. 2) Apply appropriate use criteria for selecting patients for amyloid-PET study. 3) Understand the goals of the IDEAS study as it relates to coverage with evidence development for clinical amyloid-PET scans.

RC623

Molecular Imaging Mini-Course: Advanced Molecular Imaging

Thursday, Dec. 1 8:30AM - 10:00AM Room: S404CD



AMA PRA Category 1 Credits ™: 1.50 ARRT Category A+ Credits: 1.50

FDA Discussions may include off-label uses.

Participants

Sub-Events

RC623A Novel Tracers

Participants

Timothy R. DeGrado, PhD, Rochester, MN (Presenter) Nothing to Disclose

LEARNING OBJECTIVES

1) Identify the major considerations when developing a novel molecular imaging probe. 2) Compare the strengths and weaknesses of the various imaging modalities with regard to probe development and implementation. 3) Define appropriate experiments for probe validation. 4) Gain an understanding of the process of translation of a probe to clinical practice.

ABSTRACT

Molecular imaging is rapidly advancing as new imaging biomarkers are invented to allow noninvasive assessment of biochemical function. Those who embark on the process of developing novel probes come to know the excitement of imaging biological processes for the first time, but are also well aware of the great effort and many pitfalls that can impede progress. This introductory lecture will provide an overview of the process of molecular imaging probe conception, development, preclinical validation, and translation. Specific examples will be used to illustrate the presenter's experience with meeting these challenges.

RC623B Novel Instrumentation (PET/MR)

Participants

Ciprian Catana, MD, PhD, Charlestown, MA, (ccatana@nmr.mgh.harvard.edu) (Presenter) Research Consultant, Cubresa Inc

LEARNING OBJECTIVES

1) Distinguish the technical approaches that have been proposed for integrating PET and MRI for the purpose of simultaneous data acquisition. 2) Evaluate the latest methodological developments in PET/MRI for improving PET data quantification. 3) Incorporate simultaneous PET/MRI techniques into research and clinical projects.

ABSTRACT

Molecular Imaging (New Tracers/Methods)

Thursday, Dec. 1 10:30AM - 12:00PM Room: S505AB

CT MI MR NM

AMA PRA Category 1 Credits ™: 1.50 ARRT Category A+ Credits: 1.50

FDA Discussions may include off-label uses.

Participants

Vikas Kundra, MD, PhD, Houston, TX (*Moderator*) License agreement, Introgen Therapeutics, Inc Zaver M. Bhujwalla, PhD, Baltimore, MD (*Moderator*) Nothing to Disclose

Sub-Events

SSQ11-01 Novel Intrinsically Zirconium-89 Radiolabeled Self-Destructing Mesoporous Silica Nanostructures for in Vivo Biodistribution and Tumor Vasculature Targeting Studies

Thursday, Dec. 1 10:30AM - 10:40AM Room: S505AB

Awards

Student Travel Stipend Award

Participants

Shreya Goel, Madison, WI (*Presenter*) Nothing to Disclose Feng Chen, PhD, Madison, WI (*Abstract Co-Author*) Nothing to Disclose Sixiang Shi, MS, Madison, WI (*Abstract Co-Author*) Nothing to Disclose Hector Valdovinos, MS, Madison, WI (*Abstract Co-Author*) Nothing to Disclose Todd Barnhart, Madison, WI (*Abstract Co-Author*) Nothing to Disclose Weibo Cai, PhD, Palo Alto, CA (*Abstract Co-Author*) Nothing to Disclose

PURPOSE

Long residence times and resultant toxicity remains a major roadblock in clinical translation of nanomaterials. We present synthesis of biodegradable mesoporous silica nanoparticles, to carry multiple cargos types and self-destruct over time after release of payload. Chelator-free labeling of bMSNs with 89Zr (t1/2 = 72. 8 h) was used to track their in vivo pharmacokinetics and CD105 targeting ability via positron emission tomography (PET) imaging.

METHOD AND MATERIALS

Multi-generational bMSNs with tunable pore diameters, were synthesized via biphase stratification approach and characterized. In vitro degradation and dual drug release studies were carried out in simulated body fluid (SBF) for 21 days. bMSNs were intrinsically chelated with oxophilic radionuclide 89Zr, followed by conjugation with polyethylene glycol (PEG) and TRC105 antibody to form (89Zr)bMSN-PEG-TRC05 for in vivo PET imaging in 4T1 metastatic murine breast tumor model.

RESULTS

Degradation of nanocarriers into biocompatible and non-toxic byproducts presents a favorable prospect for their clinical translation. Dendritic bMSNs with spoke-like radiating bimodal mesoporous channels showed large pore size (5.4 nm and 12 nm) resulting in rapid and complete degradation in SBF within 21 days. bMSNs showed high co-encapsulation and pH-dependent release of the drugs. Excellent 89Zr labeling yield (~ 98 % within 2 h at 75 °C) and radiostability (> 95% upto 72 h) were observed. CD105 specificity of (89Zr)bMSN-PEG-TRC05 was confirmed in vivo with PET images with significantly enhanced tumor uptake (4.5 ± 0.6 , 11.2 ± 2.1 , 11.5 ± 1.3 and 11.2 ± 0.9 %ID/g at 0.5, 6, 24 and 48 h post injection). The specificity was further confirmed with systematic ex vivo biodistribution and histological examination.

CONCLUSION

The versatile and easily tunable approach shows great potential for bench-to-bedside transition of personalized nanomedicine. The nanoparticles can be tailored to (i) label clinically relevant diagnostic and therapeutic radioisotopes without tiresome chelator chemistries, (ii) carry small-molecule and large biomolecular drugs for combination therapy, (iii) specifically target any tumor type by modifying the targeting ligand, and, (iv) auto-destruct and excrete from the body within a reasonable time period.

CLINICAL RELEVANCE/APPLICATION

Biodegradable nanoparticles with multiple cargo carrying ability combat two primary roadbloacks in clinical translation of nanomedicine.

sSQ11-02 Protein Corona: A Simple Solution that Enables Clinical Translation of Stem Cell Imaging

Thursday, Dec. 1 10:40AM - 10:50AM Room: S505AB

Awards

Student Travel Stipend Award

Participants

Hossein Nejadnik, MD, PhD, Stanford, CA (*Presenter*) Nothing to Disclose Seyedmeghdad Taghavigarmestani, MD, Stanford, CA (*Abstract Co-Author*) Nothing to Disclose Philip Yang, MD, Stanford, CA (*Abstract Co-Author*) Nothing to Disclose Morteza Mahmoudi, Stanford, CA (*Abstract Co-Author*) Nothing to Disclose Heike E. Daldrup-Link, MD, Palo Alto, CA (*Abstract Co-Author*) Nothing to Disclose

PURPOSE

To develop a new, transfection-agent free labeling approach that is clinically applicable for localizing and tracking stem cells, using MR imaging with minimum manipulation of nanoparticles and cells.

METHOD AND MATERIALS

We labeled human mesenchymal stem cells (hMSC) by ferumoxytol in media containing human serum (group 1), fetal bovine serum (group 2), StemPro® media (group 3), protamine (group 4) and protamine+heparin (group 5). Formation of protein corona around ferumoxytol was characterized by dynamic light scattering (DLS), zeta potential, and liquid chromatography-mass spectrometry (LC-MS). Iron uptake was evaluated by DAB-prussian blue, Lysotracker and inductively coupled plasma spectrometry(ICP). To evaluate the effect of different labeling methods on MR signal, labeled and unlabeled hMSCs were imaged in vitro as well as ex vivo in pig knee. MR imaging was performed in a 3T MR scanner, using T2W FSE and MESE sequences to calculate T2 relaxation times. Data was analyzed using ANOVA test with p<0.05.

RESULTS

DLS and zeta potential showed more disperse nanoparticles and decrease of negative charge of nanoparticles in all groups compared to bare nanoparticles. LC-MS revealed different proteins covering nanoparticles. Most common proteins in group 1 were Apolipoprotein A-I, E, C-I, and A-II, and in group 2 were Hemoglobin alpha and beta, Apolipoprotein A-II, Alpha-2-HS-glycoprotein, and Albumin. ICP and histology results showed higher iron uptake in group 1 compared to other groups. hMSCs in group 1 revealed significantly shorter T2 relaxation times ($17.03\pm0.23ms$) compared to unlabeled, group 2, 3, 4, and 5 hMSCs (33.29 ± 1.22 , 26.79 ± 1.46 , 20.70 ± 0.81 , 25.61 ± 0.33 , $21.90\pm0.44 ms$) (p<0.05). After implantation into pig knee, Labeled hMSCs in group 1 revealed significantly shorter T2 relaxation times ($12.68\pm0.11ms$) compared to unlabeled, group 2, 3, 4, and 5 hMSCs (35.74 ± 2.75 , 20.94 ± 3.9 , 17.50 ± 0.33 , 19.48 ± 1.13 , $17.42\pm0.21 ms$) (p<0.05). In vivo applications in pig knees are ongoing.

CONCLUSION

This study showed a significant higher ferumoxytol uptake by hMSCs labeled with human serum containing media compared to previously reported approaches with transfection agents.

CLINICAL RELEVANCE/APPLICATION

Protein-corona-mediated cell labeling represents a new and readily clinically translatable method for labeling "off the shelf" cell products with ferumoxytol.

SSQ11-03 Radiotracer Derivatives of Trimethoprim (TMP) for Imaging Transgenic Cells

Thursday, Dec. 1 10:50AM - 11:00AM Room: S505AB

Awards

Student Travel Stipend Award

Participants

Mark A. Sellmyer, MD, PhD, Philadelphia, PA (*Presenter*) Nothing to Disclose Iljung Lee, philadelphia, PA (*Abstract Co-Author*) Nothing to Disclose Catherine Hou, Philadelphia, PA (*Abstract Co-Author*) Nothing to Disclose Brian Lieberman, Philadelphia, PA (*Abstract Co-Author*) Nothing to Disclose Chenbo Zeng, philadelphia, PA (*Abstract Co-Author*) Nothing to Disclose David A. Mankoff, MD, PhD, Philadelphia, PA (*Abstract Co-Author*) Speaker, Koninklijke Philips NV; Consultant, General Electric Company; Advisory Board, RefleXion Medical Inc Robert Mach, Saint Louis, MO (*Abstract Co-Author*) Nothing to Disclose

PURPOSE

There is a clinical need for quantitative, sensitive methods to image genetically engineered cells, including immune cells used for cell-based therapy. Given the genetic manipulation inherent to gene therapy, a genetic imaging handle / reporter protein is a logical solution and positron emission tomography (PET) can provide the desired sensitivity and spatial resolution. We developed a PET imaging strategy based on the bacterial protein E. coli dihydrofolate reductase (Ec DHFR) and its highly specific small molecule inhibitor, trimethoprim (TMP). Here, we describe the initial synthesis and testing of [18F] fluoropropyl-TMP, [18F]FPTMP.

METHOD AND MATERIALS

[18F]FPTMP was synthesized via a bis-boc protected reaction. HCT116 cells were transduced with YFP-Ec-DHFR fusion gene and sorted by FACS. Cell uptake, time course and saturation assays with [18F]FPTMP were performed (and with competing cold TMP or methotrexate). Protein was quantified by Lowry method. To show in vivo activity, immune deficient mice were xenografted with HCT116 DHFR and control cells. Tumors were grown for 2 weeks prior to injection of ~ 200 μ Ci of [18F]FPTMP. PET/CT imaging, time activity curves and biodistribution studies were performed.

RESULTS

[18F]FPTMP radiosynthesis showed high specific activity and there was rapid uptake (~3-fold at 5 minutes) and excellent overall target to background (over 16-fold at 2h) in vitro in HCT116 DHFR cells. Cold TMP completely inhibited uptake and methotrexate had no effect in control cells, suggesting no cross reactivity with mammalian DHFR. [18F]FPTMP saturation studies showed an expected low Kd of 0.46 nM (+/- 0.07) and Bmax of 2870 +/- 106 fmol/mg. In a mouse xenograft model, there was over 6-fold specific signal induction in Ec DHFR tumors with [18F]FPTMP and over 40-fold induction relative to muscle. [18F]FPTMP showed a favorable biodistribution, with mixed renal and hepatobiliary metabolism.

CONCLUSION

The radiosynthesis and in vivo application of [18F]FPTMP for PET reporter gene imaging is a simple solution providing a quantitative, sensitive tool that could be easily applied to imaging cell therapy in humans.

CLINICAL RELEVANCE/APPLICATION

Clinicians are interested in basic questions for cell therapies – Are the cells getting to where they are supposed to go and are there sites of off-target accumulation? – And TMP radiotracers may provide a single, facile reporter to allow such monitoring.

Honored Educators

Presenters or authors on this event have been recognized as RSNA Honored Educators for participating in multiple qualifying educational activities. Honored Educators are invested in furthering the profession of radiology by delivering high-quality educational content in their field of study. Learn how you can become an honored educator by visiting the website at: https://www.rsna.org/Honored-Educator-Award/

David A. Mankoff, MD, PhD - 2013 Honored Educator

SSQ11-04 Non-Invasive Quantification of Macrophage Recruitment in Head and Neck Carcinoma using Flourine 19MRI

Thursday, Dec. 1 11:00AM - 11:10AM Room: S505AB

Awards

Student Travel Stipend Award

Participants Aman Khurana, MD, San Diego, CA (*Presenter*) Nothing to Disclose Fanny Chapelin, MS, Stanford, CA (*Abstract Co-Author*) Nothing to Disclose Hongyan Xu, San Diego, CA (*Abstract Co-Author*) Nothing to Disclose Quyen Nguyen, La Jolla, CA (*Abstract Co-Author*) Nothing to Disclose Eric T. Ahrens, PhD, La Jolla, CA (*Abstract Co-Author*) Nothing to Disclose

PURPOSE

Head and neck squamous cell carcinoma (HNSCC) is a source of significant morbidity and mortality worldwide with risk factors including HPV status, tobacco and alcohol. In HPV negative tumors, reduced survival outcomes associated with tumor protein 53 (TP53) mutation only occur in combination with loss of chromosome 3p with reduction in median survival from 5 years for TP53 mutations to 1.7 years for a double hit (TP53 and 3p). The reasons for worse outcomes are still unclear with potential explanations including decreased radiosensitivity of double-hit tumors and/or role of infiltrating host immune cells/macrophages. Previous studies have also shown that "double-hit/Cal27" xenografts have higher matrix metalloproteinase (MMP) activity and since a significant amount of MMP is provided by tumor associated macrophages, we expect more macrophage accumulation for the "double-hit/Cal27" group compared to the "single-hit/SCC4" group.

METHOD AND MATERIALS

A novel perfluorocarbon (PFC) emulsion was used to tag macrophages in situ with high specificity and sensitivity and no background. Approximately 5x106 cells of two different cell lines, single-hit/ SCC4 and double-hit/ Cal27, were injected in bilateral flanks of 10 mice (n=5 in each group). These mice were then injected intravenously with 0.2ml of PFC emulsion (VS-1000, Celsense, Inc., Pittsburgh, PA) and 19F and proton MRI was performed on Day 2 & 10 post-injection. Tumors were then excised for histology toevaluate immune cell recruitment and to differentiate between M1 & M2 macrophages.

RESULTS

The average number of 19F spins within the tumors were significantly more (approximately double, p<0.05) for the "double-hit/Cal27" group compared to the "single-hit/SCC4" group (3.94x1019 compared to 1.98x1019 19F / tumor) signifying ncreased tumor associated macrophage burden in the double hit tumors. The number of infiltrating macrophages per tumor decreased in both groups over the course of 8 days but not significantly.

CONCLUSION

These preliminary results show that by using a PFC nanoemulsion via an IV injection and 19F MRI, tumor associated macrophage burden of prognostically different double hit and single hit tumors can be easily differentiated in vivo.

CLINICAL RELEVANCE/APPLICATION

This non-invasive method to quantify tumor associated macrophage burden will pave the way to identify prognostically poor head and neck tumors with the 19F MRI in clinical trials.

SSQ11-05 Chelator-Free 89Zr-Labeling of Gd2O2S:Eu Nanoparticles with Super In Vivo Radio-Stability

Thursday, Dec. 1 11:10AM - 11:20AM Room: S505AB

Participants

Shreya Goel, Madison, WI (*Presenter*) Nothing to Disclose Fanrong Ai, PhD, Madison, WI (*Abstract Co-Author*) Nothing to Disclose Yonghua Zhan, Madison, WI (*Abstract Co-Author*) Nothing to Disclose Feng Chen, PhD, Madison, WI (*Abstract Co-Author*) Nothing to Disclose Todd Barnhart, Madison, WI (*Abstract Co-Author*) Nothing to Disclose Weibo Cai, PhD, Palo Alto, CA (*Abstract Co-Author*) Nothing to Disclose

PURPOSE

Owing to the special electronic shell structure of Eu atom, Gd2O2S:Eu nanoparticles can be excited by Cerenkov or γ radiation. The intense luminescence in the red region can be observed, which can be harnessed for optical imaging. Herein we report the first study of 89Zr-labeled Gd2O2S:Eu nanoparticles ([89Zr]Gd2O2S:Eu) with high radio-stability for in vivo radioluminescence imaging (RLI).

METHOD AND MATERIALS

Monodispersed Gd2O2S:Eu nanoparticles (diameter ~20 nm) were synthesized using a co-thermal decomposition of precursors Gd(ddtc)3(Phen) and Eu(ddtc)3(Phen) and surface modified with amphiphilic DSPE-PEG5k. The abundant O atoms in the Gd2O2S:Eu nanoparticles were utilized for chelator-free radiolabeling with oxophilic isotope, zirconium-89 (89Zr; t1/2 = 78.4 h). PET imaging was used to study the in vivo radiostability of the [89Zr]Gd2O2S:Eu nanoparticles.[89Zr]Gd2O2S:Eu nanoparticles were subcutaneously/intravenously injected into mice to demonstrate RLI in vivo.

RESULTS

[89Zr]Gd2O2S:Eu nanoparticles were successfully synthesized for RLI studies. ~ 76.1% 89Zr-labeling yield was achieved upon.RL intensity of [89Zr]Gd2O2S:Eu nanoparticles wasdepended on the radioactivity, concentration of [Eu] and the distance between 89Zr and Gd2O2S:Eu. In vivo, the [89Zr]Gd2O2S:Eu yielded enhanced optical signal with open (collecting both RLI signal from [89Zr]Gd2O2S:Eu and Cerenkov luminescence signal) and 620 nm (collecting only the RLI signal from [89Zr]Gd2O2S:Eu, but not the Cerenkov luminescence signal from 89Zr) filters. Separately injected 89Zr and Gd2O2S:Eu, and 89Zr only controls showed significantly reduced signal intensity.PET imaging indicated high radiostability of [89Zr]Gd2O2S:Eu complex in intravenously injected mice. Dominant liver and spleen uptake and low bone uptake was seen upto 7 days.

CONCLUSION

We demonstrate the synthesis, in vitro and in vivo applications of radioluminescent nanoparticles.89Zr could be intrinsically labeled to Gd2O2S:Eu, with high labeling yield and good in vivo radiostability.RLI overcomes the tissue penetration limitation of traditional optical imaging modalities, due to the excitation of Gd2O2S:Eu from Cerenkov radiation or higher energy particles from 89Zr decay.

CLINICAL RELEVANCE/APPLICATION

Our proof-of-principle study conveys the promising potential of [89Zr]Gd2O2S:Eu nanoparticles as multimodality (PET/Cerenkov/RL/CT) imaging probes.

SSQ11-06 Pharmacokinetic Analysis and Extravasation Study of a Novel Nanobubble Ultrasound Contrast Agent

Thursday, Dec. 1 11:20AM - 11:30AM Room: S505AB

Participants Hanping Wu, MD, Cleveland, OH (*Presenter*) Nothing to Disclose Reshani Perera, Cleveland, OH (*Abstract Co-Author*) Nothing to Disclose Agata A. Exner, PhD, Cleveland, OH (*Abstract Co-Author*) Nothing to Disclose

PURPOSE

Our group recently presented a simple strategy using the nonionic surfactant, Pluronic, as a size control excipient to produce nanobubbles in the 100 nm range which exhibited stability and echogenicity on par with clinically available microbubbles. The objective of the current study was to evaluate biodistribution and extravasation of the Pluronic-stabilized lipid nanobubbles compared to microbubbles in two experimental tumor models in mice.

METHOD AND MATERIALS

Standard microbubbles or Pluronic L10 lipid-stabilized perfluoropropane nanobubbles were bolus injected into mice bearing either an orthotropic mouse breast cancer (BC4T1) or subcutaneous mouse ovarian cancer (OVCAR-3) through tail vein. The mean echopower value in the liver, kidney and tumor as function of time was acquired and the peak enhancement and decay slope were calculated for each tissue. To quantify extravasation, fluorescently-labeled nanobubbles and microbubbles were intravenously injected into mice bearing the same tumors. Three hours later, 0.1 ml fluorescein labeled tomato lectin (1mg/ml) was i.v. injected into mice to label the vessels. The mice were then perfused with PBS, the tumor tissue was harvested and imaged to measure bubble signal in tissue.

RESULTS

The mean diameter of nanobubble and microbubble was 123.0 nm \pm 24.9 and 685.0 nm \pm 129.5, respectively. No significant differences were observed in peak enhancement between the nanobubble and microbubble groups in the three tested regions (tumor, liver and kidney). The decay rates of nanobubbles in all 3 ROIs were slower than those of microbubbles, and significant differences were noted in tumor of both models (0.79 dB/min \pm 0.40 vs 1.13 dB/min \pm 0.24 in BC4T1 tumor, and 1.66 dB/min \pm 0.76 vs 2.64 dB/min \pm 0.46 in OVCAR-3 tumor, respectively). Nanobubbles were also retained in tumor tissue to a higher extent compared to microbubbles in both tumor models.

CONCLUSION

Pluronic-stabilized nanobubbles show equivalent peak enhancement and slower washout in tumors compared to microbubbles. Histological analysis demonstrates enhanced nanobubble extravasation and enhanced retention within tumor tissue. This study demonstrates potential augmented utility of these agents in ultrasound molecular imaging and drug delivery beyond the tumor vasculature.

CLINICAL RELEVANCE/APPLICATION

Pluronic-stabilized nanobubbles can offer more robust properties in areas of molecular imaging and drug delivery.

sSQ11-07 Is Delayed Dynamic PET Acquisition Still Valuable for 18F-FLT Kinetics Quantification?

Thursday, Dec. 1 11:30AM - 11:40AM Room: S505AB

Participants

Xiaoli Liu, Columbus, OH (*Abstract Co-Author*) Nothing to Disclose Jun Zhang, PhD, Columbus, OH (*Abstract Co-Author*) Nothing to Disclose Preethi Subramanian, MS, BEng, Columbus, OH (*Abstract Co-Author*) Nothing to Disclose Bhuvaneswari Ramaswamy, Columbus, OH (*Abstract Co-Author*) Nothing to Disclose Michael V. Knopp, MD, PhD, Columbus, OH (*Presenter*) Nothing to Disclose

PURPOSE

Cancer patients with poor veins frequently have venous access problems and cannot be injected on the PET table for dynamic imaging, which leads to the loss of early kinetic information. In this study we investigate whether kinetic parameters can still be accurately estimated using a delayed dynamic FLT PET acquisition, and how long a dynamic acquisition is required for accurate quantification.

30min-dynamic FLT PET scans were acquired on a Gemini TF 64 system in continuous list mode. Dynamic PET data were reconstructed following a 26-frame protocol (8x15s, 6x30s, 5x1min, 5x2min, 2x5min). Maximum activity concentrations (Bq/mL) of both tumors and plasma in the descending aorta were obtained with 3D VOI. Ki values were calculated using Patlak Analysis based on different linear regression onset time (T0) points (1, 6, 7, 8, 9 and 10min) and end time (Td) points (16, 20, 25 and 30min). Ki of the 1-30min data set were taken as the gold standard and compared with the rest data series. Pearson product-moment correlation coefficient (R) of 0.9 was chosen as a limit for the correlation coefficient. A total of 32 data sets were evaluated.

RESULTS

Ki calculated with 6-8min injection-to-acquisition time showed excellent correlations (R>0.9) with gold standard regardless of Td value. When acquisition started 9min after dose injection, Td should be \geq 20min to ensure accurate Ki estimation. If acquisition were initiated 10min post dose injection, Td=30min was required for accurate Ki estimation. 6-25min acquisition generated the best Ki correlation (R=0.99) while the worst occurred with 10-16min acquisition (R=0.62). Equivalent acquisition durations (EAD) were calculated by Td-T0; data acquired with shorter injection-to-acquisition time generated more accurate Ki values (R=0.96 and 0.80 for 6-16min and 10-20min, respectively). Acquisitions with EAD \geq 8min could provide accurate Ki values (R>0.9) except for those of 10-20min (R=0.80) and 10-25min (R=0.89).

CONCLUSION

Dynamic FLT PET acquisition after 6-10min injection-to-acquisition delay can still generate accurate Ki values, even with equivalent acquisition duration as short as 8 minutes.

CLINICAL RELEVANCE/APPLICATION

This study demonstrated the ability of delayed dynamic FLT PET imaging without influencing the kinetic quantification, making its application more feasible for clinical therapy response assessment.

SSQ11-08 Pseudo-Cloaking Contrast Media (PCCM's) for In vivo Differentiation using Detection-based spectral CT

Thursday, Dec. 1 11:40AM - 11:50AM Room: S505AB

Participants

Khaled A. Nasr, PhD, Dallas, TX (Presenter) Nothing to Disclose

Todd C. Soesbe, PhD, Dallas, TX (Abstract Co-Author) Nothing to Disclose

Robert E. Lenkinski, PhD, Dallas, TX (*Abstract Co-Author*) Research Grant, Koninklijke Philips NV; Research Consultant, Aspect Imaging;

Matthew A. Lewis, PhD, Dallas, TX (Abstract Co-Author) Research collaboration, CMR Naviscan Corporation

PURPOSE

To develop and evaluate simultaneously administered contrast media that exhibit pseudo-cloaking (PCCM's) for in vivo differentiation using clinical detection-based spectral CT.

METHOD AND MATERIALS

Compound of elements (Z=70 to Z=78) were purchased and used for phantom studies. Nanopowder colloidal of tungsten carbide (WC, 20 mg/mL W), tungsten oxide (WO3, 20 mg/mL W) and rhenium sulfide (ReS2, 20 mg/mL Re), tantalum (Ta, 20 mg/mL), tantalum oxide (Ta2O5, 20 mg/mL) were synthesized by colloidal and microemulsion method in 2% carboxymethylcellulose. Four female Fischer rats (n = 4) averaging 150 g mass were fasted for 24 hours. The rats were then given 4 mL of oral contrast. Phantoms and animal images were obtained using a detection-based spectral CT scanner (IQon, Philips Healthcare).

RESULTS

Phantom images exhibit a clear separation between elements (Z=70 to Z=78) and iodine-based contrast media. As a result, two contrast media, one made from high-Z elements and the second made from iodine-based contrast media could be used simultaneously to distinguish between an oral and vascular contrast in a single CT examination. Unfortunately, most compounds of high-Z elements have unknown or high toxicity (LD50) making them unsuitable to be used for in vivo CT imaging. In this study we selected tungsten carbide (LD50 >2000 mg/Kg), tungsten trioxide (LD50= 1059 mg/Kg rat oral), tantalum (LD50= 2500 mg/Kg), tantalum oxide (LD50= 8000 mg/Kg) and rhenium sulfide as an oral contrast and iopamidol as iodine-based vascular contrast agent for phantoms and in vivo imaging. Both PCCM's and iodine-based contrast media appear in the conventional image with high attenuation. In the virtual non-contrast (VNC) images, contrast from iodine was removed but tungsten and rhenium contrast was not affected. In iodine-no-water images (I-n-W), iodine contrast was not affected but contrast from tungsten and rhenium was removed.

CONCLUSION

Colloidal nanoparticles of low toxicity compounds of tantalum, tungsten and rhenium were shown to be excellent candidates of PCCM's providing a clear separation from iodine-based contrast media observed in phantom and in vivo imaging using detection-based spectral CT. Both barium and bismuth-based contrast media were shown to have similar radiographic appearance as Iodine.

CLINICAL RELEVANCE/APPLICATION

High-Z element PCCM's can provide clear oral and vascular differentiation in a single CT examination detection-based spectral CT

SSQ11-09 Pharmacokinetic Monitoring of Adoptively Transferred CEA-Targeted Human T Lymphocytes with a Dual-Modal Positron Emission Tomography (PET) Near-Infrared Fluorescent (NIRF) Imaging Agent

Thursday, Dec. 1 11:50AM - 12:00PM Room: S505AB

Participants Stefan Harmsen, PhD, New York, NY (*Abstract Co-Author*) Nothing to Disclose Ilker Medine, New York, NY (*Abstract Co-Author*) Nothing to Disclose Fuat Nurili, New York, NY (*Abstract Co-Author*) Nothing to Disclose Jose Lobo, New York, NY (*Abstract Co-Author*) Nothing to Disclose Yiyu Dong, New York, NY (*Abstract Co-Author*) Nothing to Disclose Maxim A. Moroz, MD, New York, NY (*Abstract Co-Author*) Nothing to Disclose Nagavarakishore Pillarsetty, New York, NY (*Abstract Co-Author*) Nothing to Disclose Vladimir Ponomarev, MD, New York, NY (*Abstract Co-Author*) Nothing to Disclose Oguz Akin, MD, New York, NY (*Abstract Co-Author*) Nothing to Disclose Omer Aras, MD, New York, NY (*Presenter*) Nothing to Disclose

PURPOSE

Despite the remarkable progress of adoptive T cell therapy in cancer treatment, there remains an urgent need for the noninvasive tracking of the transfused T cells. Therefore, we developed a dual-modal PET/NIRF nanoparticle-based imaging agent to efficiently label human CAR T cells ex vivo and monitored the therapeutic effect of CAR T-cell in a murine model of ovarian cancer.

METHOD AND MATERIALS

Human T lymphocytes co-transduced with chimeric antigen receptors (CAR) specific for human carcinoembryonic antigen and a Renilla luciferase, were labeled with the extrinsic 89Zr-PET/NIRF nanoparticle-based imaging agent ex vivo. The labeled CEA-targeted CAR T cells were injected (i.p. and i.v.) into SCID mice bearing intraperitoneal lesions of human ovarian carcinoma cells (SKOV3) engineered to overexpress hCEA and transduced with firefly reporter gene Renilla luciferase reporter gene. The localization of adoptively transferred T cells in this peritoneal ovarian carcinomatosis model was monitored with bioluminescence imaging (BLI) as well as small-animal PET and end-point near infrared fluorescence imaging (λ max=800 nm)

RESULTS

The adoptively transferred CEA-targeted CAR T cells were efficiently labeled with the dual-modal PET/NIRF imaging agent without affecting CAR T cell viability and cytotoxic functionality on the target cells. Small animal PET imaging enabled whole-body tomographic CAR T cell tracking over a long period of time to establish the pharmacokinetic profile of these T cells following i.p. or i.v. administration. More importantly, by correlating the PET imaging with BLI, it was shown that i.p. is the most effective route of administration in terms of co-localization with the peritoneal ovarian cancer tumor deposits. Lastly, end-point NIRF imaging of the labeled CAR T cells demonstrated specific infiltration in CEA-overexpressing tumor deposits.

CONCLUSION

These results show that noninvasive monitoring of genetically engineered human T lymphocytes labeled by our dual-modal PET/NIRF imaging agent provides high resolution anatomically correlated information on T-cell trafficking and has translational implications.

CLINICAL RELEVANCE/APPLICATION

Clinically applicable strategies of noninvasive cell tracking can greatly impact the design and development of T cell-mediated cancer therapy, the assessment of patient response to antitumor treatment, and the optimization (personalization) of therapeutic plans.

Molecular Imaging Thursday Poster Discussions

Thursday, Dec. 1 12:15PM - 12:45PM Room: S503AB

MI

AMA PRA Category 1 Credit ™: .50

Participants

Pedram Heidari, MD, Boston, MA (Moderator) Nothing to Disclose

Sub-Events

MI224-SD- Pharmacokinetic Analysis and Extravasation Study of a Novel Nanobubble Ultrasound Contrast Agent THA1

Station #1

Awards

Trainee Research Prize - Resident

Participants

Hanping Wu, MD, Cleveland, OH (*Presenter*) Nothing to Disclose Reshani Perera, Cleveland, OH (*Abstract Co-Author*) Nothing to Disclose Agata A. Exner, PhD, Cleveland, OH (*Abstract Co-Author*) Nothing to Disclose

PURPOSE

Our group recently presented a simple strategy using the nonionic surfactant, Pluronic, as a size control excipient to produce nanobubbles in the 100 nm range which exhibited stability and echogenicity on par with clinically available microbubbles. The objective of the current study was to evaluate biodistribution and extravasation of the Pluronic-stabilized lipid nanobubbles compared to microbubbles in two experimental tumor models in mice.

METHOD AND MATERIALS

Standard microbubbles or Pluronic L10 lipid-stabilized perfluoropropane nanobubbles were bolus injected into mice bearing either an orthotropic mouse breast cancer (BC4T1) or subcutaneous mouse ovarian cancer (OVCAR-3) through tail vein. The mean echopower value in the liver, kidney and tumor as function of time was acquired and the peak enhancement and decay slope were calculated for each tissue. To quantify extravasation, fluorescently-labeled nanobubbles and microbubbles were intravenously injected into mice bearing the same tumors. Three hours later, 0.1 ml fluorescein labeled tomato lectin (1mg/ml) was i.v. injected into mice to label the vessels. The mice were then perfused with PBS, the tumor tissue was harvested and imaged to measure bubble signal in tissue.

RESULTS

The mean diameter of nanobubble and microbubble was 123.0 nm \pm 24.9 and 685.0 nm \pm 129.5, respectively. No significant differences were observed in peak enhancement between the nanobubble and microbubble groups in the three tested regions (tumor, liver and kidney). The decay rates of nanobubbles in all 3 ROIs were slower than those of microbubbles, and significant differences were noted in tumor of both models (0.79 dB/min \pm 0.40 vs 1.13 dB/min \pm 0.24 in BC4T1 tumor, and 1.66 dB/min \pm 0.76 vs 2.64 dB/min \pm 0.46 in OVCAR-3 tumor, respectively). Nanobubbles were also retained in tumor tissue to a higher extent compared to microbubbles in both tumor models.

CONCLUSION

Pluronic-stabilized nanobubbles show equivalent peak enhancement and slower washout in tumors compared to microbubbles. Histological analysis demonstrates enhanced nanobubble extravasation and enhanced retention within tumor tissue. This study demonstrates potential augmented utility of these agents in ultrasound molecular imaging and drug delivery beyond the tumor vasculature.

CLINICAL RELEVANCE/APPLICATION

Pluronic-stabilized nanobubbles can offer more robust properties in areas of molecular imaging and drug delivery.

Molecular Imaging Thursday Poster Discussions

Thursday, Dec. 1 12:45PM - 1:15PM Room: S503AB

MI

AMA PRA Category 1 Credit ™: .50

Participants

Pedram Heidari, MD, Boston, MA (Moderator) Nothing to Disclose

Sub-Events

MI225-SD- Characterization of Sentinel Lymph Nodes Using Targeted Ultrasound Contrast Agents THB1

.

Station #1

Awards

Trainee Research Prize - Fellow

Participants

Kibo Nam, PhD, Philadelphia, PA (Presenter) Nothing to Disclose

Maria Stanczak, MS, Philadelphia, PA (Abstract Co-Author) Nothing to Disclose

Flemming Forsberg, PhD, Philadelphia, PA (*Abstract Co-Author*) Equipment support, Toshiba Corporation; Research Grant, Toshiba Corporation; Equipment support, Siemens AG; In-kind support, General Electric Company; In-kind support, Lantheus Medical Imaging, Inc

Ji-Bin Liu, MD, Philadelphia, PA (Abstract Co-Author) Nothing to Disclose

John R. Eisenbrey, PhD, Philadelphia, PA (*Abstract Co-Author*) Support, General Electric Company; Support, Lantheus Medical Imaging, Inc

Andrej Lyshchik, MD, PhD, Philadelphia, PA (Abstract Co-Author) Nothing to Disclose

PURPOSE

The purpose of this study is to evaluate the ability of molecular ultrasound to detect metastatic involvement in the sentinel lymph nodes (SLNs) of melanoma.

METHOD AND MATERIALS

To date, 8 swine (3-7 kg; Sinclair Bio-Resources, Columbia, MO) with naturally occurring melanoma have been studied. Contrast enhanced ultrasound on a S3000 scanner with a 9L4 probe (Siemens Medical Solutions, Mountain View, CA) was used for imaging. Dual-targeted microbubbles were created from Targestar SA bubbles (Targeson, San Diego, CA) labeled with P-selection and $\alphaV\beta3$ integrin in a 1:1 ratio. IgG labeled Targestar SA was used as control. A two stage imaging approach was used to first identify and then characterize SLN. First, 0.25 ml of Sonazoid (GE Healthcare, Oslo, Norway) was injected around the tumor and SLNs were identified. Next, dual-targeted and control microbubbles were injected IV with a 30 min interval between injections. Agents were allowed to circulate for 4 min to enable binding. Sets of image clips were then collected before and after a high-power destruction sequence. The mean intensity difference in pre- and post- destruction images was calculated as a relative bubble retention measure in the nodes. Non-SLNs were also imaged by dual-targeted and control bubbles as benign controls. All imaged nodes were dissected and histologically examined.

RESULTS

Sixteen SLNs and 14 non-SLNs were analyzed. Ten SLNs showed metastatic involvement greater than 5%. All non-SLNs were benign. The mean intensity of the dual-targeted bubbles was significantly higher than that of IgG control bubbles in the metastatic SLNs (19.23 \pm 23.95 AU vs. 0.20 \pm 0.26 AU; p=0.03). Benign nodes did not show significant difference in the mean intensity of the dual-targeted and control bubbles (0.85 \pm 1.81 AU vs. 0.03 \pm 0.26 AU; p=0.93). Additionally, the mean intensity of dual-targeted bubbles for metastatic nodes was significantly different from that of benign nodes (p=0.002), while control bubbles did not differentiate between metastatic and benign nodes (p=0.91).

CONCLUSION

The results indicated that dual-targeted microbubbles labeled with P-selectin and $\alpha V\beta$ 3-integrin can help to characterize metastatic involvement in SLNs.

CLINICAL RELEVANCE/APPLICATION

It may be possible to noninvasively characterize metastatic involvement in SLNs using molecular ultrasound.

Hot Topic Session: Track and Treat - Advancements in Theranostics

Thursday, Dec. 1 3:00PM - 4:00PM Room: E352

MI

AMA PRA Category 1 Credit ™: 1.00 ARRT Category A+ Credit: 1.00

FDA Discussions may include off-label uses.

Participants

Andrei Iagaru, MD, Stanford, CA (*Moderator*) Research Grant, General Electric Company; Research Grant, Bayer AG; Research Grant, The Piramal Group

Matthias J. Eiber, MD, Muenchen, Germany (Moderator) Nothing to Disclose

LEARNING OBJECTIVES

1) Explain the concept of theranostics to referring physicians and patients. 2) Identify current theranostic agents in use for various cancers. 3) Describe emerging theranostic agents and approaches for new cancer applications.

ABSTRACT

An important aspect of Nuclear Medicine is that the same core compound of the administered radiopharmaceutical can be labeled with both diagnostic radioisotopes and therapeutic radioisotopes, allowing for the detection and subsequent targeted treatment of lesions. This concept of theranostics, the combination of therapy and diagnostics, is the basis for new approaches to advanced molecular imaging and targeted radiotherapy for specific tumor biologies. Our session will provide and highlight several examples of current and emerging theranostic applications for various diseases. These applications include: (1) intra-arterial and radioembolization therapies for neuroendocrine tumors, (2) receptor-based therapies for neuroendocrine tumors, (3) novel PET imaging, radioguided surgical and endoradiotherapy approaches using prostate-specific membrane antigen (PSMA) ligands for prostate cancer, and (4) novel imaging and therapeutic approaches which target the chemokine receptor CXCR4.

Sub-Events

SPSH54A SIRT and Intra-arterial Treatment for NET

Participants

Ghassan El-Haddad, MD, Tampa, FL (Presenter) Nothing to Disclose

LEARNING OBJECTIVES

View learning objectives under main course title.

ABSTRACT

URL

SPSH54B NET Theranostics: From Past Present to Future Perfect

Participants

Lisa Bodei, MD, PhD, New York, NY (*Presenter*) Research Consultant, Ipsen SA; Research Consultant, Advanced Accelerator Applications SA

LEARNING OBJECTIVES

View learning objectives under main course title.

SPSH54C PSMA-theranostics - Radioguided Surgery and Radioligand Therapy

Participants Matthias J. Eiber, MD, Muenchen, Germany (*Presenter*) Nothing to Disclose

LEARNING OBJECTIVES

View learning objectives under main course title.

SPSH54D CXCR4 as a Promising Theranostic Target

Participants

Ken Herrmann, Essen, Germany, (ken.herrmann@uk-essen.de) (*Presenter*) Co-founder, SurgicEye GmbH; Stockholder, SurgicEye GmbH; Consultant, Sofie Biosciences; Consultant, Ipsen SA; Consultant, Siemens AG; Research Grant, Advanced Accelerator Applications SA; Research Grant, Ipsen SA

LEARNING OBJECTIVES

View learning objectives under main course title.

Emerging Technology: Hyperpolarized MRI - Opportunities and Challenges

Thursday, Dec. 1 4:30PM - 6:00PM Room: S504CD

MI MR

AMA PRA Category 1 Credits ™: 1.50 ARRT Category A+ Credits: 1.50

FDA Discussions may include off-label uses.

Participants

Daniel M. Spielman, PhD, Stanford, CA, (spielman@stanford.edu) (Moderator) Nothing to Disclose

LEARNING OBJECTIVES

1) Understand the basic principles of hyperpolarized 13C MRS studies of human subjects. 2) Assess the potential of this technology to improve diagnosis and monitor therapy of prostate cancer, brain tumors, and cardiac pathologies.

ABSTRACT

Sub-Events

RC717A Imaging Metabolism using Hyperpolarized 13C MRS

Participants

Dirk Mayer, PhD, Baltimore, MD, (dmayer@som.umaryland.edu) (Presenter) Nothing to Disclose

LEARNING OBJECTIVES

1) Describe the basic principles of hyperpolarization/dynamic nuclear polarization. 2) Define the unique challenges applying hyperpolarzed 13C MRS in vivo. 3) Identify the most appropriate acquisition strategies. 4) Compare molecular/metabolic imaging using PET vs hyperpolarized 13C MRS.

Handout:Dirk Mayer

http://abstract.rsna.org/uploads/2016/16001575/RSNA2016_DMayer_13C.pdf

RC717B Hyperpolarized 13C MRS of Prostate Cancer

Participants

Kayvan Keshari, PhD, New York, NY (Presenter) Nothing to Disclose

LEARNING OBJECTIVES

1) Comprehend the basic principles of hyperpolarized MRS in the context of human prostate cancer. 2) Assess the potential of using this approach to stage prostate cancer aggressiveness as well as potential for response to therapy.

ABSTRACT

It has been well known that the metabolism of prostate cancer dramatically differs both from surrounding benign prostate as well as with grade. With hyperpolarized MRI as an emerging field, preclinical work has demonstrated that hyperpolarized pyruvate can play a potential role in the study of prostate cancer metabolism non-invasively. These studies have highlighted the use of pyruvate to study aggressiveness as well as response to therapy in the setting of prostate cancer. In this educational lecture, we will discuss the translation of hyperpolarized MRI to the clinic and its application in the setting of human prostate cancer.

RC717C Imaging Glioma with Hyperpolarized 13C-labeled Pyruvate

Participants

Sarah J. Nelson, PhD, San Francisco, CA (*Presenter*) Research Grant, General Electric Company; Research Grant, GlaxoSmithKline plc; Research Grant, Omniox

LEARNING OBJECTIVES

View learning objectives under the main course title.

RC717D Cardiac Application of Hyperpolarized 13C MRS

Participants Charles H. Cunningham, PhD, Toronto, ON (*Presenter*) Nothing to Disclose

LEARNING OBJECTIVES

View learning objectives under the main course title.

Molecular Imaging Mini-Course: Clinical Applications of Molecular Imaging-Neuro

Thursday, Dec. 1 4:30PM - 6:00PM Room: S504AB

NR MI OI PH

AMA PRA Category 1 Credits ™: 1.50 ARRT Category A+ Credits: 1.50

Participants Sub-Events

RC723A Oncology Applications

Participants

Hyunsuk Shim, PhD, Atlanta, GA, (hshim@emory.edu) (Presenter) Nothing to Disclose

LEARNING OBJECTIVES

1) To learn about the potential of combining an advanced spectroscopic MR imaging with standard MR images to reduce the recurrence rate in glioblatomas.

ABSTRACT

Radiation therapy (RT) is as good as the images that guide RT planning. RT based on conventional MRIs may not fully target tumor extent in glioblastomas (GBM), which may, in part, account for high recurrence rates (60-70 percent at 6 months). Magnetic resonance spectroscopy, a molecular imaging modality that quantifies endogenous metabolite levels without relying on perfusion, leakage and diffusion of injected material, may better define extent of actively proliferating tumor. In addition, advances in this technology now permit acquisition of whole-brain high-resolution 3D spectroscopic MRI (sMRI) in 12-14 minutes. We correlated state-of-the-art sMRI metabolite maps and their ratio maps with tissue histopathology to validate further its use for identifying non-enhancing and infiltrating tumors that may not be fully imaged by conventional MRI sequences and provide support for its adjunctive use in tumor contouring for RT planning. Integration of histologically-verified, whole brain 3D sMRI into RT planning is feasible and may considerably modify target volumes. Thus, RT planning for GBMs may be augmented by sMRI potentially leading to reduced or delayed recurrence rates.

RC723B Functional Applications

Participants

Satoshi Minoshima, MD, PhD, Salt Lake City, UT (*Presenter*) Royalties, General Electric Company; Research Consultant, Hamamatsu Photonics KK; Research Grant, Hitachi, Ltd; Research Grant, Nihon Medi-Physics Co, Ltd;

RC811

Emerging Technology: Immuno Imaging Probes-Opportunities and Challenges

Friday, Dec. 2 8:30AM - 10:00AM Room: E353A

MI NM OI US

AMA PRA Category 1 Credits ™: 1.50 ARRT Category A+ Credits: 1.50

FDA Discussions may include off-label uses.

Participants

Terence Z. Wong, MD, PhD, Chapel Hill, NC (Moderator) Nothing to Disclose

Sub-Events

RC811A A Primer on 89Zr-ImmunoPET

Participants Brian M. Zeglis, PhD, New York, NY (*Presenter*) Nothing to Disclose

LEARNING OBJECTIVES

1) To learn about the basic physical and chemical properties of the radioisotope 89Zr.2) To understand the basic components of a 89Zr-labeled radioimmunoconjugate.3) To understand how 89Zr-labeled radioimmunoconjugates are synthesized and purified. 4) To gain an appreciation of the forces behind the recent advent of 89Zr-based immunoPET imaging.5) To explore the PSMA-targeting radioiommunoconjugate 89Zr-DFO-J591 as a case study for the journey of an immunoPET imaging agent from the laboratory to the clinic.

ABSTRACT

RC811B Engineered Antibodies for immunoPET: Probes for Profiling Tumors and Immune Responses

Participants

Anna M. Wu, PhD, Los Angeles, CA, (awu@mednet.ucla.edu) (*Presenter*) Stockholder, ImaginAb, Inc; Consultant, ImaginAb, Inc; Consultant, Avidity NanoMedicines, LLC;

LEARNING OBJECTIVES

1) Identify key properties of antibodies that can be modified/improved to produce probes optimized for in vivo imaging. 2) Discuss applications of new immunoPET tracers to address challenges in oncology and immunology. 3) Describe the process and potential of translating immunoPET probes into clinical use.

RC811C Clinical Applications of Immuno Probes in Oncology

Participants

Elisabeth G.E. de Vries, MD, PhD, Groningen, Netherlands (*Presenter*) Institutional Research Grant, F. Hoffmann-La Roche Ltd ; Institutional Research Grant, Amgen Inc; Institutional Research Grant, Novartis Ag; Institutional Research Grant, SERVIER; Data Safety Monitoring Board, BioMarin Pharmaceutical Inc; Advisory Board, Synthon Holding BV; Advisory Board, Merck & Co, Inc; ;; ;; ;;;;;;

LEARNING OBJECTIVES

1) To learn about the answers immuno probes can provide in clinical oncology. 2) To learn about the potential of the immuno probes consisting of radioactively labeled antibodies as well as fluorescently labeled antibodies in the clinic.

ABSTRACT

Currently monoclonal antibodies (mAbs) are an expanding innovative class of cancer drugs. Numerous mAbs, including several antibody-drug conjugates, are in advanced clinical development, forming an important part of the many molecularly targeted anticancer therapeutics currently in development. Development and treatment decisions for registered mAbs could benefit from quantitative biomarkers, enabling visualization of the tissue distribution of (potentially modified) therapeutic mAbs to confirm effective whole-body target expression, engagement, and modulation and to evaluate heterogeneity across lesions and patients. Such biomarkers may be realized with positron emission tomography (PET) imaging of radioactively labeled antibodies, a process called immunoPET or with a fluorescently labeled antibodies and optical imaging. This approach could potentially increase the power and value of trials and clinical practice by improving patient selection, optimizing dose and schedule, and rationalizing observed drug responses.

RC811D Companion Imaging Diagnostics: Small Molecule Ligands versus Immune-Based Agents

Participants

Michael D. Farwell, MD, MA, New York, NY (Presenter) Nothing to Disclose

LEARNING OBJECTIVES

1) Describe desriable properties of a companion diagnostic imaigng probe. 2) Discuss likely clinical scenarios where companion diagnostic might be used. 3) List advantages and diadvantages of small molecule veruss immune-based probes as comparative diagnostics.

Honored Educators

Presenters or authors on this event have been recognized as RSNA Honored Educators for participating in multiple qualifying educational activities. Honored Educators are invested in furthering the profession of radiology by delivering high-quality educational content in their field of study. Learn how you can become an honored educator by visiting the website at: https://www.rsna.org/Honored-Educator-Award/

David A. Mankoff, MD, PhD - 2013 Honored Educator